ANKARA YILDIRIM BEYAZIT UNIVERSITY

GRADUATE SCHOOL OF NATURAL AND APPLIED SCIENCES



MODELLING AND ANALYSIS OF A HYDROPNEUMATIC RECOIL MECHANISM IN ARTILLERY

Ph.D. Thesis by

İbrahim TÜRKMEN

Department of Mechanical Engineering

May, 2021

ANKARA

MODELLING AND ANALYSIS OF A HYDROPNEUMATIC RECOIL MECHANISM IN ARTILLERY

A Thesis Submitted to

The Graduate School of Natural and Applied Sciences of

Ankara Yıldırım Beyazıt University

In Partial Fulfillment of the Requirements for the Degree of Doctor of Philosophy in Mechanical Engineering, Department of Mechanical Engineering

by

İbrahim TÜRKMEN

May, 2021

ANKARA

Ph.D. THESIS EXAMINATION RESULT FORM

We have read the thesis entitled **"MODELLING AND ANALYSIS OF A HYDROPNEUMATIC RECOIL MECHANISM IN ARTILLERY"** completed by **İBRAHİM TÜRKMEN** under the supervision of **PROF. DR. VELİ ÇELİK** and we certify that in our opinion it is fully adequate, in scope and in quality, as a thesis for the degree of Doctor of Philosophy.

Prof. Dr. Veli ÇELİK

Supervisor

Prof. Dr. Abuzer Kadir ÖZSUNAR	Prof. Dr. Sadettin ORHAN
Jury Member	Jury Member
Jury Member	Jury Member

Prof. Dr. Ergün ERASLAN

Director

Graduate School of Natural and Applied Sciences

ETHICAL DECLARATION

I hereby declare that, in this thesis which has been prepared in accordance with the Thesis Writing Manual of Graduate School of Natural and Applied Sciences,

- All data, information and documents are obtained in the framework of academic and ethical rules,
- All information, documents and assessments are presented in accordance with scientific ethics and morals,
- All the materials that have been utilized are fully cited and referenced,
- No change has been made on the utilized materials,
- All the works presented are original,

and in any contrary case of above statements, I accept to renounce all my legal rights.

ACKNOWLEDGMENTS

I would like to express my sincere gratitude to my supervisor, Prof. Dr. Veli ÇELİK for his tremendous support and motivation during my study. His immense knowledge and precious recommendations constituted the milestones of this study. His guidance assisted me all the time of my research and while writing this thesis.

I am grateful to Prof. Dr. Abuzer Kadir ÖZSUNAR and Prof. Dr. Sadettin ORHAN for their valuable contributions and constructive criticisms during my thesis progress and thesis defense examination.

I would like to thank TUBİTAK for its financial support within the scope of 2214-A International Research Fellowship Programme for PhD Students.

I also would like to thank Republic of Turkey Ministry of Industry and Technology and Mechanical and Chemical Industry Company Heavy Weapons and Steel Factory for their financial supports and contributions within the scope of SAN-TEZ program with the contract number 0504.STZ.2013-2.

I must express my profound appreciations to my parents for providing me emotional support, loving care and continuous encouragement.

I cannot thank my wife enough for her love and patience and being stand by me throughout all these years and through the period of writing this thesis. This accomplishment would not have been possible without her.

2021, 20 May **İbrahim TÜRKMEN**

MODELLING AND ANALYSIS OF A HYDROPNEUMATIC RECOIL MECHANISM IN ARTILLERY

ABSTRACT

In this study, the recoil movement of heavy weapons with hydropneumatic recoil mechanism is modeled. The primary purpose of the study is to obtain the equation of motion of the recoiling parts in the weapon systems. For this purpose, the forces acting on the recoiling parts were determined, and the effects of each force were examined. Breech force is calculated via LeDuc equations for in bore period and verified by comparing with experimental studies from literature for a typical 105 mm howitzer and from MKEK for a new generation lighter 105 mm weapon system. Additionally, velocity of projectile in barrel is calculated from the model and compared with test data. Breech force which is generated during the discharge of the remaining gases after the projectile leaves the barrel is also calculated and total breech force is obtained. Then, net retarding force that consists of friction, hydraulic brake and recuperator forces are calculated. After determining breech and net retarding forces, the equation of motion is obtained, and solved via MATLAB. Recoil distance, velocity and acceleration of recoiling parts are calculated and effects of firing angle, weight of recoiling parts, orifice discharge coefficient, muzzle brake efficiency are investigated.

Comparisons show that model results are compatible with test data and the differences between them is less than three percent. Additionally, it is deduced from this study that if firing angle and orifice discharge coefficient increase, maximum recoil displacement, maximum velocity, and maximum acceleration values of recoiling parts increase. When orifice discharge coefficient is increased by 20 percent, maximum recoil displacement, velocity, and acceleration of recoiling parts are increased from 1109 mm to 1220 mm, from 45.2 m/s to 49.7 m/s and from 21.6 m/s^2 to 23.7 m/s^2, respectively.

In addition, maximum recoil displacement, maximum velocity, and maximum acceleration values of recoiling parts decrease if weight of recoiling parts and muzzle brake efficiency increase. When weight of recoiling parts is increased by 20 percent,

maximum recoil displacement, velocity and acceleration of recoiling parts are decreased from 1109 mm to 921 mm, from 45.2 m/s to 37.5 m/s and from 21.6 m/s^2 to 17.9 m/s^2, respectively. Besides, as the muzzle brake efficiency increases from 1 to 1.5, maximum recoil displacement and velocity of recoiling parts decreased from 1109 mm to 1075 mm, 45.2 m/s to 43.8 m/s, respectively.

Keywords: Hydropneumatic recoil mechanism, heavy weapons, modelling, analysis, MATLAB.

AĞIR SİLAHLARDAKİ HİDROPNÖMATİK GERİ TEPME MEKANİZMASININ MODELLENMESİ VE ANALİZİ

ÖZ

Bu çalışmada hidropnömatik geri tepme mekanizmasına sahip ağır silahların geri tepme hareketi modellenmiştir. Çalışmanın öncelikli amacı silah sistemlerindeki geri tepen parçaların hareket denklemini elde etmektir. Bu amaç doğrultusunda, geri tepen parçalara etki eden kuvvetler belirlenmiş ve her bir kuvvetin etkileri incelenmiştir. Silahın ateşlenmesi ile namlu içerisinde oluşan yüksek basıncın neden olduğu geri tepme kuvveti, merminin namluyu terk etmesine kadar geçen süre boyunca LeDuc denklemlerinin yardımı ile hesaplanmış ve hesaplanan değerler literatürden ve MKEK'den alınan deneysel çalışmalarla karşılaştırılarak doğrulanmıştır. Ayrıca merminin namlu içerisindeki hızı modelden hesaplanmış ve testlerden elde edilen verilerle kıyaslanmıştır. Mermi namluyu terk ettikten sonra namlu içerisinde kalan gazların boşaltımı sırasında oluşan geri tepme kuvveti de hesaplanmış ve toplam geri tepme kuvveti elde edilmiştir. Bu kuvvetin neden olduğu geri tepme hareketi, geri tepme mekanizmasındaki hidrolik fren ve reküperatör kuvveti ile sürtünme sayesinde durdurulmaktadır. Geri tepme kuvveti ile net durdurucu kuvvetin belirlenmesinden sonra elde edilen hareket denklemi MATLAB programında çözülmüştür. Geri tepen parçaların hız ve ivme değerleri ile geri tepme mesafesi hesaplanmış ve atış açısı, geri tepen parçaların ağırlığı, orifis boşaltım katsayısı, namlu ağız baskısı frenleme faktörü gibi parametrelerin etkisi incelenmiştir.

Yapılan karşılaştırmalar, model sonuçları ile test atışlarından elde edilen verilerin uyumlu olduğunu ve aradaki farkın yüzde üçten az olduğunu göstermektedir. Bu çalışma, maksimum geri tepme mesafesi ile maksimum geri tepme hızı ve ivmesi değerlerinin; atış açısı ve orifis boşaltım katsayısı arttıkça arttığını ortaya koymuştur. Orifis boşaltım katsayısı yüzde 20 arttığında, maksimum geri tepme mesafesi 1109 mm'den 1220 mm'ye, maksimum geri tepme hızı 45.2 m/s'den 49.7 m/s'ye maksimum geri tepme ivmesi 21.6 m/s^2'den 23.7 m/s^2'ye artmaktadır.

Bu çalışmada ayrıca, maksimum geri tepme mesafesi ile maksimum geri tepme hızı ve ivmesi değerlerinin; geri tepen ağırlık ve namlu ağız baskısı frenleme faktörü arttıkça azaldığını göstermiştir. Geri tepen ağırlık yüzde 20 arttırıldığında, maksimum geri tepme mesafesi 1109 mm'den 921 mm'ye, maksimum geri tepme hızı 45.2 m/s'den 37.5 m/s'ye maksimum geri tepme ivmesi 21.6 m/s^2'den 17.9 m/s^2'ye azalmaktadır. Namlu ağız baskısı frenleme faktörü 1'den 1.5'e arttığında ise; maksimum geri tepme mesafesi 1109 mm'den 1075 mm'ye, maksimum geri tepme hızı 45.2 m/s'den 43.8 m/s'ye azalmaktadır.

Anahtar Kelimeler: Hidropnömatik geri tepme mekanizması, ağır silahlar, modelleme, analiz, MATLAB.

CONTENTS

Ph.D. THESIS EXAMINATION RESULT FORM ii
ETHICAL DECLARATION iii
ACKNOWLEDGMENTS iv
ABSTRACT v
ÖZ vii
NOMENCLATURE xi
LIST OF TABLES xv
LIST OF FIGURES xvi

CHAPTER 1 - INTRODUCTION 1
1.1 Recoil Mechanisms 2
1.1.1 Purpose and Working Principle of Recoil Mechanisms 2
1.1.2 Functions of Recoil Mechanisms 4
1.1.3 Components of Recoil Mechanisms 7
1.2 Types of Recoil Mechanisms 8
1.2.1 Hydropneumatic Recoil Mechanisms 8
1.2.2 Hydro Spring Recoil Mechanisms 11
1.2.3 Soft Recoil Mechanisms 12
1.2.4 Magneto Rheologic Recoil Mechanisms 12
1.3 Literature Review 13
1.4 Aim of the Study 21

CHAPTER 2 - MATHEMATICAL MODELLING 23
2.1 Equation of Motion 23
2.2 Breech Force 24
2.2.1 In-bore Period 24
2.2.2 Gas Ejection Period 27
2.2.3 Muzzle Brake 32
2.3 Weight Force 33
2.4 Net Retarding Force 33
2.4.1 Recuperator Force 35
2.4.2 Frictional Force 36
2.4.3 Hydraulic Brake 40

2.5 Numerical Solution 42

CHAPTER 3 - RESULTS AND DISCUSSION 44

3.1 Breech Force 44

3.1.1 In-bore Period 44

3.1.2 Gas Ejection Period 46

3.2 Velocity of Projectile 47

3.3 Acceleration of Projectile 49

3.4 Recoil Displacement 51

3.5 Effect of Firing Angle on Recoil Displacement 52

3.6 Velocity of Recoiling Parts 53

3.7 Effect of Firing Angle on Velocity of Recoiling Parts 53

3.8 Acceleration of Recoiling Parts 54

3.9 Effect of Firing Angle on Acceleration of Recoiling Parts 55

3.10 Effect of Recoiling Weight on Recoil Displacement 56

3.11 Effect of Recoiling Weight on Velocity of Recoiling Parts 57

3.12 Effect of Recoiling Weight on Acceleration of Recoiling Parts 59

3.13 Effect of Orifice Discharge Coefficient on Recoil Displacement 61

3.14 Effect of Orifice Discharge Coefficient on Recoil Velocity 62

3.15 Effect of Orifice Discharge Coefficient on Recoil Acceleration 64

3.16 Effect of Muzzle Brake Efficiency on Breech Force 66

3.17 Effect of Muzzle Brake Efficiency on Recoil Displacement 67

3.18 Effect of Muzzle Brake Efficiency on Recoil Velocity 69

3.19 Effect of Muzzle Brake Efficiency on Recoil Acceleration 71

CHAPTER 4 - CONCLUSION AND FUTURE WORKS 74

4.1 Conclusion 74

4.2 Future Works 76

REFERENCES 78

CURRICULUM VITAE 81

NOMENCLATURE

Roman Letter Symbols

a	Distance between bearings, m
a	Linear acceleration of projectile, m/s^2
a	Acceleration of recoiling parts, m/s^2
a	LeDuc parameter, m/s
a_0	Average area of orifice, m^2
a_t	Peripheral acceleration of projectile, m/s^2
A	Cross section area of hydraulic cylinder, m^2
A	Bore area, m^2
A_b	Bore area, m^2
A_p	Effective area of the piston, m^2
A_R	Recuperator cylinder area, m^2
b	LeDuc parameter, m
b	Distance between CG and rear bearing, m
B	Breech force, N
B_e	Mean breech force, N
B_M	Maximum breech force, N
B_0	Breech force at projectile exit, N
$B(t)$	Breech force as a function of time, N
$B(t)_{max}$	Maximum breech force, N
c	Specific heat of hydraulic fluid, J/kg.°C
C_0	Orifice discharge coefficient
d_f	Depth of bearing from CG, m
d_p	Depth of bearing from tube centerline, m
d_r	Distance between cradle slide and recoil cylinder, m
d_r	Distance between supports, m
F	Force on projectile, N
F_a	Inertial force due to acceleration of recoiling parts, N
F_0	Hydraulic brake force, N
F_R	Recuperator force, N
F_r'	Normal force, N

f_r'	Frictional force due to riffling torque, N
G	Momentum imparted to breech by propellant gases during gas ejection without a muzzle brake, kg.m/s
g	Gravity, 9.81 m/s^2
H	Hydraulic brake force, N
I_p	Mass moment of inertia of projectile, kg/m^2
K	Total resistance force (Net retarding force), N
k	Radius of gyration of projectile, m
k	Fraction of heat loss from propellant gases to tube
$\overline{k}$	Constant
K_a	Recuperator force, N
K_f	Friction force of bearings or slides, N
K_m	Muzzle brake force, N
K_0	Ideal constant recoil force, N
K_R	Rod pull, N
$K(t)$	Sum of resisting forces, N
L	Recoil length, m
$m_{c_{eff}}$	Effective mass of charge, kg
m_f	Mass of hydraulic fluid, kg
m_p	Mass of projectile, kg
$m_{p_{eff}}$	Effective mass of projectile, kg
m_r	Mass of recoiling parts, kg
n	Ratio of specific heats
N_r	Twist of rifling
P	Gas pressure in recuperator, Pa
p_b	Peak interior ballistic pressure, Pa
P_e	Mean chamber pressure, Pa
P_f	Breech pressure at end of gas ejection period, Pa
P_h	Pressure in high pressure chamber, Pa
P_l	Pressure in low pressure chamber, Pa
P_M	Peak chamber pressure, Pa
P_0	Gas pressure in recuperator at in-battery position, Pa

P_0	Breech pressure at projectile exit, Pa
P_x	Gas pressure in recuperator at any recoil distance x, Pa
R	Gas constant, J/kg.K
R	Frictional forces, N
R_1	Reaction force, N
R_2	Reaction force, N
R_b	Radius of bore, m
RT_b	Specific impetus of propellant, m^2/s^2
T	Gas temperature in bore, K
T_b	Gas temperature at breech, K
t_f	Time at end of recoil force or end of gas ejection period, s
T_0	Gas temperature in breech at projectile exit, K
t_0	Time of projectile exit, s
T_r	Rifling torque, N.m
u	Projectile travel in bore, m
U_0	Tube length, m
V	Gas volume in recuperator, m^3
V_0	Gas volume in recuperator at in-battery position, m^3
v	Velocity of piston, m/s
v	Velocity of recoiling parts, m/s
v'	In-bore velocity of projectile, m/s
v_f	Velocity of recoiling parts at end of gas ejection period, m/s
v_0	Velocity of recoiling parts at projectile exit, m/s
v_0'	Muzzle velocity of projectile, m/s
V_x	Gas volume in recuperator at any recoil distance x, m^3
W_c	Weight of propellant charge, N
W_p	Weight of projectile, N
W_r	Total weight of recoiling parts, N
W_t	Work done by hydraulic fluid, J
x	Absolute travel of recoiling parts, m
x_f	Travel of recoiling parts at end of gas ejection period, m
x_0	Travel of recoiling parts at projectile exit, m

$\dot{x}_p$ Velocity of projectile, m/s

x_R Displacement of control piston rod, m

$\dot{x}_r$ Velocity of recoiling parts, m/s

Greek Letter Symbols

α Angular acceleration of projectile, rad/s^2

β Muzzle brake efficiency factor

ρ Fluid density, kg/m^3

ϕ Duration of gas ejection period, s

θ Firing angle

θ_r Helix angle of rifling

μ Velocity of gases in bore, m/s

μ Coefficient of friction

λ Speedup factor

γ Ratio of specific heats

Δ Chamber volume plus bore volume, m^3

ΔP Pressure difference between high and low pressure chambers, Pa

ΔT Temperature change, °C

ΔV Velocity change, m/s

ΔV_x Change in gas volume, m^3

Acronyms

BMG Browning Machine Gun

CG Centre of Gravity

FEM Forward Euler Method

MKEK Mechanical and Chemical Industry Company

MR Magneto Rheologic

RKM Runge-Kutta Method

LIST OF TABLES

Table 1.1 Mass of recoiling parts vs maximum recoil distance 13
Table 1.2 Orifice discharge coefficient vs maximum recoil distance 14
Table 1.3 Model results and test data for different firing angles 14
Table 1.4 Experimental and predicted peak values 14
Table 1.5 Simulation results 21
Table 1.6 Simulation results 21
Table 3.1 Effect of firing angle on recoil displacement 52
Table 3.2 Effect of recoiling weight on recoil displacement 56
Table 3.3 Effect of recoiling weight on velocity of recoiling parts 57
Table 3.4 Effect of recoiling weight on acceleration of recoiling parts 58
Table 3.5 Effect of orifice discharge coefficient on recoil displacement 59
Table 3.6 Effect of orifice discharge coefficient on velocity of recoiling parts 60
Table 3.7 Effect of orifice discharge coefficient on acceleration of recoiling parts . 61
Table 3.8 Effect of muzzle brake efficiency on recoil displacement 63
Table 3.9 Effect of muzzle brake efficiency on velocity of recoiling parts 64
Table 3.10 Effect of orifice discharge coefficient on acceleration of recoiling parts 65

LIST OF FIGURES

Figure 1.1 Weapon reactions of initial and modern designs 1
Figure 1.2 Hydro-pneumatic type recoil mechanism 3
Figure 1.3 Movement of projectile and recoiling parts 5
Figure 1.4 Classification of recoil mechanisms 8
Figure 1.5 Independent type recoil mechanism 9
Figure 1.6 Dependent type recoil mechanism 10
Figure 1.7 Hydro spring recoil mechanism 11
Figure 1.8 Soft recoil mechanism 12
Figure 1.9 Surface plot of the orifice area versus recoil travel at different elevation 15
Figure 1.10 Optimization result 16
Figure 1.11 Barrel assembly dynamics with (a) 1 air spring, (b) 2 air springs, (c) 3 air springs, (d) 4 air springs 17
Figure 1.12 Dynamic response of barrel assembly at (a)0°, (b)10°, (c)30°, (d)50° .. 18
Figure 1.13 (a) Maximum displacement and (b) settling time of barrel assembly ... 19
Figure 1.14 Comparison of experimental and theoretical (a) buffer pressure, (b) buffer velocity 19
Figure 1.15 Effect of (a) recuperator stiffness, (b) recoil damping, (c) tire stiffness, (d) friction coefficient on recoil displacement 20
Figure 1.16 (a) Recoil force vs time and, (b) recoil stroke vs time 20
Figure 2.1 One degree of freedom model for recoiling parts 24
Figure 2.2 Forces contributing net retarding force 34
Figure 2.3 Spring and gas recuperator behaviors 35
Figure 2.4 Forces and reaction on recoiling parts 37
Figure 2.5 Cross section through barrel 39
Figure 2.6 Flowchart of the model 43
Figure 3.1 Comparison of model and test data from literature for breech force vs projectile travel 45
Figure 3.2 Comparison of model and test data from MKEK for breech force vs projectile travel 45
Figure 3.3 Model data of new 105 mm howitzer for breech force vs time for gas ejection period 46
Figure 3.4 Model data of new 105 mm howitzer for total breech force vs time 47
Figure 3.5 Comparison of model and test data from literature for velocity of projectile vs projectile travel 48

Figure 3.6 Comparison of model and test data from MKEK for velocity of projectile vs projectile travel 49

Figure 3.7 Comparison of model and test data from literature for acceleration of projectile vs projectile travel 50

Figure 3.8 Model data of new 105 mm howitzer for acceleration of projectile vs projectile travel 50

Figure 3.9 Model data of new 105 mm howitzer for recoil displacement vs time 51

Figure 3.10 Effect of firing angle on recoil displacement 52

Figure 3.11 Model data of new 105 mm howitzer for velocity of recoiling parts vs time 53

Figure 3.12 Effect of firing angle on velocity of recoiling parts 54

Figure 3.13 Model data of new 105 mm howitzer for acceleration of recoiling parts vs time 55

Figure 3.14 Effect of firing angle on acceleration of recoiling parts 56

Figure 3.15 Effect of recoiling weight on recoil displacement 57

Figure 3.16 Effect of recoiling weight on velocity of recoiling parts 58

Figure 3.17 Effect of recoiling weight on velocity of recoiling parts (0-80 ms) 59

Figure 3.18 Effect of recoiling weight on acceleration of recoiling parts 60

Figure 3.19 Effect of recoiling weight on acceleration of recoiling parts (0-40 ms) 61

Figure 3.20 Effect of orifice discharge coefficient on recoil displacement 62

Figure 3.21 Effect of orifice discharge coefficient on velocity of recoiling parts 63

Figure 3.22 Effect of orifice discharge coefficient on velocity of recoiling parts (0-60 ms) 64

Figure 3.23 Effect of orifice discharge coefficient on acceleration of recoiling parts65

Figure 3.24 Effect of orifice discharge coefficient on acceleration of recoiling parts (0-40 ms) 66

Figure 3.25 Effect of muzzle brake efficiency on breech force 67

Figure 3.26 Effect of muzzle brake efficiency on recoil displacement 68

Figure 3.27 Effect of muzzle brake efficiency on recoil displacement (50-205 ms) 69

Figure 3.28 Effect of muzzle brake efficiency on velocity of recoiling parts 70

Figure 3.29 Effect of muzzle brake efficiency on velocity of recoiling parts (0-25 ms) 70

Figure 3.30 Effect of muzzle brake efficiency on acceleration of recoiling parts 72

Figure 3.31 Effect of muzzle brake efficiency on acceleration of recoiling parts (5-30 ms) 73

CHAPTER 1

INTRODUCTION

Artillery weapons had been used in thirteenth century firstly and have developed until today. In initial artillery designs which do not have a recoil mechanism, barrel assembly was mounted directly to the carriage and this cause weapon systems to jump. Additionally, those weapon systems were very heavy which is a major disadvantage for mobility. Then, late in the nineteenth century, recoil mechanisms were designed and started to be used in weapon systems. Recoil mechanisms allow some components to move opposite to firing direction and decrease the effect of backward forces [1]. The performance of the weapon systems increased significantly by using of the recoil mechanisms. Figure 1.1 shows the reactions of initial and modern weapon systems.

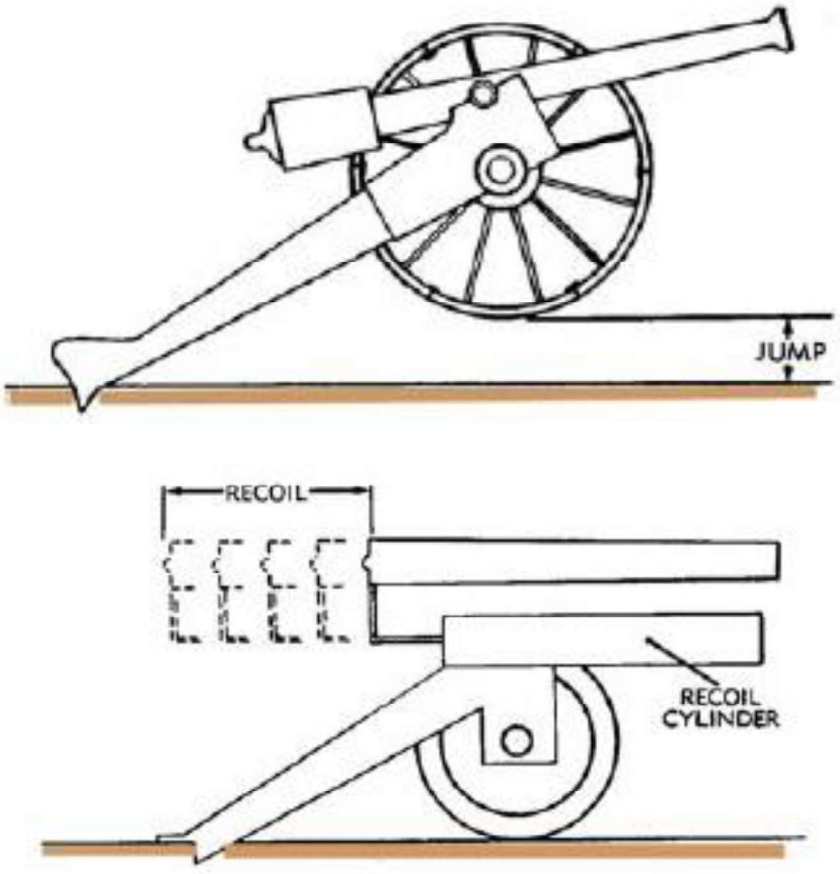

Figure 1.1 Weapon reactions of initial and modern designs [2]

Studies in recent years have focused on the decreasing the weight of weapon systems to improve mobility. Hence, there is a need for recoil mechanism that has high recoil efficiency and small volume to improve vehicular integration of weapon systems.

1.1 Recoil Mechanisms

When a round is fired, extremely high interior ballistic forces is formed due to the burning propellant. While these high forces accelerate the projectile inside barrel, they also act on the breech and push it backward. Recoil mechanisms dissipate most of the recoil energy and store some of it to return the weapon system back to in battery position. All recoil mechanisms in artillery weapon systems use hydraulic cylinder to damp recoil energy via fluid throttling. However, there are two main options for energy storage. Some weapon systems have mechanical springs and some other has pneumatic cylinder to initiate counter recoil motion of the weapon system. Both types have been used since they first patented at the end of 19th century. Hydro spring or hydro mechanical system, and hydropneumatic system were first patented in 1890 and 1894 respectively. Both have advantages and disadvantages, and these are discussed in following chapters. Additionally, purpose, functions, working principle and components of recoil mechanisms are also explained.

1.1.1 Purpose and Working Principle of Recoil Mechanisms

Burning of propellant over a very short time (5-20 ms) causes extremely high internal ballistic forces that act on the gun tube. The main purpose of the recoil mechanism is to decrease magnitude of this recoil force and transfer it to carriage in a much longer period (0.2-0.5 s). In other words, the design objective of recoil mechanism is to change short duration and higher peak loads into long period and lower peak loads.

Although it is possible to mount weapon system directly on to the carriage, this is not preferred in practice due to that it requires enormous structure to resist huge peak loads. In the practical design of artillery, a recoil mechanism is used to allow gun tube and other recoiling parts to move back. This backward motion which is caused by internal ballistic forces is resisted mostly by recoil mechanism and partly by muzzle

brake and frictional forces. A hydro-pneumatic type recoil mechanism is demonstrated in Figure 1.2 to explain working principle of recoil mechanisms.

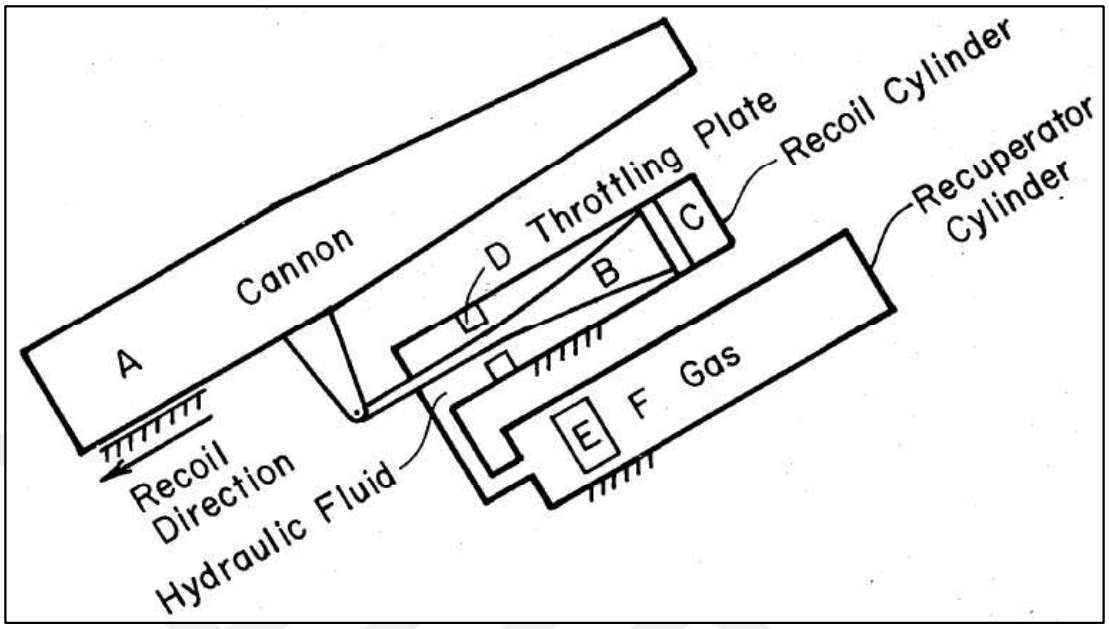

Figure 1.2 Hydro-pneumatic type recoil mechanism [3]

Rod B and piston C are connected to barrel A. When the projectile is fired A, B and C move backward and piston C forces fluid in the recoil cylinder to pass through the throttling plates D. The orifice between plates D is wide enough to let fluid passing fast initially. While B is moving backward, orifice decreases due to the increase in diameter of rod B. Even at low fluid velocities, constant throttling pressure difference can occur. Thus, constant recoil force can be obtained, and barrel A is balanced at the end of recoil distance.

The fluid that forced to flow from recoil cylinder to recuperator makes piston E move forward and this piston compress nitrogen gas that is in F region of recuperator. After recoiling parts stop, compressed gas forces the piston E to move rearward and thus fluid moves back into the recoil cylinder and the fluid forces piston C forward to bring the weapon back into the initial position. The velocity of recoiling parts during counter recoil cycle much lower than recoil cycle due to counter recoil forces are much lower than recoil forces. A large resistance occurs while the fluid is passing through the orifice, this results in low fluid velocity and accordingly low recoiling parts velocity.

But still some external buffers may be needed to slow recoiling parts to prevent from slamming.

One of the most important points of recoil mechanism design is selecting the orifice area vs recoil distance so that the retarding force acting on the recoiling parts is essentially constant throughout the recoil travel. Selecting a recoil mechanism type among all types depends on the artillery system. For example, recoil stroke must be short for an armored vehicle while it should be long for a light weighted towed howitzer. It is very important to keep the peak recoil force minimum acting on the lightweight vehicles and support carriages. Additionally, a designer should consider some other system design parameters such as ammunition characteristics, available space for crew, carriage strength, weapon stability.

1.1.2 Functions of Recoil Mechanisms

Apart from the main purpose, which is indicated in the previous chapter, a recoil mechanism has three important functions:

- Momentum transfer
- Recoil force control
- Energy transfer

1.1.2.1 Momentum Transfer

Relative movement of projectile and recoiling parts is schematically shown in Figure 1.3. Gas pressure that is formed after burning of gun powder moves the projectile forward and barrel and other connected parts rearward. Breech force B(t) is calculated from multiplying this pressure and cross sectional bore area.

While the projectile is leaving the barrel, the forward momentum of it is approximately equal to momentum of recoiling parts,

$$m_r \dot{x}_r + m_p \dot{x}_p = 0 \tag{1.1}$$

Where, m_r is mass of recoiling parts (kg), $\dot{x}_r$ is velocity of recoiling parts (m/s), m_p is projectile mass (kg), and $\dot{x}_p$ is velocity of projectile (m/s).

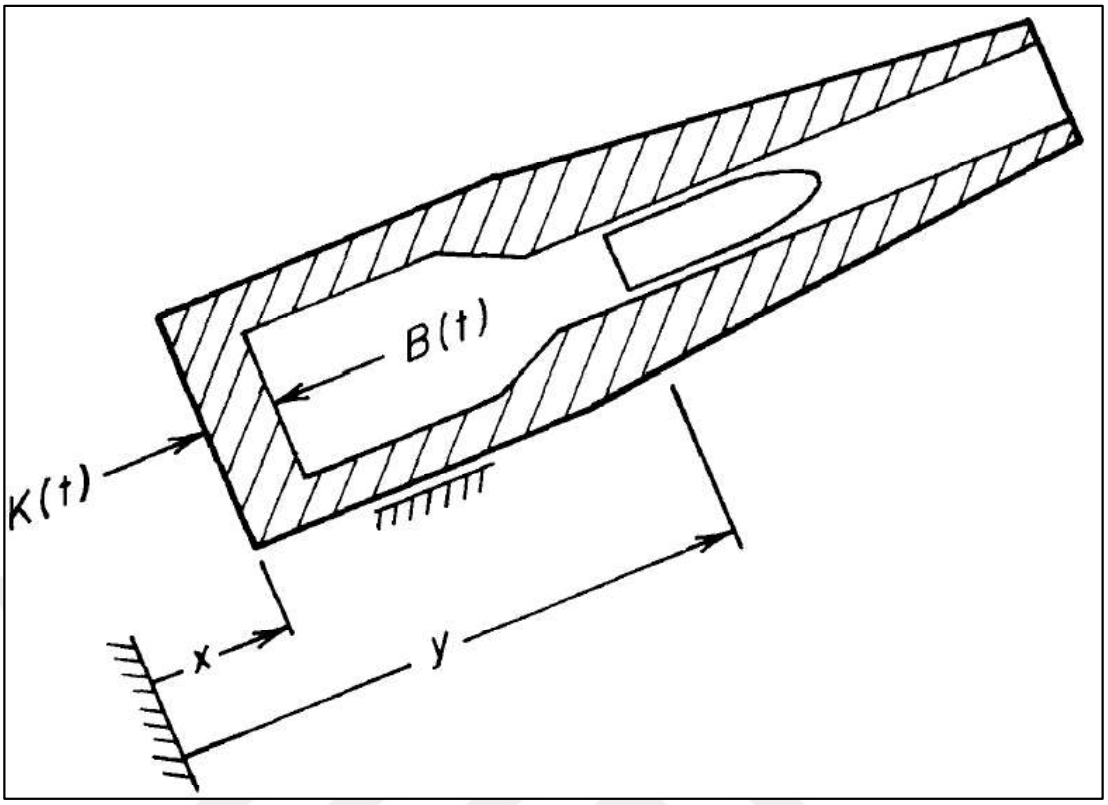

Figure 1.3 Movement of projectile and recoiling parts [3]

As an example, consider a modern 155 mm artillery weapon. Projectile mass is 45 kg, the projectile muzzle velocity is 660 m/s and the mass of recoiling parts is 3600 kg for this weapon system. Velocity of recoiling parts is calculated from Eq. 1.1.

$$3600\ \dot{x_r} + (45)(660) = 0$$

$$\dot{x_r} = -8.25\ m/s$$

1.1.2.2 Recoil Force Control

Recoil length must be known to calculate recoil force. Kinetic energy change of recoiling parts is equal to work done by all forces that act on recoiling parts.

$$LK_0 = \frac{(m_r)(\Delta V)^2}{2} \tag{1.2}$$

Where, ΔV is velocity change (m/s), L is recoil length (m), and K_0 is ideal constant recoil force (N). Considering again 155 mm weapon system, L and ΔV can be assumed 1.5 m and 8.25 m/s respectively. Then, K_0 can be calculated from Eq. 1.2.

$$K_0 = \frac{(3600)(8.25)^2}{(2)(1.5)} = 81675\ N$$

To make a comparison, peak breech force should be calculated from equation below via using peak chamber pressure value p_b as 344.7 MPa for 155 mm bore.

$$B(t)_{max} = A_b p_b \tag{1.3}$$

$$B(t)_{max} = (\pi/4)(0.155)^2(344.7) = 6.504\ MN$$

This huge force is 80 times greater than K_0 that acts on recoiling parts and if a recoil mechanism is not applied $B(t)_{max}$ acts on the carriage directly. This reduction explains the importance and necessity of using recoil mechanisms.

1.1.2.3 Energy Transfer

Kinetic energy of the recoiling parts that occurs during recoil is equal the energy which is dissipated by friction force, recuperator force and fluid throttling. Friction and recuperator forces can be neglected for an approximate solution due to that they are small comparing to fluid throttling. Work done by hydraulic fluid W_t can be obtained from the equation below.

$$W_t = LK_0 \tag{1.4}$$

$$W_t = (1.5)(81675) = 122513\ J$$

The work done by recoil force causes an increase in fluid temperature and it is calculated by equation below.

$$W_t = m_f c \Delta T \tag{1.5}$$

Where, m_f is mass of hydraulic fluid (kg), c is specific heat (J/kgK), and ΔT is temperature change. m_f and c are 40 kg and 646.2 J/kgK respectively.

$$\Delta T = \frac{122513}{(40)(646.2)} = 4.74\ ^{\circ}\mathrm{C}$$

If a series of rounds is fired without waiting enough time for cooling of the fluid, temperature of it increases significantly, and this may cause damages. Therefore, this has to be taken in consideration during design process.

1.1.3 Components of Recoil Mechanisms

Various recoil mechanisms types are used in artillery system designs and these mechanisms have various components. All types of recoil mechanisms are used to stop recoil motion in specified distance and to bring artillery system back in firing position. Accordingly, recoil mechanisms have to be designed with suitable components for suitable artillery system due to that they affect performance, stability and weight directly.

Recoil mechanisms consist of three main components:

- Recoil Brake
- Counter Recoil Mechanism
- Buffer

Recoil brake consists of one hydraulic cylinder and one piston and is used to stop recoiling parts by fluid throttling. Fluid is forced to pass through an orifice and recoil energy of the recoiling parts is dissipated as heat.

Counter recoil mechanism consists of recuperator and/or counter recoil cylinder. This recuperator is used to store energy and it can be hydro spring or hydropneumatic type. Recoiling parts return firing position by the energy that is stored by recuperator. Storing energy is obtained by compressing the spring in spring type and by compressing gas in pneumatic type. To provide stability for all firing angles in weapon system, some energy has to be loaded to recuperator initially.

Buffer mechanism absorbs energy at the end of counter recoil to prevent recoiling parts from crashing. In some systems there is no buffer. Friction force between sliding surfaces, packings, and seals provides enough resistance to stop recoiling parts.

1.2 Types of Recoil Mechanisms

Recoil mechanisms can be divided into four main groups: Hydro-pneumatic, hydro-spring, soft and, magneto-rheologic. This classification with subgroups is given in Figure 1.4.

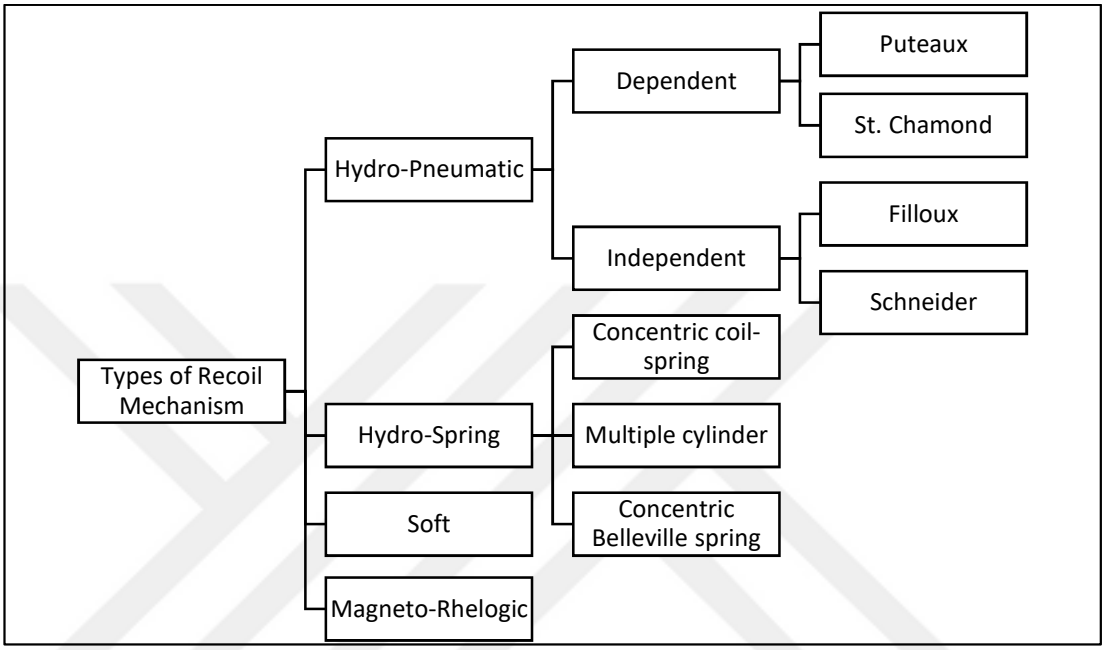

Figure 1.4 Classification of recoil mechanisms [3]

1.2.1 Hydropneumatic Recoil Mechanisms

Hydropneumatic type recoil mechanisms mainly consist of a hydraulic cylinder and a recuperator (pneumatic cylinder). Recuperator is used for counter recoil in hydropneumatic recoil mechanism type and some of recoil energy is stored by compressing nitrogen. After recoil ends compressed nitrogen expands and recoiling parts return to the firing position. Most of the rest energy absorbs by flow of hydraulic fluid from high pressure side to low pressure side through an orifice [4].

Hydropneumatic type recoil mechanism separated into two groups: dependent and independent. Independent type mechanism that is shown in Figure 1.5, recuperator and recoil brake are discrete. Piston rods of recuperator and recoil brake are directly connected to recoiling parts. Flowing of the fluid in brake cylinder from one side to other through orifice provides necessary retarding force. At the same time, fluid in

counter recoil cylinder flows into recuperator and compress the gas. Gas and hydraulic fluid in recuperator are separated by floating piston.

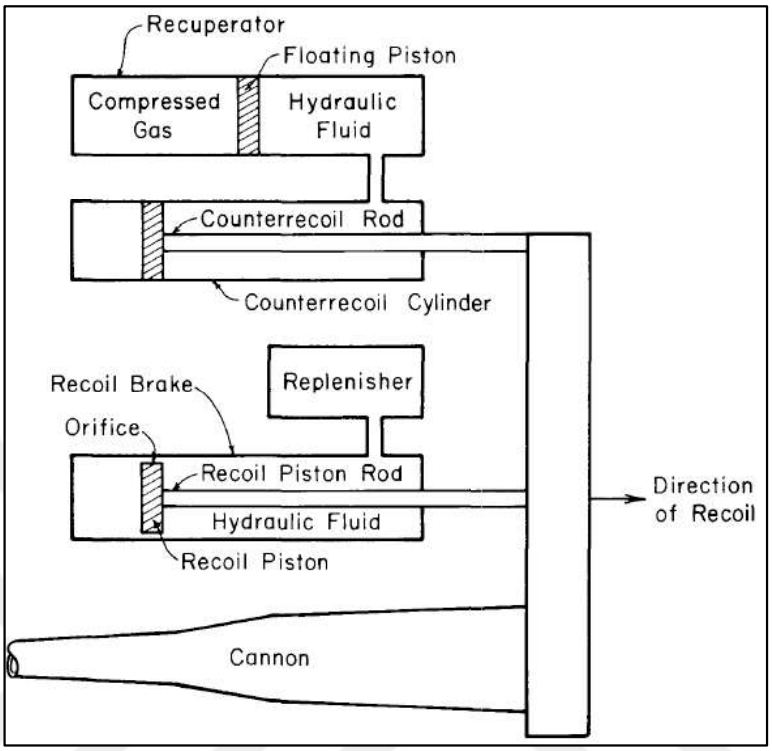

Figure 1.5 Independent type recoil mechanism [3]

Dependent type recoil mechanism that is shown is Figure 1.6, only brake piston rod is connected to recoiling parts. Fluid in brake cylinder flows into recuperator and is forced to pass through the orifice. Recuperator is directly connected to brake cylinder. There is a floating piston in recuperator to separate gas and fluid as same in independent type.

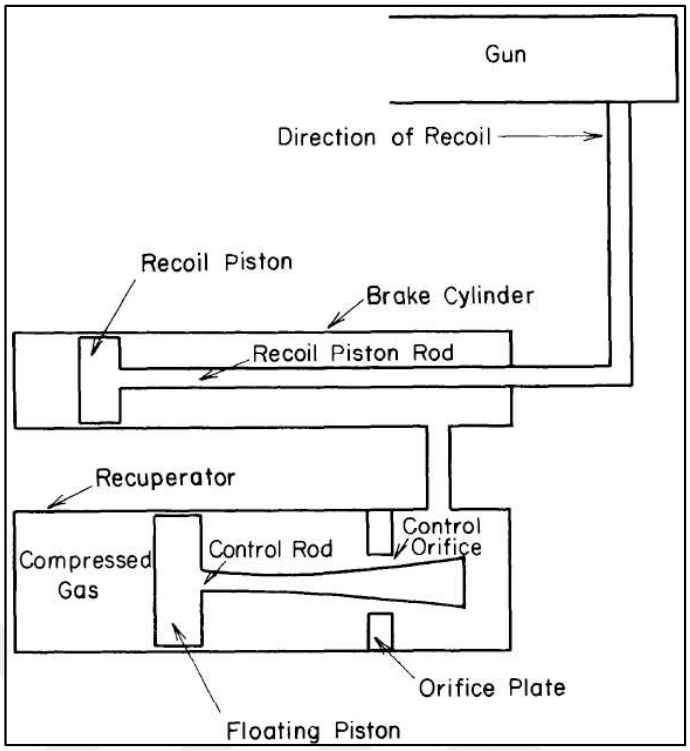

Figure 1.6 Dependent type recoil mechanism [3]

Dependent type is usually used for towed artillery systems while independent type is commonly used for self-propelled systems.

Advantages of hydropneumatic mechanisms:

- Reliability
- Long duration
- Sensitive adjustability
- To allow long recoil distance
- Ease of design

Disadvantages of hydropneumatic mechanisms:

- Expensive manufacturing and to be an expert for manufacturing
- Internal corrosion
- High surface quality (smoothness) requirement
- Additional precaution to prevent gas pressure changes in different conditions
- Need time between two shots

1.2.2 Hydro Spring Recoil Mechanisms

Hydro spring recoil systems include mechanical springs to store energy for counter recoil which is different from hydropneumatic mechanisms (Figure 1.7).

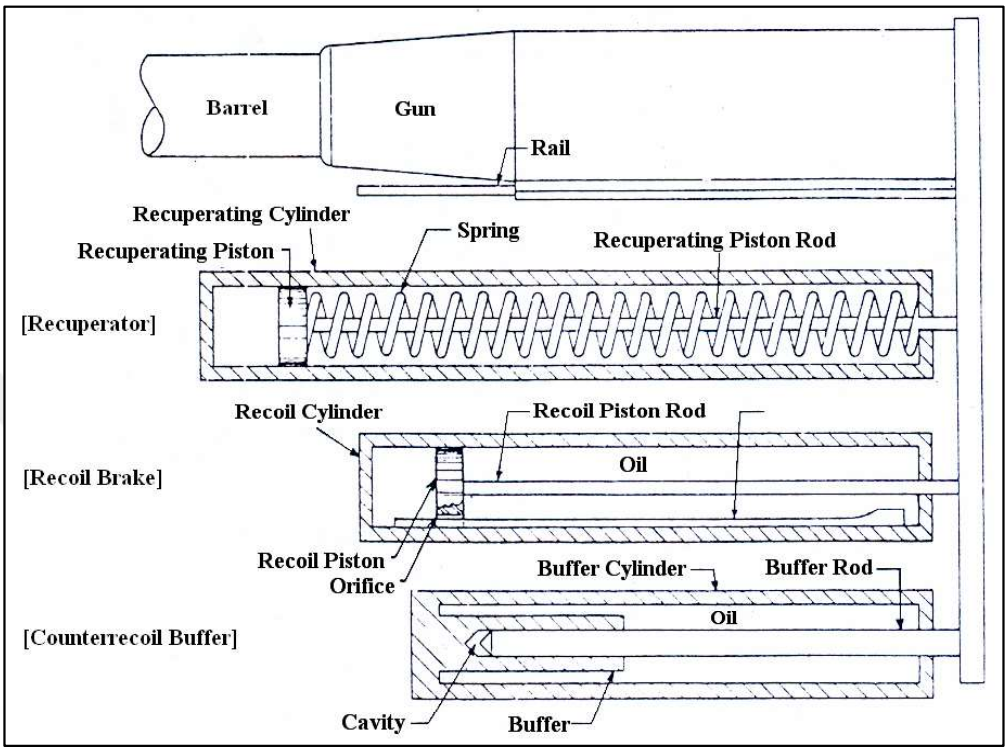

Figure 1.7 Hydro spring recoil mechanism [5]

There are three types of hydro spring mechanisms and these are:

- Concentric coil-spring
- Multiple cylinder
- Concentric belleville spring

Hydro spring mechanism are not as common as hydropneumatic systems. However, it still has some advantages and disadvantages. Advantages of hydro spring mechanisms:

- Simple design
- Easy to manufacture
- Low cost
- Easy to adjust
- Less leakage problems

Disadvantages of hydro spring mechanisms:

- Unpredictable life
- Bigger volume
- Maintenance frequency

1.2.3 Soft Recoil Mechanisms

The working principle of soft recoil mechanisms is different from hydropneumatic and hydro spring type recoil mechanisms. As shown in Figure 1.8, there is no orifice for fluid throttling and counter recoil stroke. The basic of this mechanism is storing the energy instead of dissipating it.

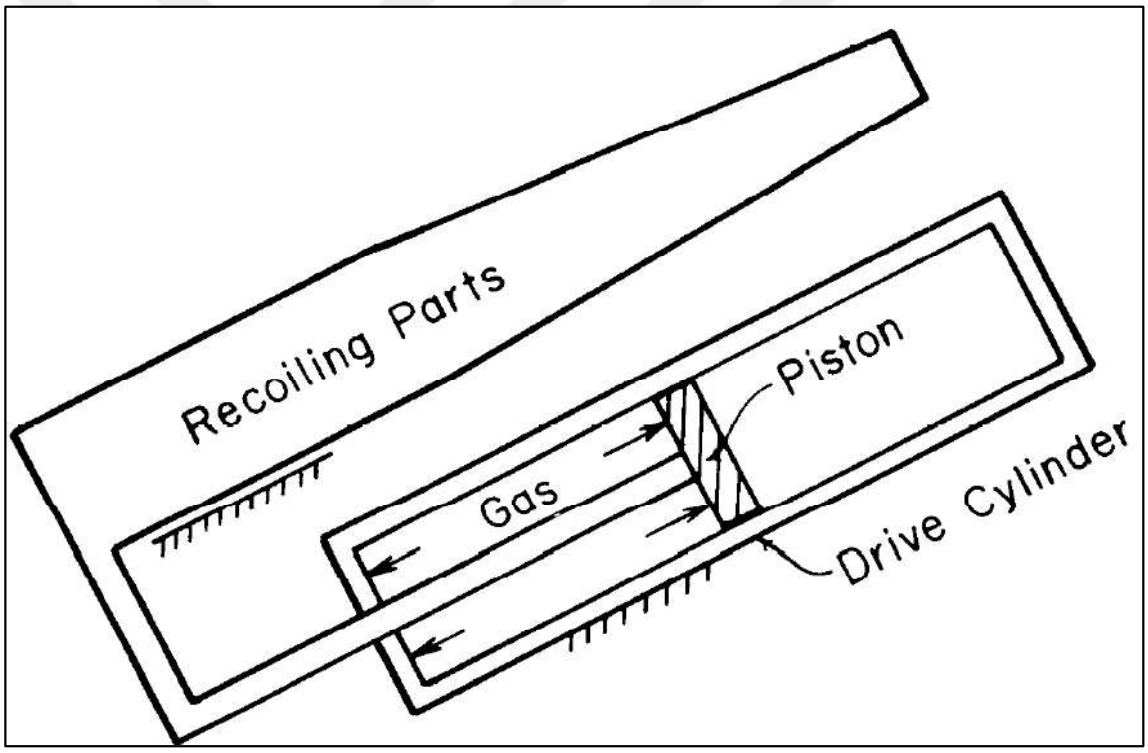

Figure 1.8 Soft recoil mechanism [3]

1.2.4 Magneto Rheologic Recoil Mechanisms

Magneto rheologic (MR) fluids are used in this type of recoil mechanisms. MR fluids usually consist of carrier fluid and iron powders with specific concentrations that suspend in this fluid. Size of iron powders is about several microns. There are some chemicals that prevent iron powders to be pellet in the fluid. When these fluids are

influenced by magnetic field, iron powders order as a sieve in the cross-section and this affects the flow of the fluid that pass though this cross-section. Therefore, the fluid behaves as having a changeable viscosity. Viscosity of the fluid increases with the magnitude of the magnetic field and it behaves as a Newtonian fluid when the magnetic field is removed. This situation provides us to control fluid flow by altering the magnetic field. These types of recoil mechanisms are mostly used for weapons in helicopters and warplanes.

1.3 Literature Review

Different methods such as analytical, numerical and experimental have been implemented for modeling of recoil mechanisms. Summary of those studies in the literature is prepared and given below.

Tuncer and Alli [6] has built a mathematical model of an independent type hydropneumatic recoil mechanism and improve a simulation that uses firing test data of the chosen weapon system. Breech force and projectile velocity are calculated from the model and compared with test results and model is validated. Tuncer [7] has built a similar model to analyze recoil performance of 120 mm weapon system in her master thesis. It is revealed from her model that mass of recoiling system and orifice discharge coefficient in the hydraulic cylinder are directly affect the recoil length. Recoil length increases with the mass of recoiling parts, but this results in decrease in recoil velocity due to the conservation of momentum. Additionally, increasing orifice discharge coefficient reduces the recoil length and these results are given in Table 1.1 and 1.2.

Table 1.1 Mass of recoiling parts vs maximum recoil distance

Mass of recoiling parts (kg)	Maximum recoil distance (m)
1650	0.2933
1700	0.2943
1750	0.2952
1800	0.2961
1850	0.2970
1900	0.2979
1950	0.2988
2000	0.2996
2050	0.3005
2100	0.3013
2150	0.3021
2200	0.3029

Table 1.2 Orifice discharge coefficient vs maximum recoil distance

Orifice discharge coefficient	Maximum recoil distance (m)
0.6	0.2676
0.65	0.2778
0.7	0.2863
0.75	0.2938
0.8	0.3031
0.85	0.3081
0.9	0.3153

Taşkıran [8] has focused on the dynamics of a heavy weapon that has independent type short stroke recoil mechanism. Results of his studies explain the relationship between recoil distance, recoil velocity and firing angle. His studies show that maximum recoil distance increases with firing angle. Comparison of model results and experimental data is given in Table 1.3.

Table 1.3 Model results and test data for different firing angles

Angle (degree)	Maximum recoil distance (m)	
	Tests average	Model result
0	0.2903	0.2882
17	0.2948	0.2898

Elaldı and Akçay [9] has developed a model to predict important parameters of the recoil mechanism by using method of Runge-Kutta. A hydropneumatic recoil mechanism is designed, produced and tested for 155 mm weapon system. Oil pressure, hydraulic brake force and recoil length are measured via experimental setup and compared with the predicted values from model and values are compatible with each other. Experimental and predicted peak values are given in Table 1.4.

Table 1.4 Experimental and predicted peak values

Charge Zone	Maximum oil pressure (bar)		Maximum hydraulic braking force (kN)	
	Experimental	Predicted	Experimental	Predicted
3	31	26	31	33
5	60	53	70	66
8	450	441	517	517

Zaloğlu [10] has performed a comprehensive finite element based analysis of recoil springs in automatic weapons which includes effects of all important parameters such as nonlinear force deflection characteristics, dynamic stress etc. In addition, an experimental study is carried out to validate the results from analysis. Yang [5] has

studied on optimization of recoil mechanism via dynamic simulation analysis. Small volume, high efficiency and low cost are considered as optimization parameters for the vehicular integration of artillery weapons. It can be inferred from the study that maximum recoil distance can be limited within a certain value by controlling the orifice area.

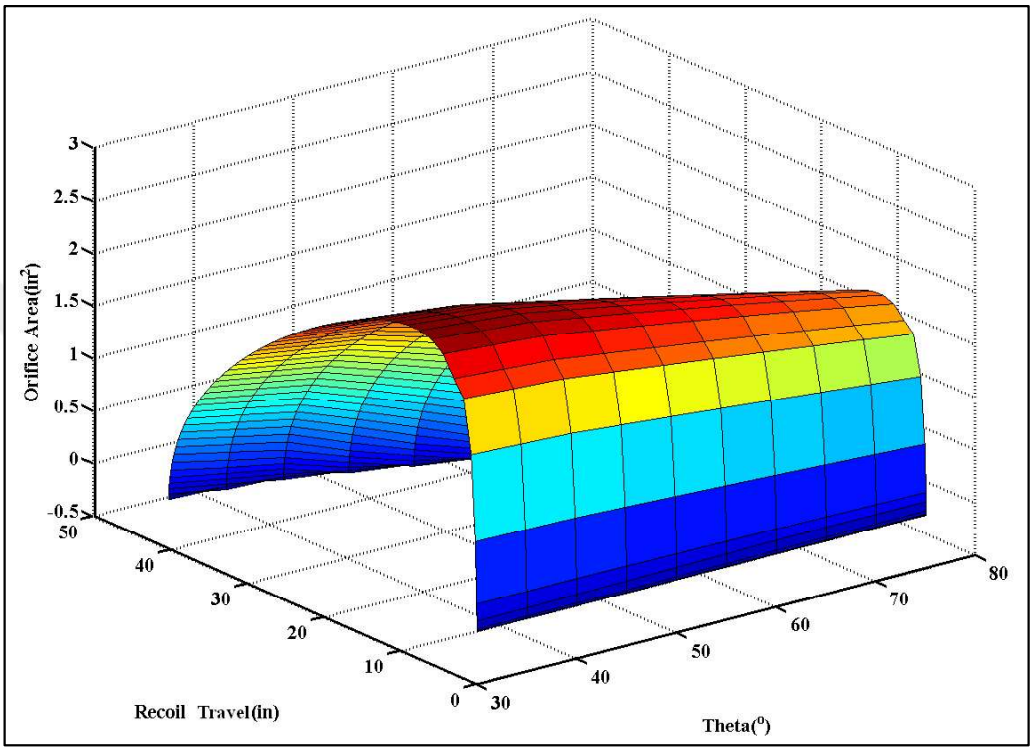

Figure 1.9 Surface plot of the orifice area versus recoil travel at different elevation [5]

Lin et al. [11] have studied on dynamics of the recoil mechanism of 155 mm self-propelled howitzer and they have obtained recoil length, velocity and acceleration. To find the required force, free body analysis is applied on the system component firstly and experience data and curve fitting methods are also applied together for more complex systems. Additionally, the maximum recoil distance that is aimed to be minimized is specified as cost function of the optimization procedure. And it seems from Figure 1.10 that maximum recoil distance is decreased about 5 % after optimization.

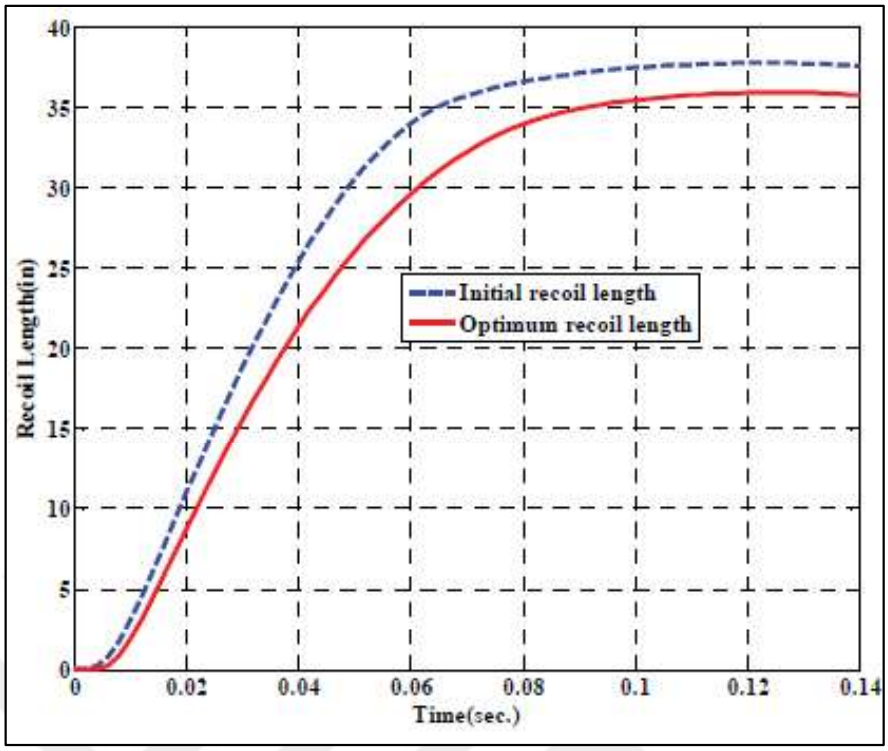

Figure 1.10 Optimization result [11]

Hassaan [12] has investigated recoil mechanisms of cannons which have air springs and hydraulic damper with constant damping coefficient. A nonlinear barrel assembly model is built and solved via Runge-Kutta 4 method. The effect of number of air springs used on the recoil mechanism performance is studied and results are given in Figure 1.11. It is obvious from the figure that maximum barrel displacement and barrel settling time decreases with increasing the number of air springs.

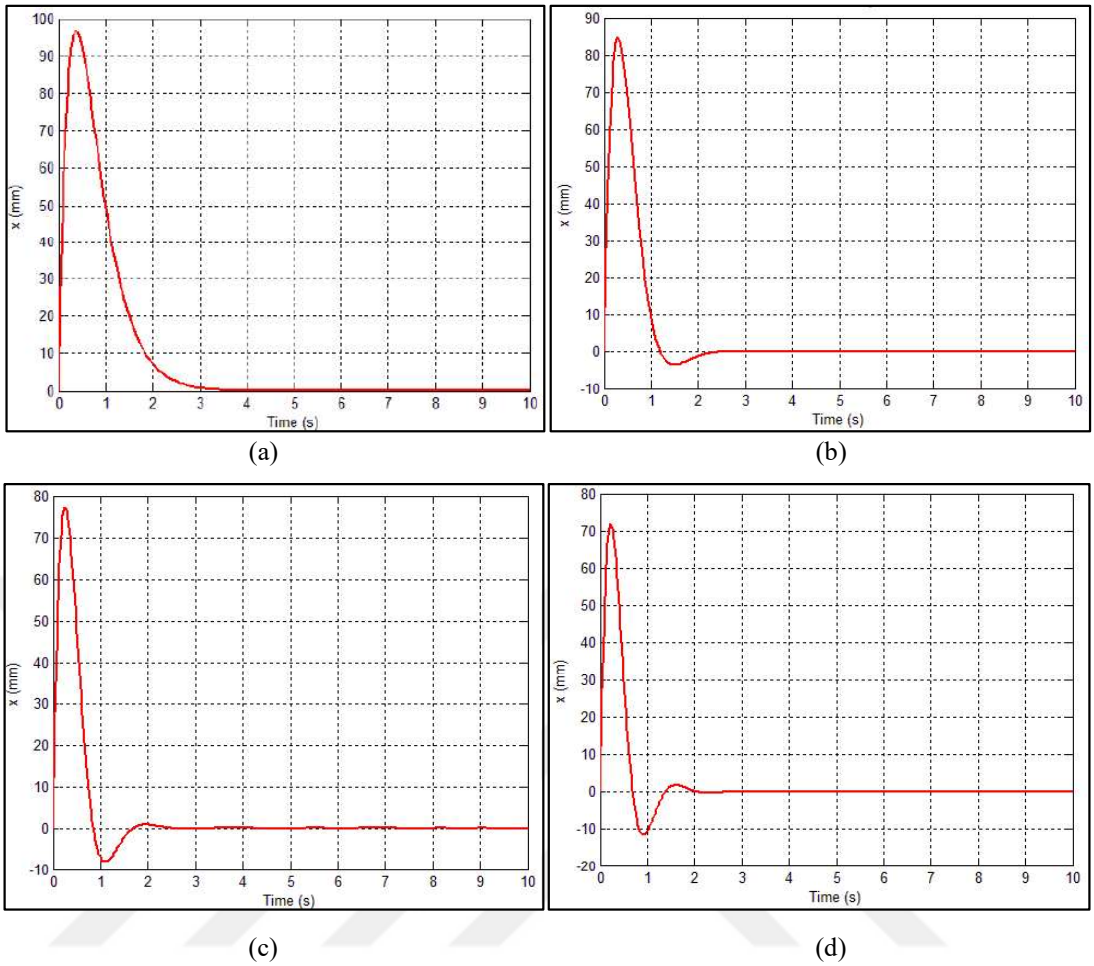

Figure 1.11 Barrel assembly dynamics with (a) 1 air spring, (b) 2 air springs, (c) 3 air springs, (d) 4 air springs [12]

Hassaan [13] has also studied recoil mechanism of 155 mm howitzer which has a hydraulic damper with nonlinear damping characteristic and helical spring with constant stiffness. Dynamic response of the barrel assembly to firing is investigated by using extremely nonlinear model for different firing angles and results are given in Figure 1.12. It is understood from the figure that increasing the firing angles increases maximum displacement and settling time of the barrel assembly.

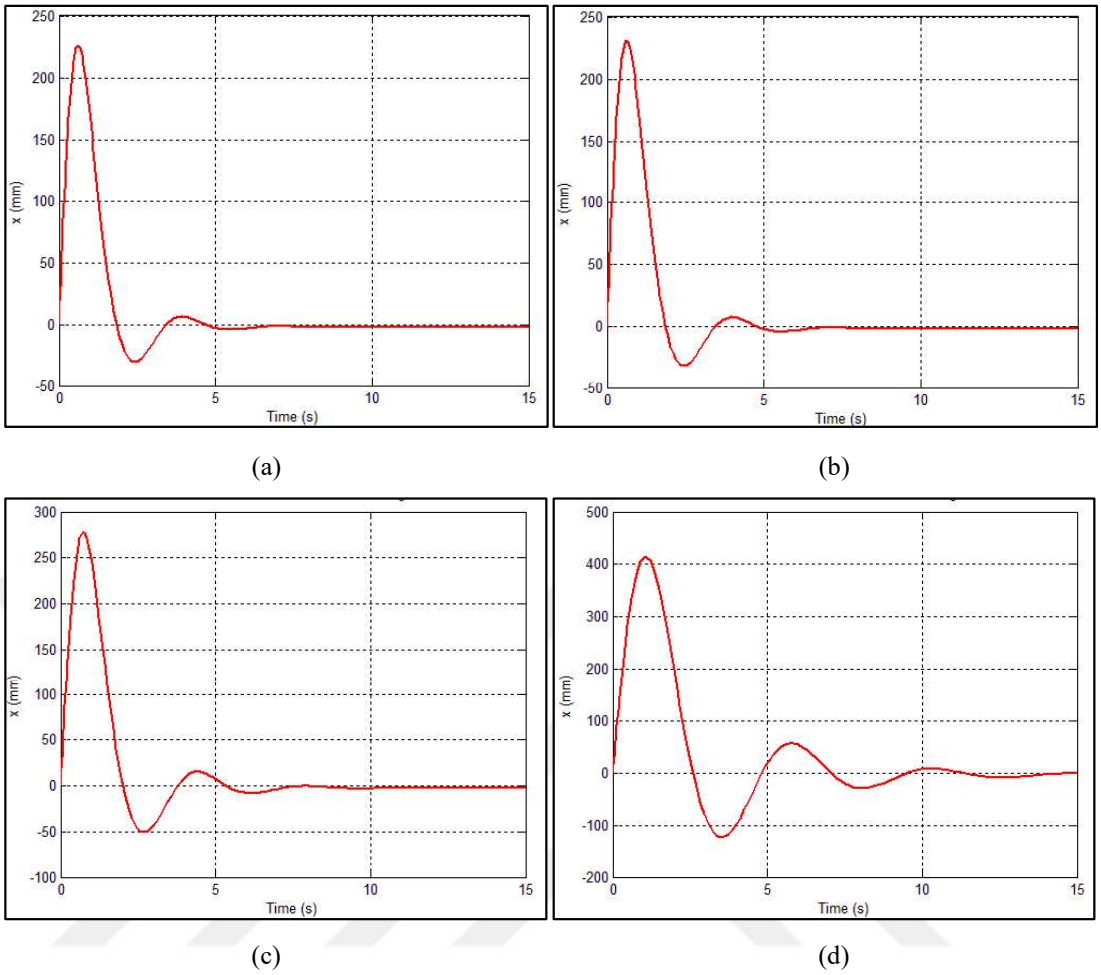

Figure 1.12 Dynamic response of barrel assembly at (a) 0°, (b) 10°, (c) 30°, (d) 50° [13]

Hassaan [14] has made another study on recoil mechanism of 155 mm howitzer which has hydraulic dampers and air springs and all of them have nonlinear characteristics. Dynamic response of the barrel assembly is investigated by using the same model for up to 4 number of elements and results are given in Figure 1.13. It is seen from the figure that increasing the number of recoil elements decreases the maximum recoil displacement and settling time of the barrel assembly.

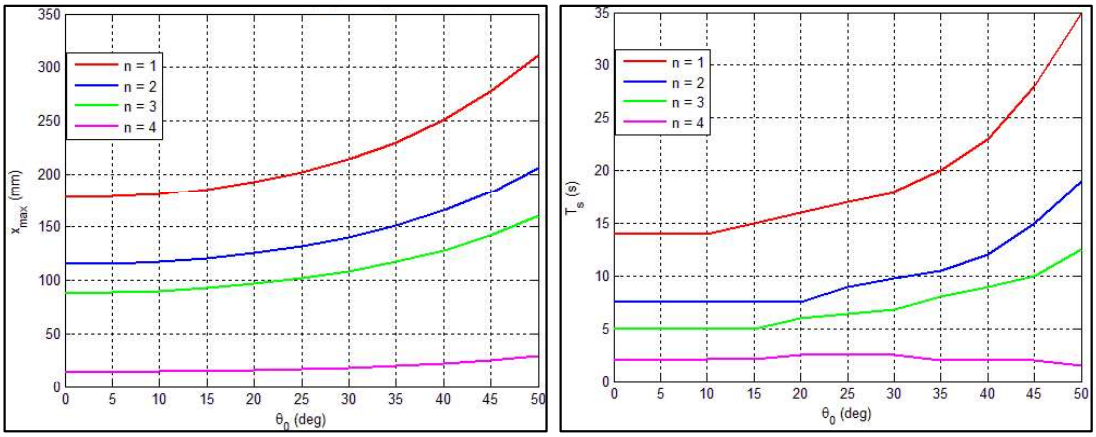

(a) (b)

Figure 1.13 (a) Maximum displacement and (b) settling time of barrel assembly [14]

Hajihosseinloo et al. [15] has investigated the performance of high energy gun recoil absorbers. An experimental setup that simulates gun reaction loads is prepared for measurements and a theoretical model which predicts recoil velocity and buffer pressure is built for calculations. Results from both experiments and model are compared and given in Figure 1.14. Additionally, it is explained in their study that discharge coefficient is very important for the buffer performance.

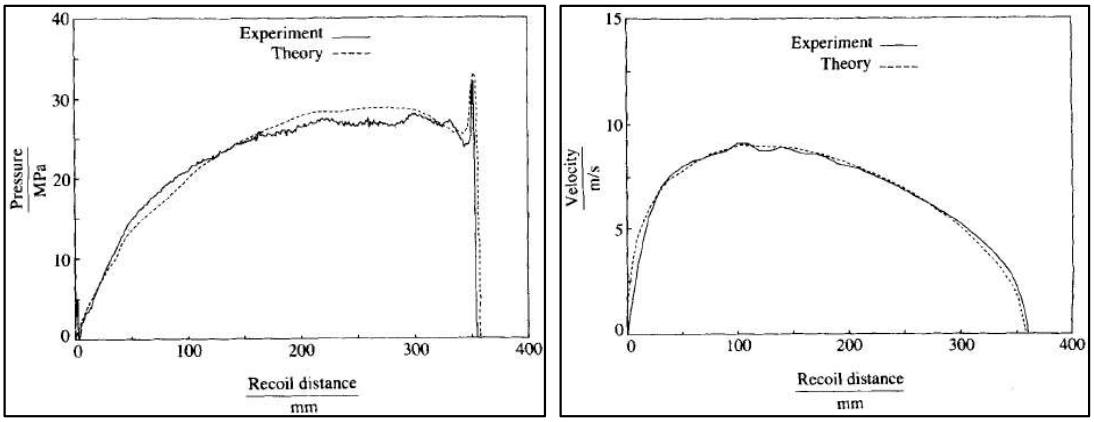

(a) (b)

Figure 1.14 Comparison of experimental and theoretical (a) buffer pressure, (b) buffer velocity [15]

Tiwari et al. [16] has improved a rigid body dynamics model and an experimental setup to investigate the effect of recuperator stiffness, recoil damping, tire stiffness and friction coefficient on recoil displacement. It is induced from the study that increasing recoil damping coefficient is the most effective way of decreasing recoil displacement.

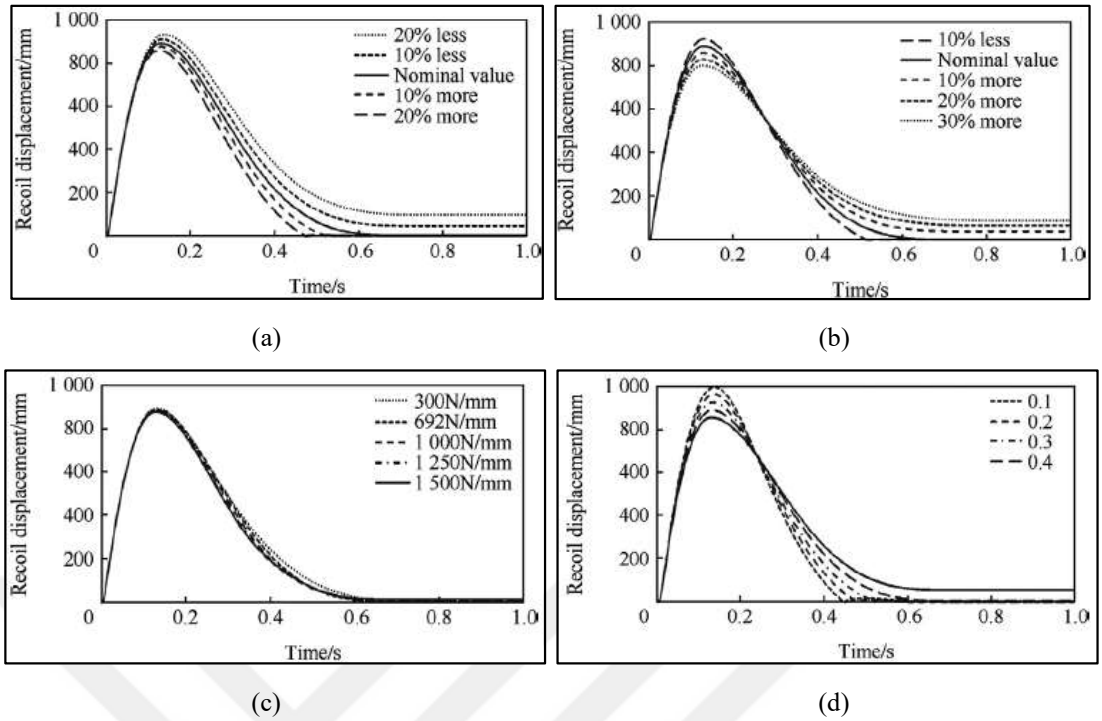

Figure 1.15 Effect of (a) recuperator stiffness, (b) recoil damping, (c) tire stiffness, (d) friction coefficient on recoil displacement [16]

Ahmadian and Poynor [17] has studied on recoil dynamics control by using magneto rheological dampers on 50 caliber BMG rifle. It is seen in Figure 1.16 that increasing damping force by increasing the applied current results in decrease in recoil stroke and increase in recoil force.

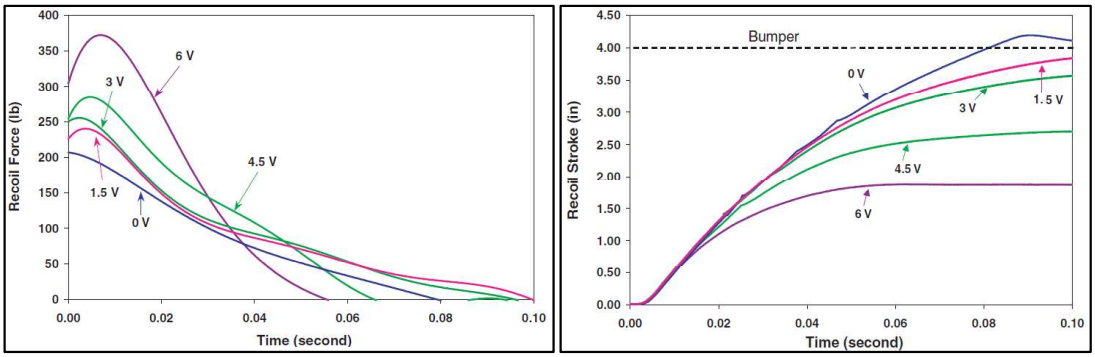

Figure 1.16 (a) Recoil force vs time and, (b) recoil stroke vs time [17]

Ahmadian et al. [18] has studied on recoil dynamics control of fire out-of-battery recoil systems by using magneto rheological dampers on dynamic simulation of 105 mm

cannon. Results show that hydraulic recoil dampers as effective as magneto rheological dampers under normal conditions. However, hydraulic dampers do not show good performance when firing faults occur.

Table 1.5 Simulation results [18]

	Impact momentum (force) at bumper [lb-s (lb)]		**Impact velocity at bumper (in-s)**	
	with MR damper	without MR damper	with MR damper	without MR damper
FOOB	0	0	0	0
Pre-fire	0	533 (2553)	0	76.2
Hang-fire	0	0	0	0
Misfire	0	1584 (135000)	0	226.5

Ahmadian et al. [19] has made a similar study about recoil dynamics control of fire out-of-battery recoil systems on larger calibers and obtain similar results. Magneto rheological dampers can remove the effects of fault modes that may occur fire out-of-battery recoil systems.

Table 1.6 Simulation results [19]

	Impact momentum (force) at bumper [kN-sec (kN)]		**Impact velocity at bumper (m/sec)**	
	with MR damper	without MR damper	with MR damper	without MR damper
FOOB	0	0	0	0
Pre-fire	0	2.37 (11.36)	0	1.94
Hang-fire	0	0	0	0
Misfire	0	7.05 (622.8)	0	5.75

Different types of modeling and simulating methods were used in literature and most of them validated by experimental results. However, all these studies have focused on one or limited number of parameters that affect the design of recoil mechanisms and there are not any studies on 105 mm light-weight howitzer. Therefore, there is a need for comprehensive model which includes all parameters and focus on new generation light weight artilleries.

1.4 Aim of The Study

The primary purpose of the study is to obtain the equation of motion for the recoiling parts in the weapon systems. For this purpose, the forces acting on the recoiling parts such as breech force, hydraulic brake force, recuperator force, and frictional forces are determined, and the effects of each force are examined. Additionally, an analytical

model that based on equation of motion is solved via MATLAB and results for recoil distance, breech force and projectile velocity are compared with experimental test data to validate the model.

Modeling and analysis of recoil motion is very important for designing recoil mechanisms and weapon systems accordingly. This kind of modeling can help designers to predict maximum recoil distance or determine some critical parameters such as orifice area, initial gas pressure etc. to stop recoiling parts in a specified recoil distance.

Additionally, studies in recent years have focused on decreasing the weight of weapon systems to improve mobility. These changes necessitate to make some modification in design of recoil mechanisms. The model that is validated in this study can be used to define what kind of change is necessary in which parameters.

CHAPTER 2

MATHEMATICAL MODELLING

In this chapter, equation of motion for recoiling parts of a hydropneumatic recoil mechanisms is obtained. Before beginning mathematical modelling, some assumptions that have applied are given below.

- The mathematical modelling is only focusing on recoil mechanism itself. It is assumed that recoil motion is not affected by external forces or disturbances such as vibration.
- The motion of supporting structure during firing is neglected and it is assumed as a rigid body with very small quantity of motion.
- Frictional resistance of packings and seals inside hydraulic and pneumatic cylinders is neglected due to that its magnitude is relatively small.

The model become simpler and the equation of motion for recoiling parts can be defined with these assumptions.

2.1 Equation of Motion

When a round is fired, very high internal ballistic pressure is formed in a short time and this induces recoiling parts to move backward. Recoil mechanism is used to stop this movement. Equation of motion for recoiling parts can be obtained by using one degree of freedom model (Figure 2.1).

From the Newton's second law of motion,

$$m_r\ddot{x} = B(t) - K(t) + W_r \sin\theta \tag{2.1}$$

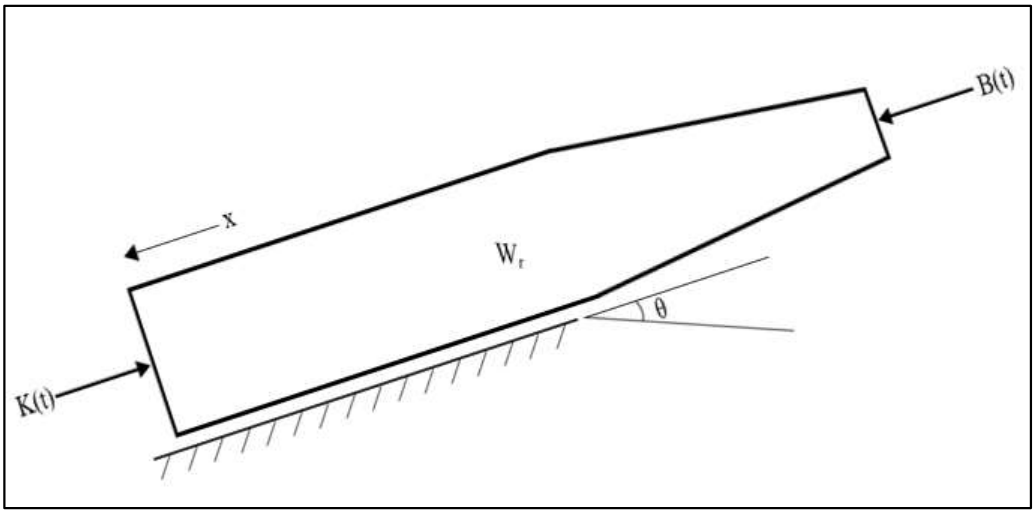

Figure 2.1 One degree of freedom model for recoiling parts

$B(t)$ represents breech force and is formed by internal ballistic pressure. This force initiates recoil movement and is active for very short period. $K(t)$ is the sum of resisting forces to recoil movement. W_r is the total weight of recoiling parts and θ is the firing angle. All forces that act on recoiling parts is investigated in following sections.

2.2 Breech Force

It is very important to develop a convenient analytical equation for estimating the breech force to obtain a realistic recoil mechanism design. It seems reasonable to start design studies with parameters that rarely vary such as peak chamber pressure and muzzle velocity. Breech force is analyzed for two time periods: in-bore and gas ejection.

2.2.1 In-Bore Period

A relation between breech force and projectile travel is firstly formed then using that relation other relations between breech force, projectile and recoiling parts' velocities, travel of projectile and time are developed. To do these LeDuc, an empirical equation, is used.

Velocity of projectile as a function of in-bore travel of the projectile according to LeDuc equation is given below [20]:

$$v' = \frac{a\,u}{b+u} \tag{2.2}$$

Where, v' is in-bore velocity of projectile (m/s), u is projectile travel in bore (m), a is LeDuc parameter (m/s) and b is LeDuc parameter (m).

LeDuc parameters are given as [3]:

$$a = v_0'(Q+1) \tag{2.3}$$

$$b = QU_0 \tag{2.4}$$

$$Q = \left(\frac{27}{16}\frac{P_M}{P_e} - 1\right) - \sqrt{\left(\frac{27}{16}\frac{P_M}{P_e} - 1\right)^2 - 1} \tag{2.5}$$

$$\frac{P_M}{P_e} = \frac{2gU_0P_MA}{v_0'^2\left(W_p + \frac{W_c}{2}\right)} \tag{2.6}$$

Where, v_0' is muzzle velocity of projectile (m/s), U_0 is tube length (m), P_M is peak chamber pressure (Pa), P_e is mean chamber pressure (Pa), g is gravity, A is bore area (m^2), W_p is weight of projectile (N) and W_c is weight of propellant charge (N).

Substitute the values of a and b into Eq 2.2:

$$v' = \frac{a\,u}{b+u} = \frac{v_0'(Q+1)u}{QU_0+u} \tag{2.7}$$

The relation between breech force and projectile travel is given below:

$$B = \left(\frac{W_p + \frac{W_c}{2}}{W_p}\right)F \tag{2.8}$$

$$F = \frac{W_p}{g}\left[\frac{a^2bu}{(b+u)^3}\right] \tag{2.9}$$

Substitute a, b and F into Eq. 2.8:

$$B = \left[\frac{\left(W_p + \frac{W_c}{2}\right)v_0'^2(Q+1)^2}{g}\right]\left[\frac{QU_0u}{(QU_0+u)^3}\right] \tag{2.10}$$

When $u = b/2 = QU_0/2$ maximum breech force occurs and Eq. 2.10 yields:

$$B_M = \frac{4}{27}\left[\frac{W_p+\frac{W_c}{2}}{g}\right]\frac{v_0'^2(Q+1)^2}{QU_0} \tag{2.11}$$

Where, B_M is maximum breech force (N).

Substitute Eq. 2.11 into Eq. 2.10:

$$B = B_M\left[\frac{27Q^2U_0^2u}{4(QU_0+u)^3}\right] \tag{2.12}$$

Besides breech force is obtained as a function of u, U_0, B_M and Q. LeDuc equation can also be used for projectile travel versus time relation.

$$v' = \frac{du}{dt} = \frac{a\,u}{b+u} \tag{2.13}$$

$$dt = \left(\frac{b+u}{au}\right)du \tag{2.14}$$

Integrating Eq. 2.14 with the boundary conditions at projectile exit $u = U_0$ and $t = t_0$:

$$t = t_0 - \left[\frac{b}{a}\ln\left(\frac{U_0}{u}\right) + \frac{U_0-u}{a}\right] = t_0 - \frac{QU_0\ln\left(\frac{U_0}{u}\right)+(U_0-u)}{v_0'(Q+1)} \tag{2.15}$$

Where, t_0 is time of projectile exit (s).

To find the t_0, an equation between impulse of the breech force and momentum of the recoiling parts is used.

$$B_e t_0 = \frac{W_r}{g}v_0 \tag{2.16}$$

Where, B_e is mean breech force (N), W_r is weight of recoiling parts (N) and v_0 is velocity of recoiling parts at $t = t_0$, projectile exit (s).

The relation between projectile velocity and velocity of recoiling parts is found from the equation below [21]:

$$v = \left(\frac{W_p+\frac{W_c}{2}}{W_r}\right)v' \tag{2.17}$$

Where, v' is in-bore velocity of projectile (m/s) and v is velocity of recoiling parts (m/s).

If the work done by mean breech force is equated to the work done by actual breech force:

$$B_e U_0 = \int_u^{U_0} B du \tag{2.18}$$

Substitute B from Eq. 2.12 into Eq. 2.18 and integrate:

$$B_e = \left(\frac{27}{8} B_M\right) \frac{Q}{(Q+1)^2} \tag{2.19}$$

Substitute Eq. 2.19 into Eq. 2.16:

$$t_0 = \frac{8 W_r v_0 (Q+1)^2}{27 g B_M Q} \tag{2.20}$$

Substitute Eq. 2.17 into Eq. 2.20:

$$t_0 = \frac{8\left(W_p + \frac{W_c}{2}\right) v_0' (Q+1)^2}{27 g B_M Q} \tag{2.21}$$

Eq. 2.7 and Eq. 2.12 can be used to find velocity of projectile and breech force respectively through the projectile travel.

2.2.2 Gas Ejection Period

After projectile leaves the barrel, propellant gases go out to the atmosphere passing through the muzzle. These gasses have significant momentum due to their high velocity and this momentum causes a backward movement on recoiling parts. Therefore, gas ejection period should be involved to modeling to estimate recoil dynamics.

To make the calculations of gas ejection period, time of projectile exit t_0 and velocity of free recoil v_0 are obtained from Eq. 2.21 and Eq. 2.17 as initial conditions.

Since $u = U_0$ at projectile exit, Eq. 2.10 is reduced to:

$$B_0 = P_0 A = \left[\frac{\left(W_p + \frac{W_c}{2}\right) v_0'^2 Q}{g U_0 (Q+1)}\right] \tag{2.22}$$

Where, B_0 is breech force at time t_0 (N), P_0 is breech pressure at time t_0 (Pa).

The absolute velocity of recoiling parts [21]:

$$v = \frac{dx}{dt} \tag{2.23}$$

Where, x is absolute travel of recoiling parts, (m).

Forward projectile displacement is represented by u and u is relative to the tube that moves backward a distance x with the recoiling parts. So the absolute displacement of the projectile is $u - x$.

$$v' = \frac{d}{dt}(u - x) \tag{2.24}$$

When at time $t = 0$, $x = 0$ and $u = 0$, substitute Eq. 2.23 and Eq. 2.24 into Eq. 2.17 and then integrate:

$$W_r x = \left(W_p + \frac{W_c}{2}\right)(u - x) \tag{2.25}$$

At projectile exit $u = U_0$, recoil travel at projectile exit is:

$$x_0 = \left(\frac{W_p + W_c/2}{W_r + W_p + W_c/2}\right) U_0 \tag{2.26}$$

Where, x_0 is recoil travel at projectile exit (m).

The barrel is assumed as a convergent-divergent nozzle and the process is assumed to be adiabatic and the propellant gas is a perfect gas. The velocity of gas μ is obtained from energy and continuity equations together with these assumptions [21].

$$\mu = \sqrt{\frac{2\gamma}{\gamma - 1} R (T_b - T)} \tag{2.27}$$

Where, μ is velocity of gases in bore (m/s), γ is ratio of specific heats, R is gas constant (J/kg.K), T is gas temperature in bore (K), T_b is gas temperature at breech (K).

RT_b is one of the propellent characteristics and it is called specific impetus. $RT_b/(\gamma-1)$ is a known property that represents the potential energy of unit mass of propellant.

Breech pressure can be calculated from the equation below [21]:

$$P_b = P_0\left(1+\frac{t-t_0}{\phi}\right)^{2\gamma/(1-\gamma)} \tag{2.28}$$

$$P_0 = \frac{W_c R T_0}{g\Delta} \tag{2.29}$$

$$\phi = \frac{2\Delta}{A(\gamma-1)}\left[\frac{W_c}{g\gamma P_0 \Delta}\left(\frac{\gamma+1}{2}\right)^{(\gamma+1)/(\gamma-1)}\right]^{1/2} \tag{2.30}$$

where, P_0 is breech pressure at projectile exit (Pa), T_0 is gas temperature in breech at time t_0 (K), ϕ is duration of gas ejection period (s), Δ is chamber volume plus bore volume (m^3).

A correction from literature is applied to Eq. 2.29 and a more complicated model is obtained [21].

$$P_0 = \frac{W_c R T_0}{g\Delta}\left(1+\frac{W_c}{6W_p}\right) \tag{2.31}$$

When substitute Eq. 2.31 into Eq. 2.28 and Eq. 2.30:

$$P_b = \frac{W_c R T_0}{g\Delta}\left(1+\frac{W_c}{6W_p}\right)\left(1+\frac{t-t_0}{\phi}\right)^{2\gamma/(1-\gamma)} \tag{2.32}$$

$$\phi = \frac{2\Delta}{A(\gamma-1)}\left[\frac{1}{\gamma R T_0\left(1+\frac{W_c}{6W_p}\right)}\left(\frac{\gamma+1}{2}\right)^{(\gamma+1)/(\gamma-1)}\right]^{1/2} \tag{2.33}$$

It should be noted that W_c is much less than $6W_p$ which means the correction is very small.

To find the momentum G that applied to the breech by the propellant gases after projectile leaves the barrel during gas ejection period without a muzzle brake, the equation below should be integrated.

$$G = \int_{t_0}^{\infty} AP_b dt \tag{2.34}$$

$$= \frac{AW_c RT_0}{g\Delta}\left(1 + \frac{W_c}{6W_p}\right)\int_{t_0}^{\infty}\left(1 + \frac{t-t_0}{\phi}\right)^{2\gamma/(1-\gamma)} dt$$

$$= \frac{W_c}{g}\left(1 + \frac{W_c}{6W_p}\right)^{1/2}(RT_0)^{1/2}\left(\frac{2}{\gamma+1}\right)\left[\frac{1}{\gamma}\left(\frac{\gamma+1}{2}\right)^{(\gamma+1)/(\gamma-1)}\right]^{1/2}$$

Where, G is momentum imparted to the breech during gas ejection without a muzzle brake (kg.m/s).

When $\gamma = 1.26$ is assumed according to literature and using $W_c \ll 6W_p$, Eq. 2.34 yields [22];

$$G = 1.34\frac{W_c}{g}\left(1 + \frac{W_c}{12W_p}\right)\sqrt{RT_0} \tag{2.35}$$

Kinetic energy of the projectile and charge at muzzle should be equal to energy given by propellant and T_0 can be found from that equation.

$$\frac{W_c}{g(\gamma-1)}R(T_b - T_0) = \frac{1}{2}\left(m_{p_{eff}} + m_{c_{eff}}\right)v_0'^2 \tag{2.36}$$

where, $m_{p_{eff}} = \frac{(1+k)W_p}{g}$ is effective mass of projectile, (kg), $m_{c_{eff}} = \frac{W_c}{3g}$ is effective mass of charge, (kg) and k is fraction of heat loss from propellant gases to tube ($k \approx 1/7$) [21, 22].

From using these effective masses together with k and γ values, the equation below is obtained.

$$RT_0 = RT_b - \left(0.0433 + 0.1486\frac{W_p}{W_c}\right)v_0'^2 \tag{2.37}$$

Substitute Eq. 2.37 into Eq. 2.35:

$$G = 1.34\frac{W_c}{g}\left(1 + \frac{W_c}{12W_p}\right)\sqrt{RT_b - \left(0.0433 + 0.1486\frac{W_p}{W_c}\right)v_0'^2} \tag{2.38}$$

To find gas ejection period substitute Eq. 2.28 into Eq. 2.34 and integrate Eq. 2.30.

$$G = \int_{t_0}^{\infty} AP_b dt = AP_0 \int_{t_0}^{\infty} \left(1 + \frac{t-t_0}{\phi}\right)^{2\gamma/(1-\gamma)} dt = B_0 \phi \left(\frac{\gamma-1}{\gamma+1}\right) \quad (2.39)$$

Where, B_0 is breech force at muzzle.

$\gamma = 1.26$ is applied on Eq. 2.39.

$$\phi = \left(\frac{\gamma+1}{\gamma-1}\right)\frac{G}{B_0} = \frac{8.7G}{B_0} \quad (2.40)$$

Breech force due to the propellant gasses during gas ejection period is found from Eq. 2.28. And an efficiency factor that shows the effect of muzzle brake is accounted to determine the force on the recoiling parts.

$$B = (1-\beta)P_b A = (1-\beta)AP_0 \left(1 + \frac{t-t_0}{\phi}\right)^{2\gamma/(1-\gamma)} \quad (2.41)$$

The acceleration of the recoiling parts is determined from equation of motion.

$$a = \frac{g(1-\beta)B_0}{W_r}\left(1 + \frac{t-t_0}{\phi}\right)^{2\gamma/(1-\gamma)} \quad (2.42)$$

Integrating Eq. 2.42:

$$v = v_0 + \frac{g(1-\beta)B_0\phi}{W_r\left(\frac{\gamma+1}{1-\gamma}\right)}\left[\left(1 + \frac{t-t_0}{\phi}\right)^{(\gamma+1)/(1-\gamma)} - 1\right] \quad (2.43)$$

$\gamma = 1.26$ is applied on Eq. 2.43.

$$v = v_0 + \bar{k}\left[1 - \left(1 + \frac{t-t_0}{\phi}\right)^{-8.7}\right] \quad (2.44)$$

Where,

$$\bar{k} = \frac{Gg}{W_r}(1-\beta) \quad (2.45)$$

Integrating Eq. 2.44:

$$x = x_0 + (v_0 + \bar{k})(t-t_0) + \frac{\phi\bar{k}}{7.7}\left[\left(1 + \frac{t-t_0}{\phi}\right)^{-7.7} - 1\right] \quad (2.46)$$

$\gamma = 1.26$ is applied on Eq. 2.41

$$B = (1-\beta)AP_0\left(1+\frac{t-t_0}{\phi}\right)^{-9.69} \tag{2.47}$$

When t approaches ∞, B approaches zero. But B is never zero for any time. When $t - t_0 = \phi$, the value in parenthesis will be $2^{-9.69}$ which is very small. Therefore, B is assumed zero for practical purposes. Since the gas ejection period is assumed to be ended at $t - t_0 = \phi$:

$$t_f = t_0 + \phi \tag{2.48}$$

Where, t_f is time at end of recoil force or end of gas ejection period (s).

Likewise:

$$P_f = 0.0012\ P_0 \text{ (from Eq. 2.28)} \tag{2.49}$$

$$v_f = v_0 + \bar{k} \quad \text{(from Eq. 2.44)} \tag{2.50}$$

$$x_f = x_0 + \left(v_0 + \bar{k}\right)\phi \quad \text{(from Eq. 2.46)} \tag{2.51}$$

2.2.3 Muzzle Brake

The role of muzzle brake is to use some of the propellant gases' kinetic energy to decrease the backward motion of recoiling parts. Therefore, a muzzle brake contributes to have effective retarding force.

A muzzle brake contains many baffles that are completely or nearly perpendicular to barrel axis. Thus, the direction of the propellant gas flow causes a forward impulse on the tube and this decreases the recoil momentum.

The muzzle brake force can be calculated from the equation below [23]:

$$K_m = \beta P_b A \tag{2.52}$$

Where, K_m is muzzle brake force (N), $\beta = \lambda\gamma\left(\frac{2}{\gamma+1}\right)^{\gamma/(\gamma-1)}$ is muzzle brake efficiency factor and λ is speedup factor. The speedup factor is dependent to geometry of the muzzle brake.

The net momentum tranferred to recoiling parts is:

$$\int_0^\infty (B - K_m)\, dt = A(1-\beta)\int_0^\infty P_b\, dt = G(1-\beta) \tag{2.53}$$

To understand (1-β) better, it is given as a ratio below:

$$(1-\beta) = \frac{\begin{array}{c}impulse\ applied\ to\ recoiling\ parts\ during\\ gas\ ejection\ period\ with\ a\ muzzle\ brake\end{array}}{\begin{array}{c}impulse\ applied\ to\ recoiling\ parts\ during\\ gas\ ejection\ period\ without\ a\ muzzle\ brake\end{array}} \tag{2.54}$$

β is determined from the geometry of muzzle brake. If there is no muzzle brake then β equals zero. If the flow of gases completely reversed which is not possible then β equals two. It is convenient to take β value between 0.3 and 1.5.

2.3 Weight Force

A gravitational force occurs depending on the firing angle due to the weight of recoiling parts. Angle between recoiling parts and horizontal is constant so this force is constant and sin component of this force ($W_r \sin\theta$) is added to equation of motion.

2.4 Net Retarding Force

There are three main forces that contribute the net retarding force. These forces are listed below and a curve that shows the magnitute of these forces is also given in Figure 2.2.

- Recuperator Force
- Frictional Forces
- Hydraulic Brake Force

In that curve, F_R is recuperator force, R represents frictional forces an H is hydraulic brake force. Hydraulic brake force makes the biggest contribution to net retarding

forces while frictional forces make the smallest contribution. It can be said based on experiences that frictional force is only between 3-7 % of total retarding force [24]. Therefore, neglecting frictional effects of packings and seals seems reasonable to make calculations easier.

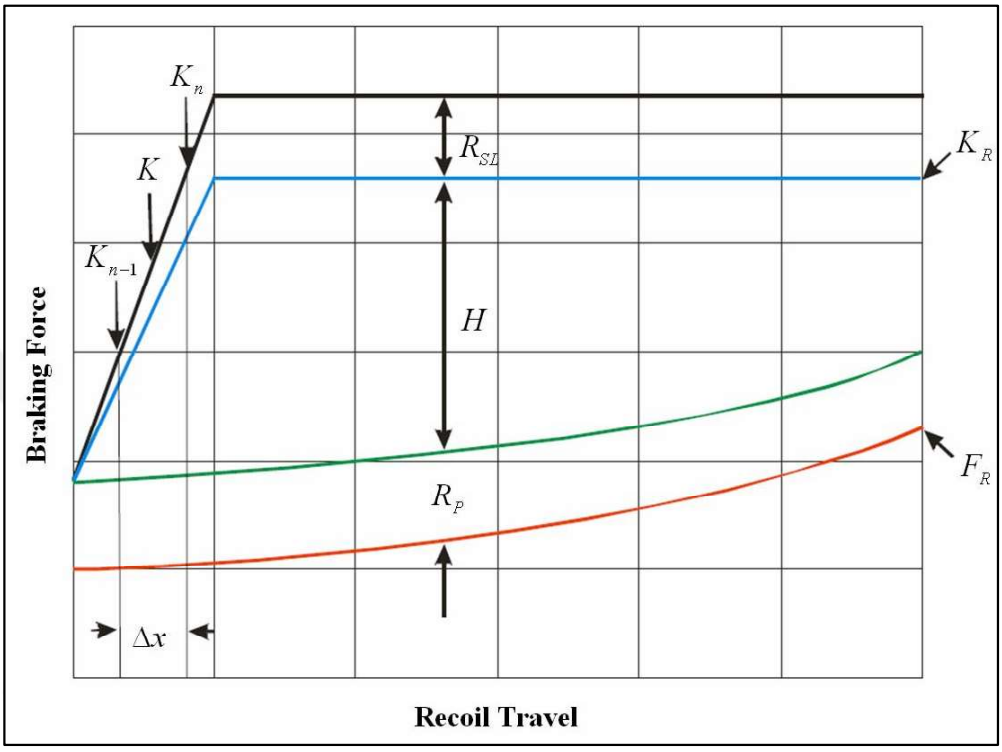

Figure 2.2 Forces contributing net retarding force [5]

There are several assumptions that are made during net retarding force calculations and these are:

- Compression and expansion processes of the gas inside recuperator cylinder are adiabatic and gas is ideal.
- Coefficient of friction is constant.
- Flow inside hydraulic cylinder is quasi-steady, incompressible, inviscid and one directional.

All these forces that form total resisting force to recoil motion are calculated as a function of recoil distance or time. Thus, equation of motion for recoiling parts can be obtained.

2.4.1 Recuperator Force

The main purpose of the gas inside the recuperator cylinder is to store energy during recoil and bring the weapon system back in battery position by using this stored energy. The force that is formed during recoil by compression of gas or spring is called recuperator force and contributes to net retarding force against recoil motion. Behavior of spring and gas as recuperator is different from each other and it is shown in Figure 2.3.

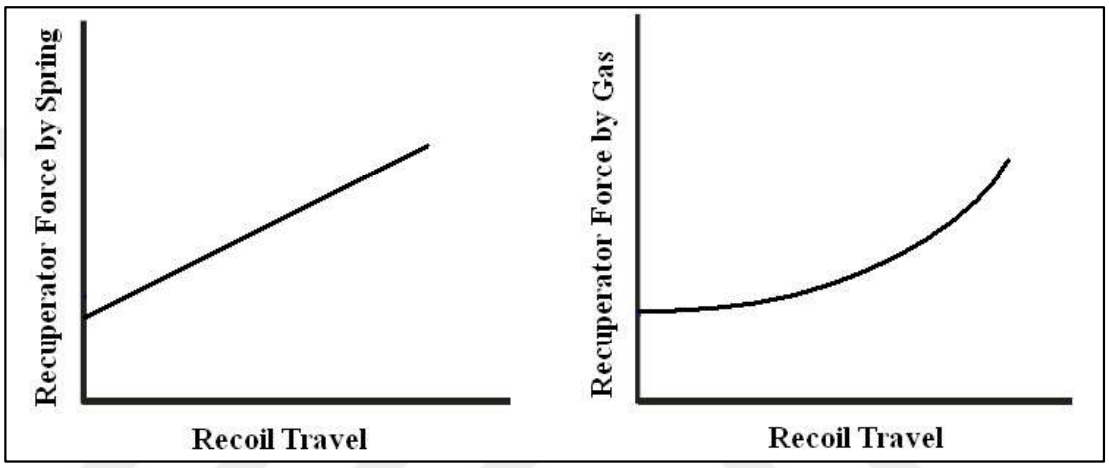

Figure 2.3 Spring and gas recuperator behaviors [5]

Weapon system that is studied has hydropneumatic recoil mechanism with gas recuperator. Compression and expansion processes of the gas are assumed polytropic and recuperator force can be calculated from equation below.

$$P\,V^n = constant \tag{2.55}$$

Where, P is gas pressure (Pa), V is gas volume (m^3) and n is ratio of specific heats.

Nitrogen is used in recuperator cylinder for most of the recoil mechanisms and 1.4 can be used as its ratio of specific heats. Eq. 2.55 can be rewritten below during recoil.

$$P_0 V_0^n = P_x V_x^n$$

$$P_x = P_0 (P_0/V_x)^n \tag{2.56}$$

Where, P_0 is gas pressure at in-battery position (Pa), V_0 is gas volume at in-battery position (m^3), P_x is gas pressure at any recoil distance x (Pa) and V_x is gas volume at any recoil distance x (m^3).

V_x is given as,

$$V_x = V_0 - \Delta V_x \tag{2.57}$$

Where ΔV_x is the change in gas volume (m^3) and is calculated from the equation below.

$$\Delta V_x = A_R x_R \tag{2.58}$$

Where, A_R is recuperator cylinder area (m^2) and x_R is control piston rod displacement (m).

Gas pressure and gas volume at in-battery position and at any recoil distance can be calculated from Eq.2.56, 2.57 and 2.58. Then, recuperator force is obtained from the equation below.

$$K_a = A_R P_x = A_R P_0 . \left(\frac{V_0}{V_0 - A_R x_R}\right)^{1.4} \tag{2.59}$$

Definition of minimum and maximum initial gas pressure has significant importance. Minimum initial gas pressure value must satisfy that recuperator force at the end of recoil is bigger than the weight of recoiling parts and friction to bring weapon system back to initial position. Additionally, maximum initial gas pressure should not be very high to avoid slamming at the end of counterrecoil motion and should not go over the limit of sealings.

2.4.2 Frictional Forces

There are two different frictional forces in recoil mechanisms, and these are:

- Frictional resistance of bearings

- Frictional resistance of riffling torque

2.4.2.1 Frictional Resistance of Bearings

Bearing frictional forces occur between sliding surfaces which are recoiling parts and cradle. Figure 2.4 is used to calculate frictional resistance of bearings.

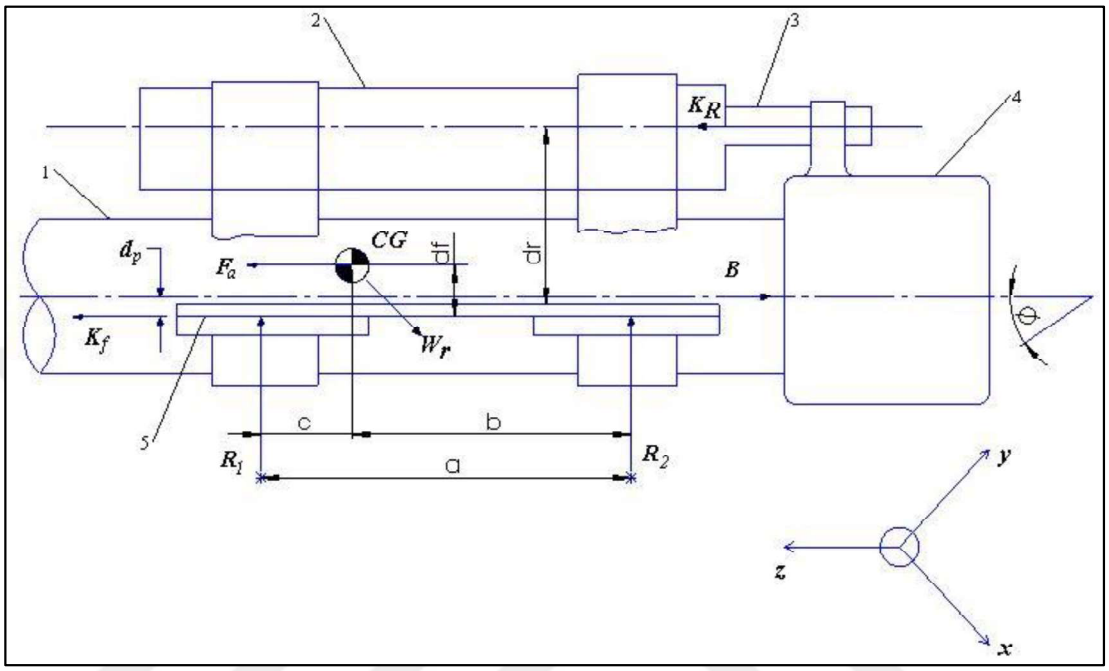

Figure 2.4 Forces and reaction on recoiling parts [8]

R_1 can be calculated from the equation below.

$$R_1 a + B d_p + (W_r \sin\theta) d_f = K_R d_r + (W_r \cos\theta) b + F_a d_f \tag{2.60}$$

$$R_1 = \left(\frac{d_r}{a}\right) K_R + \left(\frac{b}{a}\right) W_r \cos\theta + \frac{d_f}{a}(F_a - W_r \sin\theta) - \left(\frac{d_p}{a}\right) B \tag{2.61}$$

Where, R_1 and R_2 are reaction forces (N), K_R is rod pull (N), F_a is inertial force due to acceleration of recoiling parts (N), d_r is distance between cradle slide and recoil cylinder (m), a is distance between bearings (m), b is distance between CG and rear bearing about which moments are taken (m), d_f is depth of bearing from CG (m) and d_p is depth of bearing from tube centerline (m).

F_a is obtained from Eq. 2.62.

$$F_a = B + W_r \sin\theta - K \tag{2.62}$$

Where, K is total resistance force and is given as follows.

$$K = K_R + K_f \tag{2.63}$$

Where, K_f is friction force of bearings or slides.

$$K_f = \mu(|R_1| + |R_2|) \tag{2.64}$$

The relation between R_1 and R_2 is,

$$R_2 = W_r \cos\theta - R_1, \quad R_1 < W_r \cos\theta \tag{2.65}$$

$$R_2 = R_1 - W_r \cos\theta, \quad R_1 > W_r \cos\theta \tag{2.66}$$

Substitute Eq. 2.65 and Eq. 2.66 into Eq. 2.64.

$$K_f = \mu(W_r \cos\theta) \tag{2.67}$$

2.4.2.1 Frictional Resistance of Riffling Torque

Another force can be considered is riffling torque which is produced by the projectile riffling and Figure 2.5 is used to calculate this force.

$$F_r' = \frac{T_r}{d_r} \tag{2.68}$$

Where, T_r is rifling torque, (Nm), F_r' is normal force (N) and d_r is distance between supports (m).

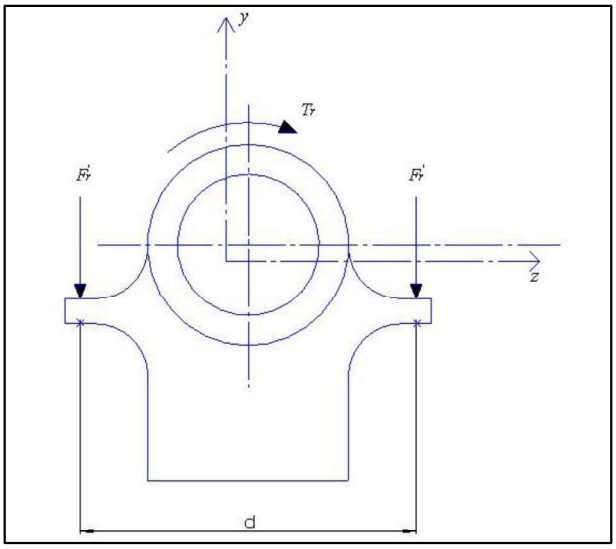

Figure 2.5 Cross section through barrel [8]

The linear acceleration a of a projectile is given as:

$$a = \frac{B(t)}{m_p + 0.5m_c} \tag{2.69}$$

The peripheral acceleration a_t of projectile in the bore is:

$$a_t = a \tan \theta_r = \frac{\pi\, B(t)}{N_r(m_p + 0.5m_c)} \tag{2.70}$$

Where, θ_r is helix angle of rifling (rad) and N_r is twist of rifling, calibers per turn.

The angular acceleration α is given as:

$$\alpha = \frac{a_t}{R_b} = \frac{\pi\, B(t)}{N_r R_b(m_p + 0.5m_c)} \tag{2.71}$$

Where, R_b is radius of bore (m).

The rifling torque T_r is,

$$T_r = I_p \alpha \tag{2.72}$$

$$I_p = m_p k^2 \tag{2.73}$$

Where, I_p is mass moment of inertia of projectile (kg/m^2) and k is radius of gyration of projectile (m).

Substitution of Eq. 2.71 and Eq. 2.73 into Eq. 2.72 yields:

$$T_r = \frac{\pi m_p k^2 B(t)}{N_r R_b (m_p + 0.5 m_c)} \tag{2.74}$$

Substituting Eq. 2.74 into Eq. 2.68 with $k = 0.74 R_b$ yields:

$$F_r' = \frac{0.5476 \pi m_p R_b B(t)}{N_r (m_p + 0.5 m_c) d_r} \tag{2.75}$$

The frictional force due to riffling torque is obtained from the equation below.

$$f_r' = \mu \, 2F_r' \tag{2.76}$$

Total frictional force is the sum of Eq. 2.67 and 2.76.

$$F_f = K_f + f_r' = \mu (W_r \cos\theta) + \mu \, 2F_r' \tag{2.78}$$

Frictional force due to riffling torque is very small comparing to friction force of bearings and can be neglected. Hence Eq.2.78 is reduced to Eq. 2.79.

$$F_f = K_f = \mu (W_r \cos\theta) \tag{2.79}$$

2.4.3 Hydraulic Brake Force

During recoil, hydraulic fluid is forced to flow through orifices by piston inside the hydraulic cylinder. While piston moves, hydraulic fluid causes a resistance to this motion and this resistive force is called hydraulic brake force. This force is calculated from the pressure difference between two sides of the effective piston area.

$$F_0 = (P_h - P_l) \, A_p = \Delta P \, A_p \tag{2.80}$$

Where, F_0 is hydraulic brake force (N), $P_h$is pressure in high pressure chamber (Pa), P_l is pressure in low pressure chamber (Pa) and A_p is effective area of the piston (m^2). Pressure difference between high and low pressure chambers are calculated from the equation below:

$$\Delta P = \frac{A^2 v^2 \rho}{2C_0^2 a_0^2} \tag{2.81}$$

Where, A is cross section area of cylinder (m^2), v is velocity of piston or in other words velocity of recoil (m/s), ρ is fluid density (kg/m^2), C_0 is orifice discharge coefficient and a_0 is average area of orifice (m^2).

Substitute Eq. 2.81 into Eq. 2.80 gives the equation for hydraulic brake force.

$$F_0 = \frac{A^2 v^2(x) \rho A_p}{2C_0^2 a_0^2} \tag{2.82}$$

Net retarding force equals the summation of recuperator force, frictional force and hydraulic brake force.

$$K = K_a + K_f + F_0 \tag{2.83}$$

Subtitute Eq. 2.59, Eq. 2.79 and Eq. 2.82 into Eq.2.83.

$$K = \mu W_r \cos\theta + A_R P_0 . \left(\frac{V_0}{V_0 - A_R x_r}\right)^{1.4} + \left(\frac{A^2 v^2(x) \rho A_p}{2C_0^2 a_0^2}\right) \tag{2.84}$$

Additionally, total breech force equals to summation of breech forces of in-bore and gas ejection periods which are Eq. 2.10 and 2.47. If muzzle brake efficiency factor is assumed 1, total breech force is obtained from the equation below.

$$B(t) = \left[\frac{\left(W_p + \frac{W_c}{2}\right) v_0'^2 (Q+1)^2}{g}\right] \left[\frac{QU_0 u}{(QU_0 + u)^3}\right] + AP_0 \left(1 + \frac{t - t_0}{\phi}\right)^{-9.69} \tag{2.85}$$

Substitution of Eq. 2.84 and Eq. 2.85 into Eq. 2.1 gives the equation of motion for recoiling parts.

$$m\ddot{x} = \left[\frac{\left(W_p + \frac{W_c}{2}\right) v_0'^2 (Q+1)^2}{g}\right] \left[\frac{QU_0 u}{(QU_0 + u)^3}\right] + AP_0 \left(1 + \frac{t - t_0}{\phi}\right)^{-9.69} +$$

$$W_r \sin\theta - \mu W_r \cos\theta - A_R P_0 . \left(\frac{V_0}{V_0 - A_R x_r}\right)^{1.4} - \left(\frac{A^2 v^2(x) \rho A_h}{2C_0^2 a_0^2}\right) \tag{2.86}$$

2.5 Numerical Solution

Runge-Kutta Method (RKM) which is included in Forward Euler Method (FEM) is used to solve Eq. 2.86. A numerical solution approaches to exact solution when the step size approaches zero. Therefore, time step is chosen as 10^{-5} second and the equation is solved by using MATLAB.

FEM is a method for solving ordinary differential equations by using the formula below.

$$y_{n+1} = y_n + h\, f(x_n, t_n) \tag{2.87}$$

FEM is based on Taylor series expansion.

$$y(t_n + h) \equiv y_{n+1} = y(t_n) + h \frac{d_y}{d_t}\Big|_{t_n} + O(h^2)$$

$$= y_n + h\, f(x_n, y_n) + O(h^2) \tag{2.88}$$

It is understood from Eq. 2.88 that an error occurs for each time step and it is local truncation errror. Local truncation error is $O(h^2)$ for this method, so it is first order technique.

Runge-Kutta methods are a class of methods which use the information on the slope at more than one point to extrapolate the solution to the future time step. One of the most common methods for the solution of initial value problems and used in this study is forth order Runge Kutta technique and it is given below.

$$y_{n+1} = y_n + (k_1 + 2k_2 + 2k_3 + k_4)/6 \tag{2.89}$$

The system in our model consists of breech force for in bore and gas ejection periods, weight force and net retarding force that includes frictional force, recuperator force and hydraulic brake force. Additionally main outputs of the model are accleration, velocity and recoil displacement of the recoiling parts. Figure 2.6 shows the flowchart of the model.

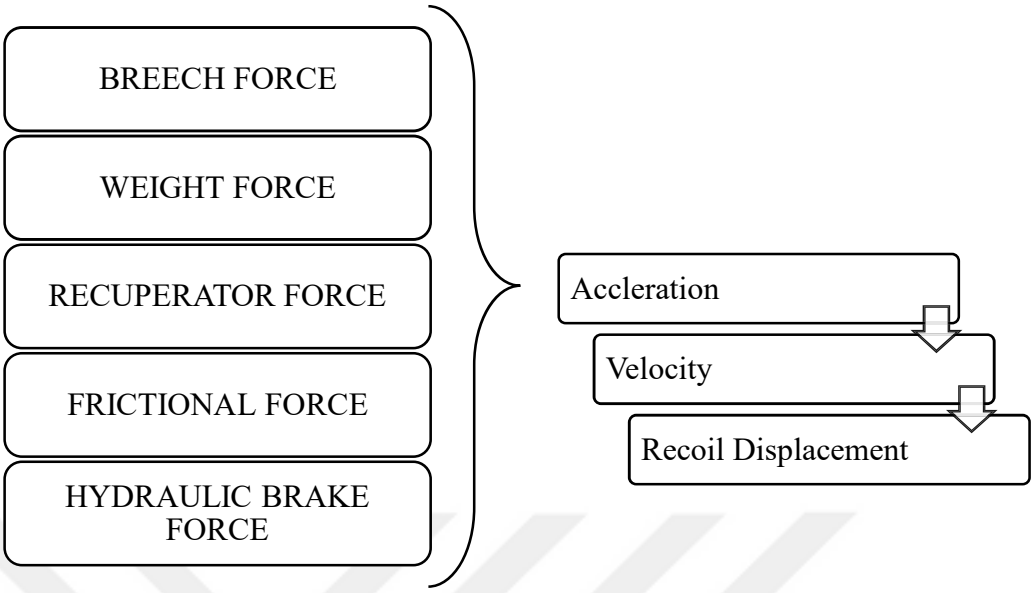

Figure 2.6 Flowchart of the model

CHAPTER 3

RESULTS AND DISCUSSION

The model is solved, and results are compared with the data that are obtained from firing tests. Firing test data are belong to 105 mm howitzer weapon systems. Most of these data are taken from Mechanical and Chemical Industry (MKEK) Company Heavy Weapons and Steel Factory and some of them are taken from literature [25].

3.1 Breech Force

Breech force calculations should include in-bore and gas ejection period together. Although most of the breech force is formed in-bore period, gas ejection period has also some effects on recoil movement and should be considered.

Total breech force change in one round cycle is necessary to solve equation of motion for recoiling parts. Therefore, breech force for in-bore period is calculated firstly from the model for two 105 mm weapon systems. The model is validated by comparing results with test data. After the model is verified, breech force for gas ejection period is also calculated and total breech force is obtained from the model for new generation 105 mm howitzer.

3.1.1 In-Bore Period

Results are obtained from the model are compared with two different firing test data. Firstly, Figure 3.1 shows the comparison of model results and a typical 105 mm howitzer firing test data from literature.

It is obviously seen from the Figure 1 that calculated results from the model and measured data from firing tests are compatible with each other. Peak breech force is about 2 MN for both measured and calculated results.

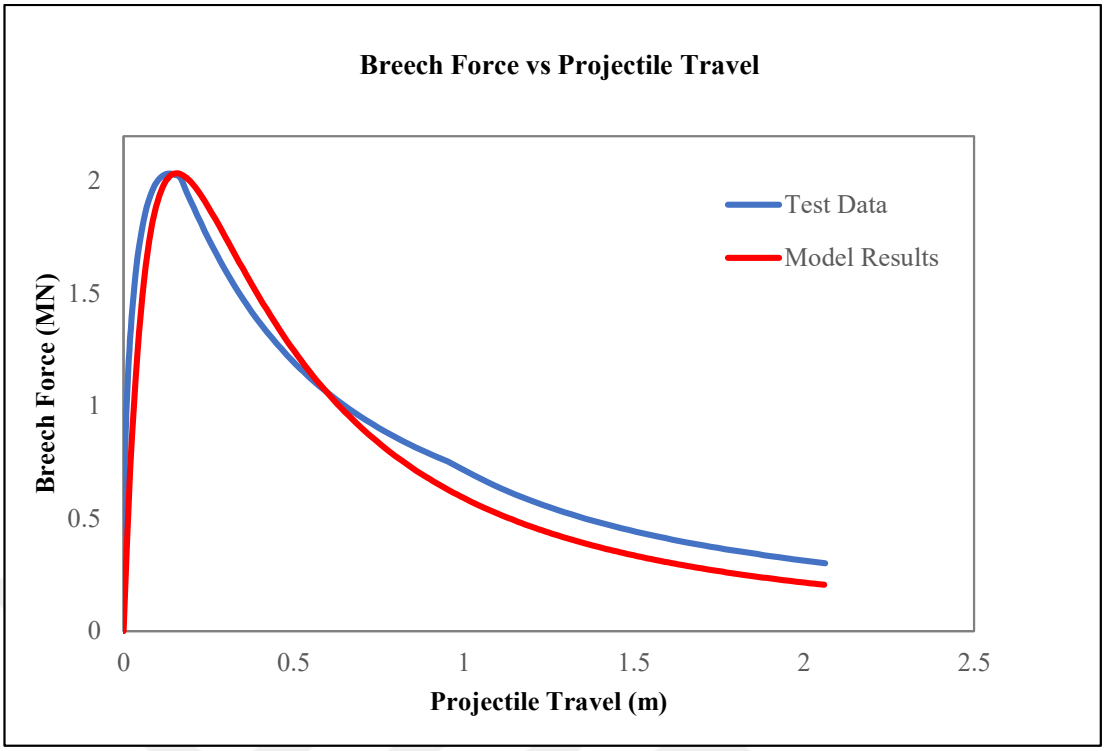

Figure 3.1 Comparison of model results and test data from literature for breech force vs projectile travel

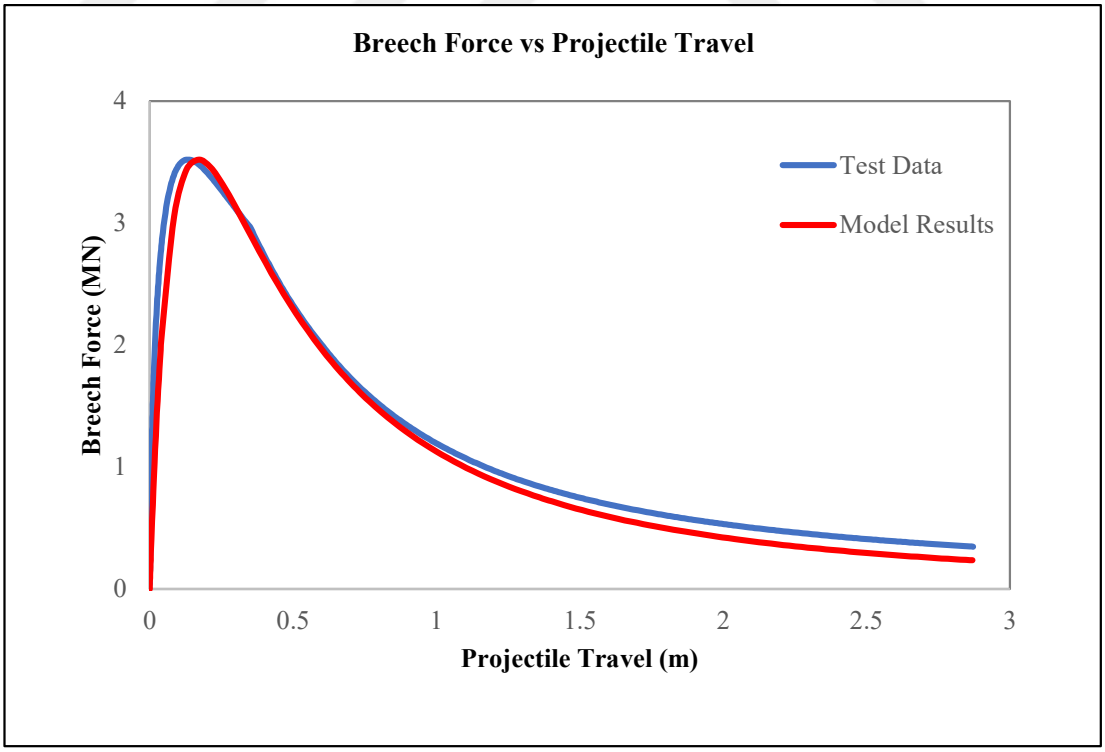

Figure 3.2 Comparison of model results and test data from MKEK for breech force vs projectile travel

Secondly, comparison of model results and firing test data for a new generation lighter 105 mm howitzer is given in Figure 3.2. It seems from the figure that model results and test data are very close to each other. It can be said that the model is verified for breech force change during projectile travel by firing tests for two different weapon systems.

3.1.2 Gas Ejection Period

As explained in previous chapter, propellant gasses contribute the breech force and recoil movement because of its high velocity. Hence, breech force for this period is considered and results from the model for new generation 105 mm howitzer is given in Figure 3.3.

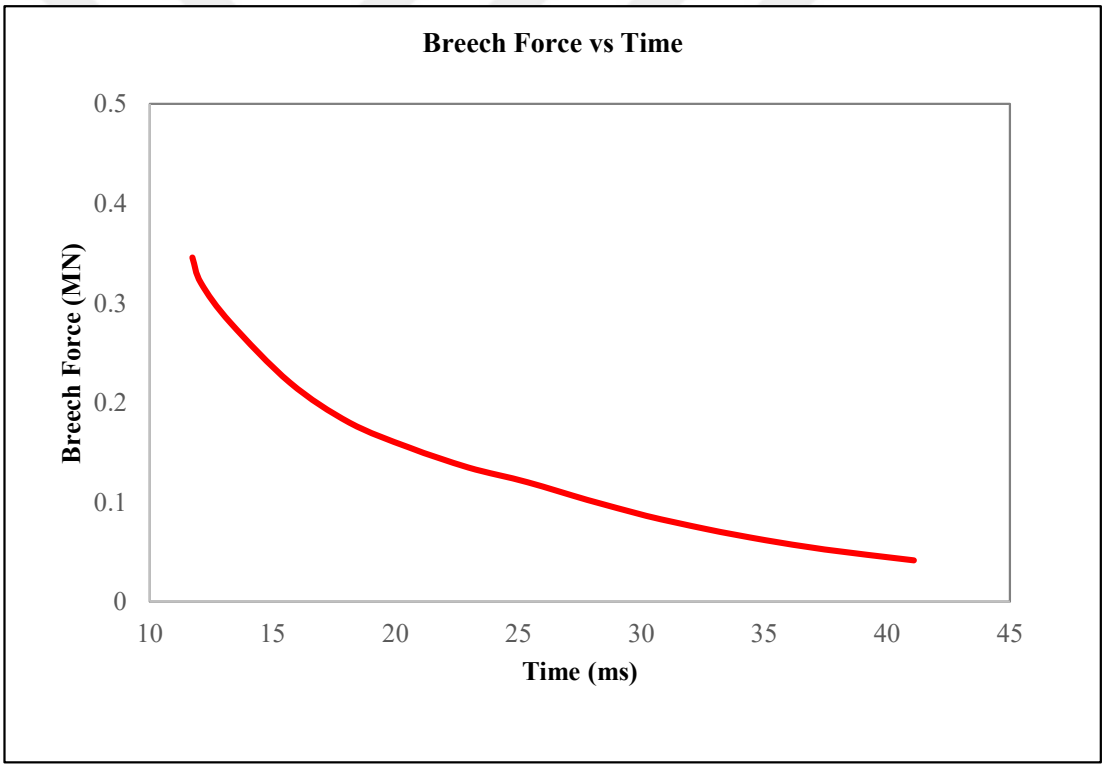

Figure 3.3 Model results of new 105 mm howitzer for breech force vs time for gas ejection period

Total breech force is calculated from Eq. 2.85 and total breech force vs time curve is given in Figure 3.4

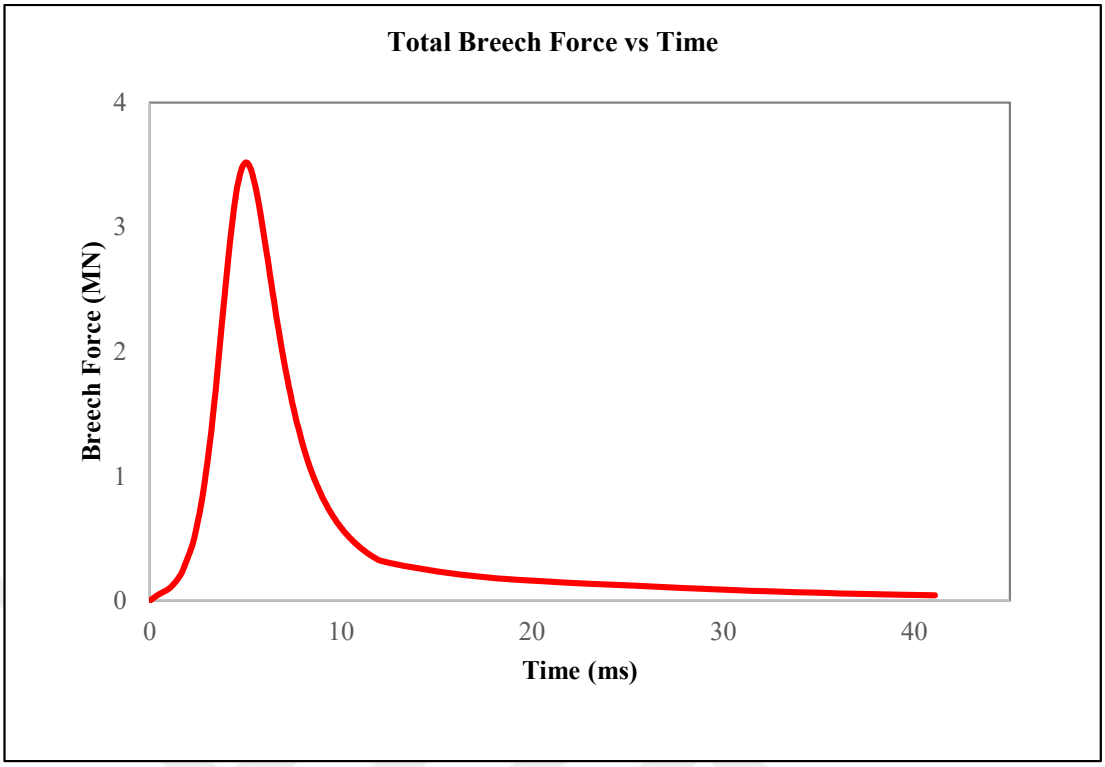

Figure 3.4 Model results of new 105 mm howitzer for total breech force vs time

3.2 Velocity of Projectile

Results are obtained from the model for velocity of projectile are also compared with two different firing test data. Figure 3.5 shows the comparison of model results and a typical 105 mm howitzer firing test data from literature for velocity of projectile.

Muzzle velocity is calculated from the model as 455.2 m/s and is measured from firing test as 455.4 m/s. The difference between these values is about 0.1 %. Figure 3.5 shows that calculated results from the model and measured data from firing tests are compatible with each other.

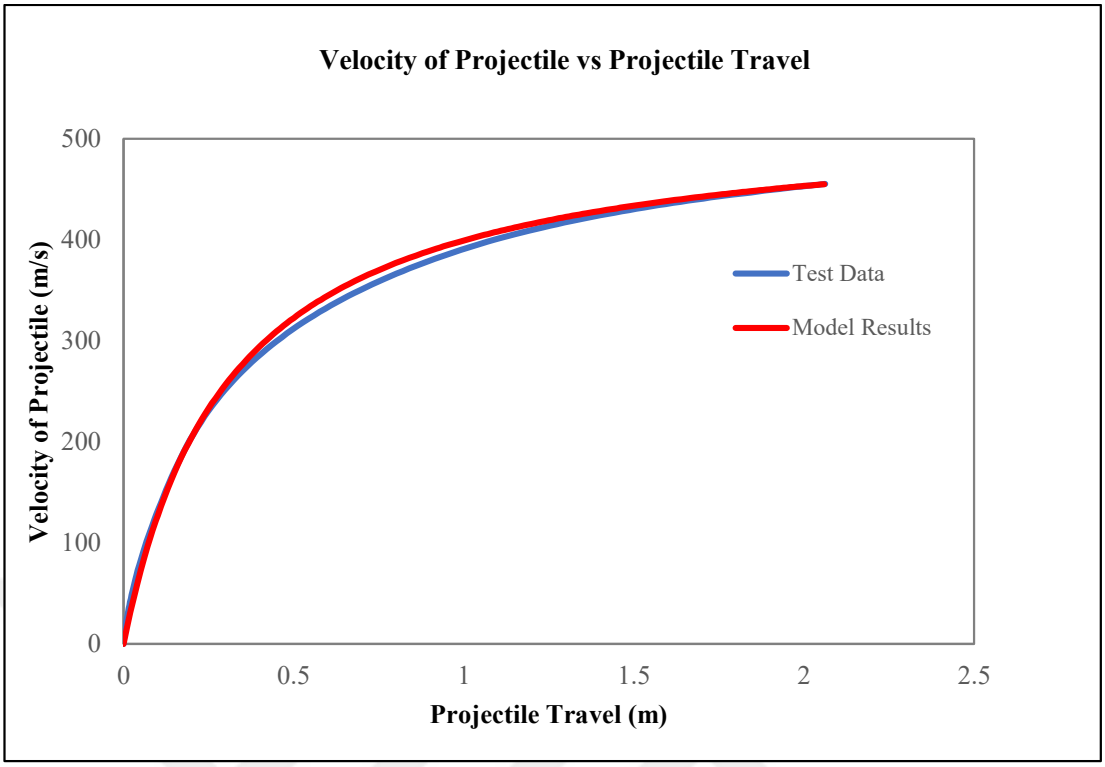

Figure 3.5 Comparison of model results and test data from literature for velocity of projectile vs projectile travel

Comparison of model results and firing test data for a new generation lighter 105 mm howitzer is given in Figure 3.6. Muzzle velocity is calculated from the model as 680 m/s and is measured from firing test as 695 m/s. The difference between these values is about 2 % and calculated results from the model and measured data from firing tests are very close to each other. It is understood from Figure 3.5 and Figure 3.6 that the model is verified for velocity of projectile change during projectile travel by firing tests for two different weapon systems.

Additionally, change in velocity of projectile is compatible with change in breech force. It increases with higher acceleration where the breech force is very high, and it increases with lower acceleration where the breech force has low values.

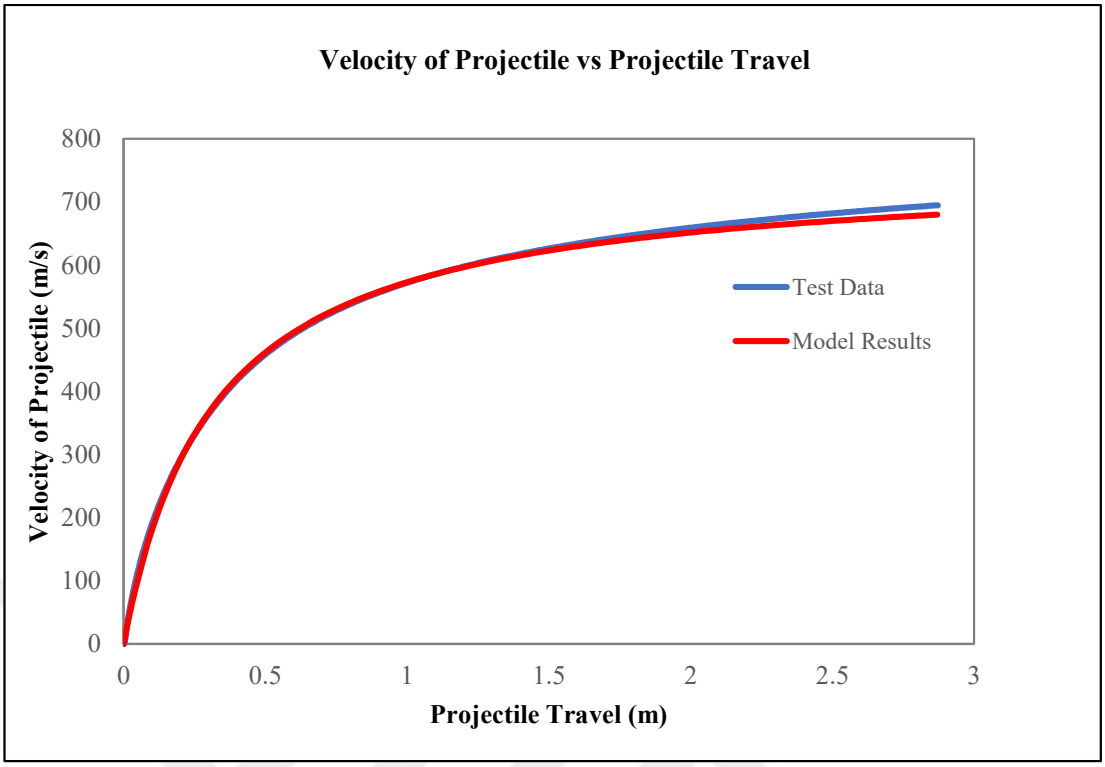

Figure 3.6 Comparison of model results and test data from MKEK for velocity of projectile vs projectile travel

3.3 Acceleration of Projectile

Firing test data for acceleration of projectile is only valid for a typical 105 mm weapon system. Therefore, results which are obtained from the model for acceleration of projectile are only compared with firing tests from literature and this comparison is given in Figure 3.7.

Peak acceleration is calculated from the model as 128090 m/s^2 and is measured from firing tests as 129200. The difference between peak values is less than 0.1% and it is seen from figure that other values are also close to each other. Additionally, acceleration values of projectile are also compatible with breech force values and this satisfies the Newton's second law of motion.

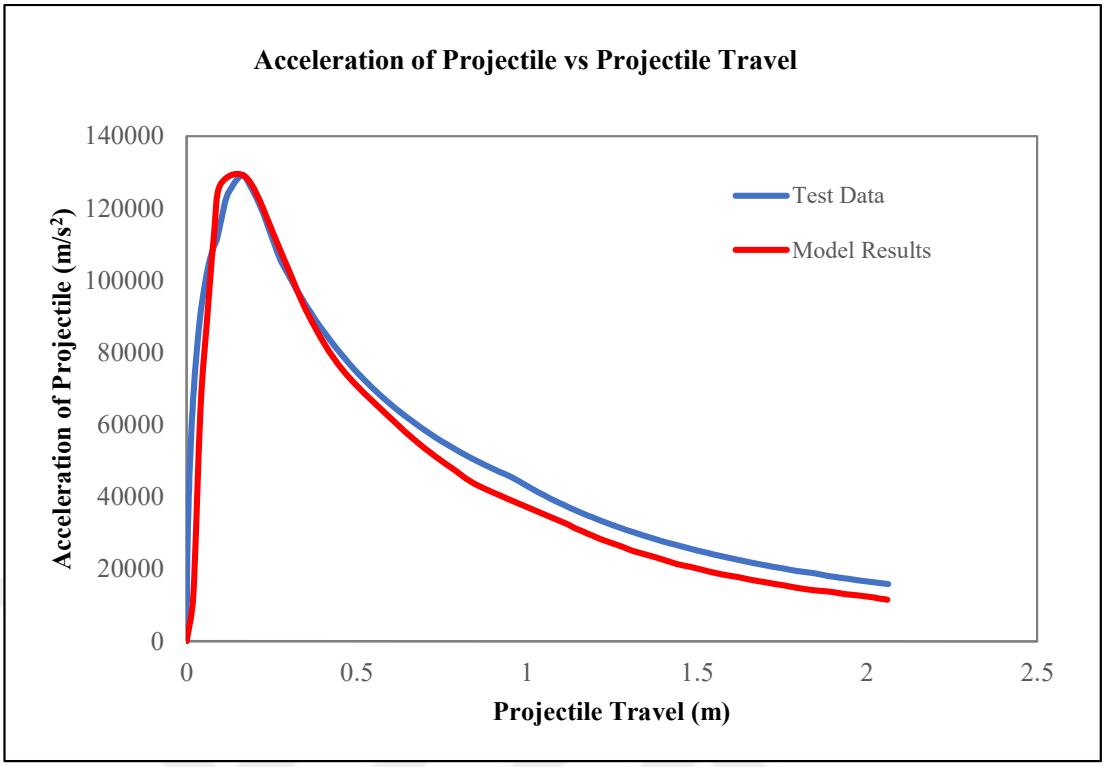

Figure 3.7 Comparison of model results and test data from literature for acceleration of projectile vs projectile travel

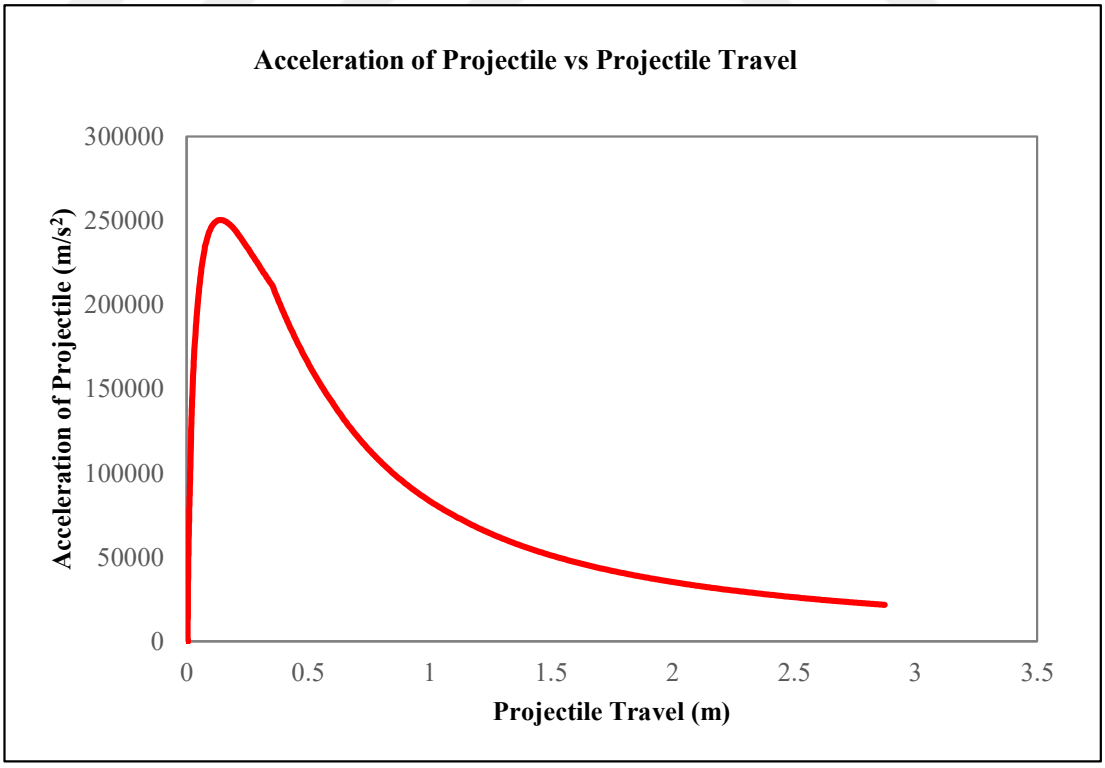

Figure 3.8 Model results of new 105 mm howitzer for acceleration of projectile vs projectile travel

Acceleration of projectile for the new generation 105 mm howitzer is calculated from the model and given in Figure 3.8 without any comparison due to the lack of test data. Maximum acceleration value for the projectile is calculated as 250350 m/s^2 from the model.

3.4 Recoil Displacement

Firing test data for recoil displacement is only valid for new generation 105 mm howitzer and these data are supplied by MKEK. Recoil displacement change vs time is calculated from the model for zero-degree firing angle and is given in Figure 3.9.

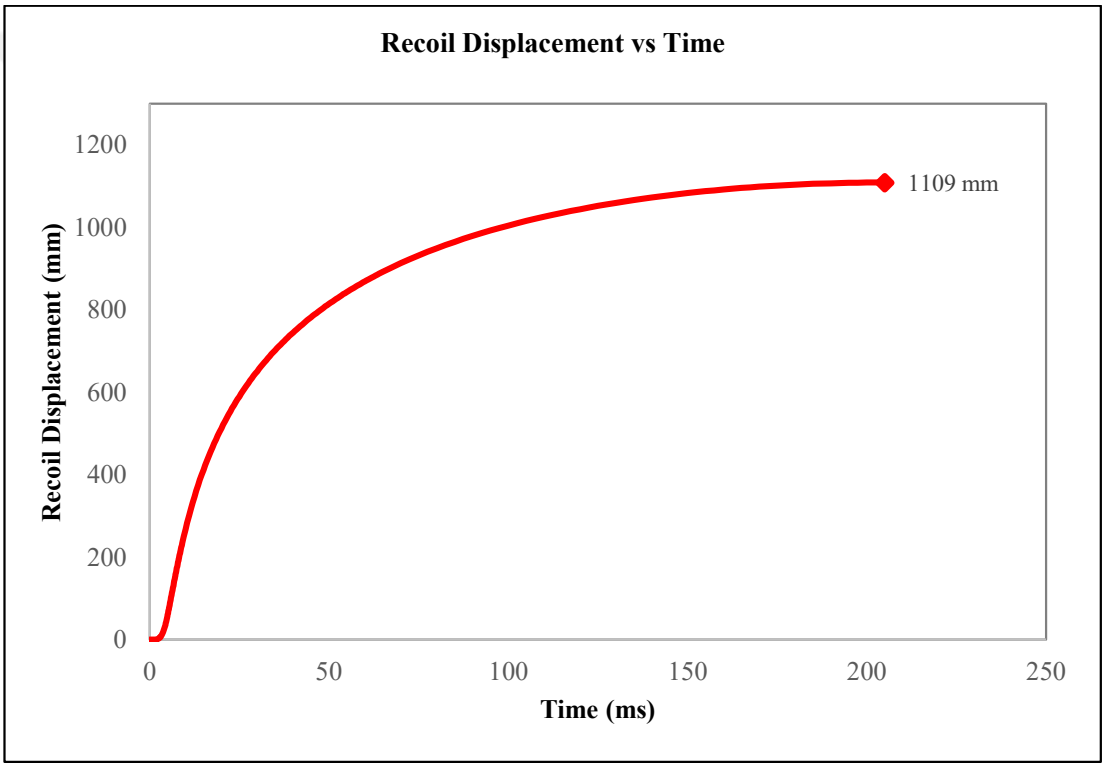

Figure 3.9 Model results of new 105 mm howitzer for recoil displacement vs time

Firing tests and measurements are repeated several times for zero-degree firing angle and average of maximum recoil displacement values is 1135 mm. And maximum recoil displacement is calculated from the model as 1109 mm. The difference between these values is about 2 % which is acceptable.

3.5 Effect of Firing Angle on Recoil Displacement

Effect of firing angle on recoil displacement is investigated in the model and maximum recoil displacement values are compared with the result from firing tests. The model is solved for 0° and 45° (800 mils) values and results are given in Figure 3.10.

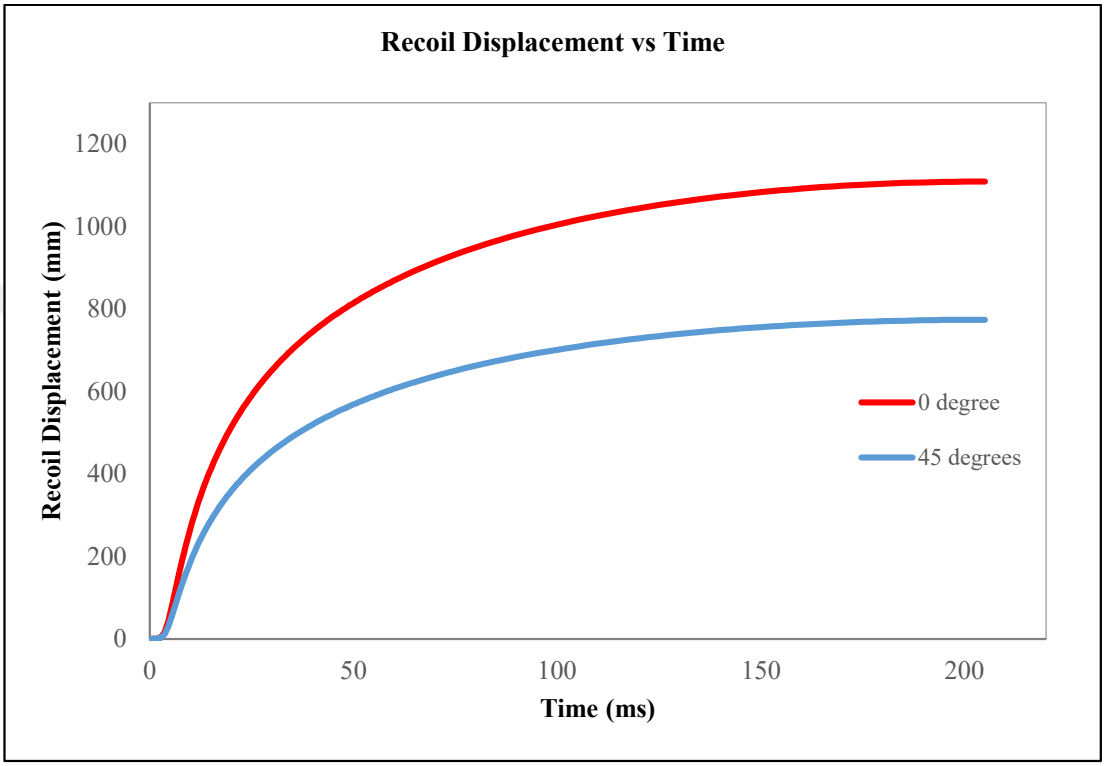

Figure 3.10 Effect of firing angle on recoil displacement

Comparison of firing data and model results for maximum recoil displacement values is given in Table 3.1. It should be noted that given maximum recoil displacement value for test data is the average value.

Table 3.1 Effect of firing angle on recoil displacement

Angle (degree)	Maximum recoil displacement (mm)		Difference (%)
	Model result	Test data	
0	1109	1135	2.3
45	774	792.5	2.3

Model results and test data are compatible with each other and difference between them is 2.3%. It is understood both from model and firing tests that maximum recoil displacement decreases when firing angle is increased.

3.6 Velocity of Recoiling Parts

Firing test data for velocity of recoiling parts is not valid for any of the 105 mm gun system. Therefore, any comparison with test data is not given in this section. However, results that are given in this section are obtained from the model which is validated by test data in previous sections.

Velocity of recoiling parts vs time curve is given in Figure 3.11. It is calculated from the model that maximum velocity value of recoiling parts is 45.19 m/s. It can also be said that velocity of recoiling parts curve is similar to breech force curve.

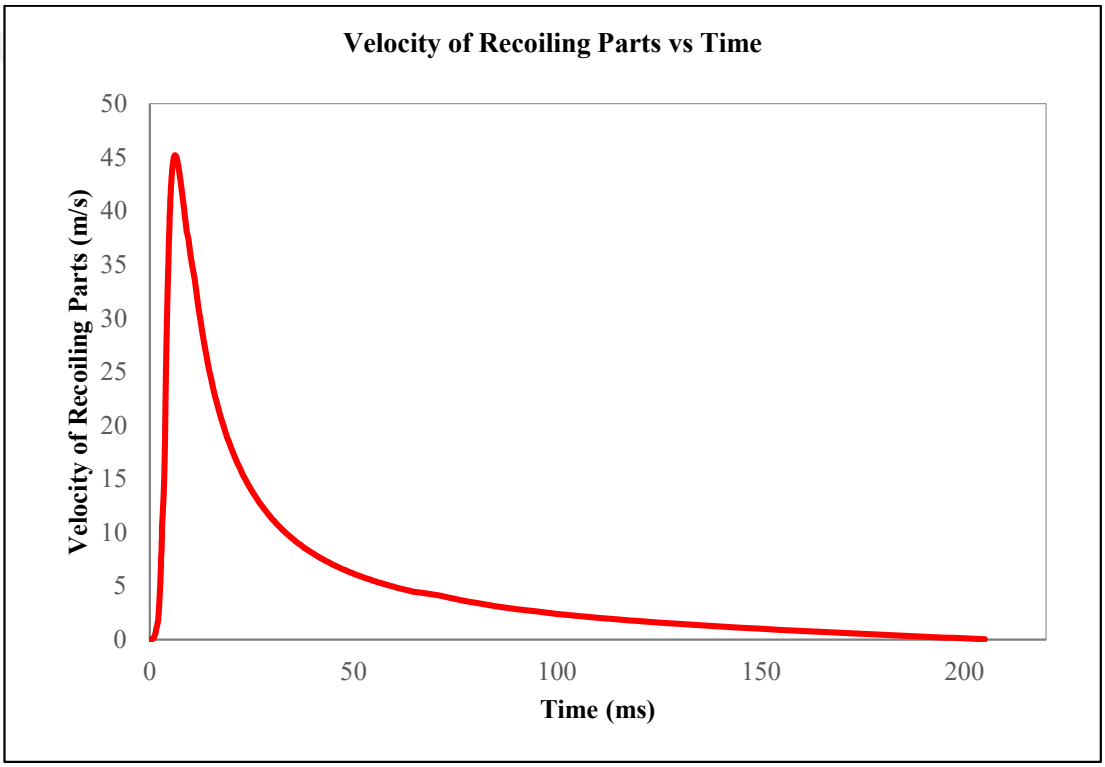

Figure 3.11 Model results of new 105 mm howitzer for velocity of recoiling parts vs time

3.7 Effect of Firing Angle on Velocity of Recoiling Parts

Effect of firing angle on velocity of recoiling parts is analyzed by using model. The model is solved for 0° and 45° (800 mils) values and results are given in Figure 3.12.

Maximum velocity values of recoiling parts are 45.19 m/s for 0° while it is 31.54 m/s for 45°. It is seen from Figure 3.12 that maximum velocity of recoiling parts decreases when firing angle is increased.

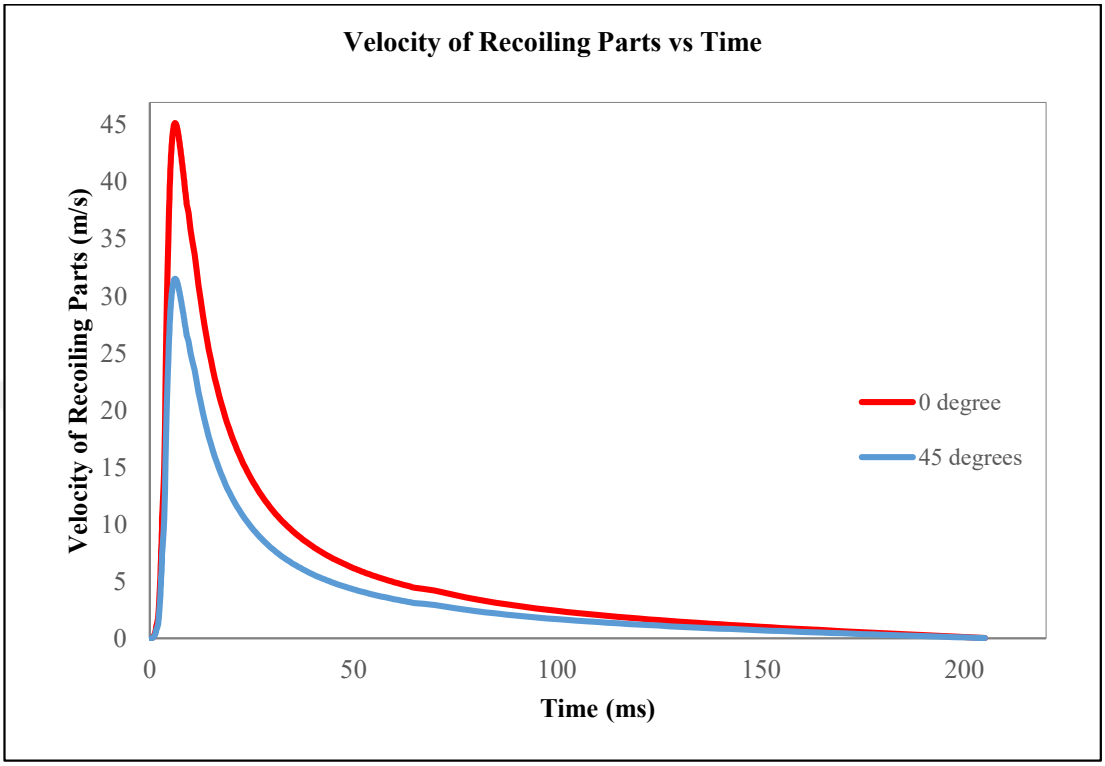

Figure 3.12 Effect of firing angle on velocity of recoiling parts

3.8 Acceleration of Recoiling Parts

Acceleration of recoiling parts vs time is calculated from the model and results are given in Figure 3.13. It is seen from the figure that acceleration increases where the breech force increased rapidly, and maximum acceleration of recoiling parts is calculated as 21.57 m/s^2. After that acceleration decreases due to that net retarding forces starts to overcome breech force and then it reaches minus values which means recoiling parts begins to slow down. Minimum acceleration value is -3.20 m/s^2.

Additionally, it can be said that recoil mechanism does its duty successfully which is dissipating recoil energy that is formed in very short duration by extremely high internal ballistic forces.

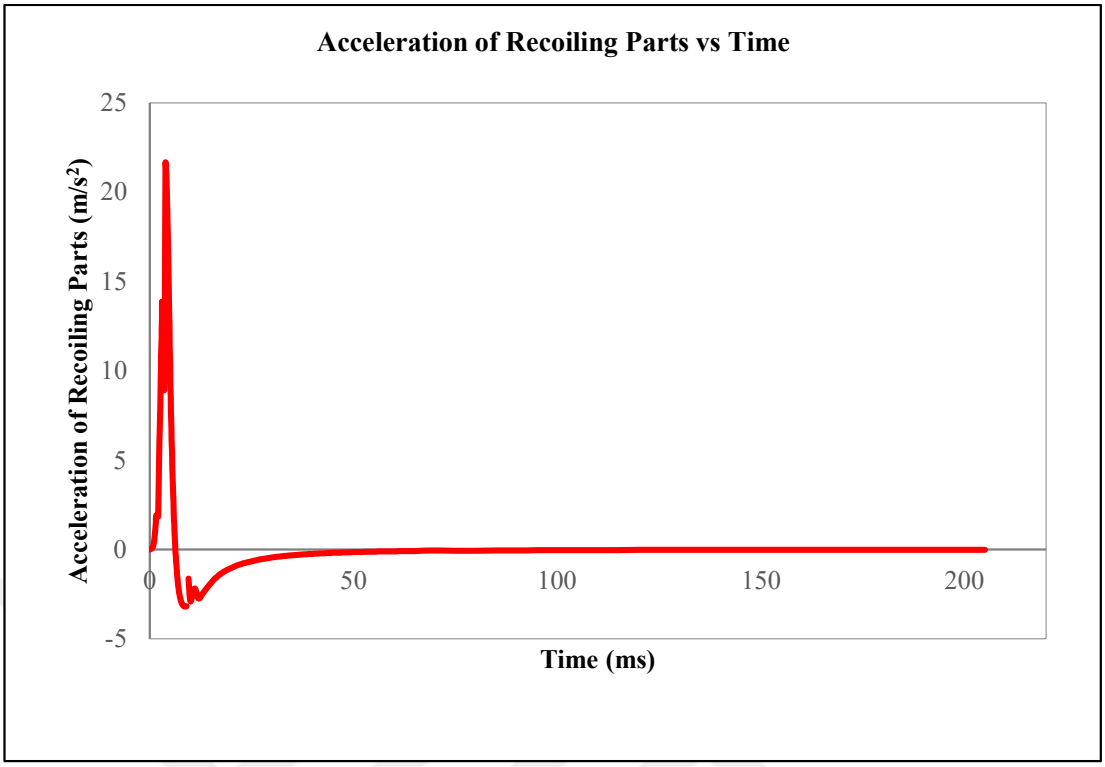

Figure 3.13 Model results of new 105 mm howitzer for acceleration of recoiling parts vs time

3.9 Effect of Firing Angle on Acceleration of Recoiling Parts

Effect of firing angle on acceleration of recoiling parts is investigated by using model. The model is solved for 0° and 45° (800 mils) values and results are given in Figure 3.14.

Maximum acceleration values of recoiling parts are 21.57 m/s^2 for 0° while it is 15.05 m/s^2 for 45°. In addition, minimum acceleration values of recoiling parts are -3.20 m/s^2 for 0° and -2.23 m^2 for 45°.

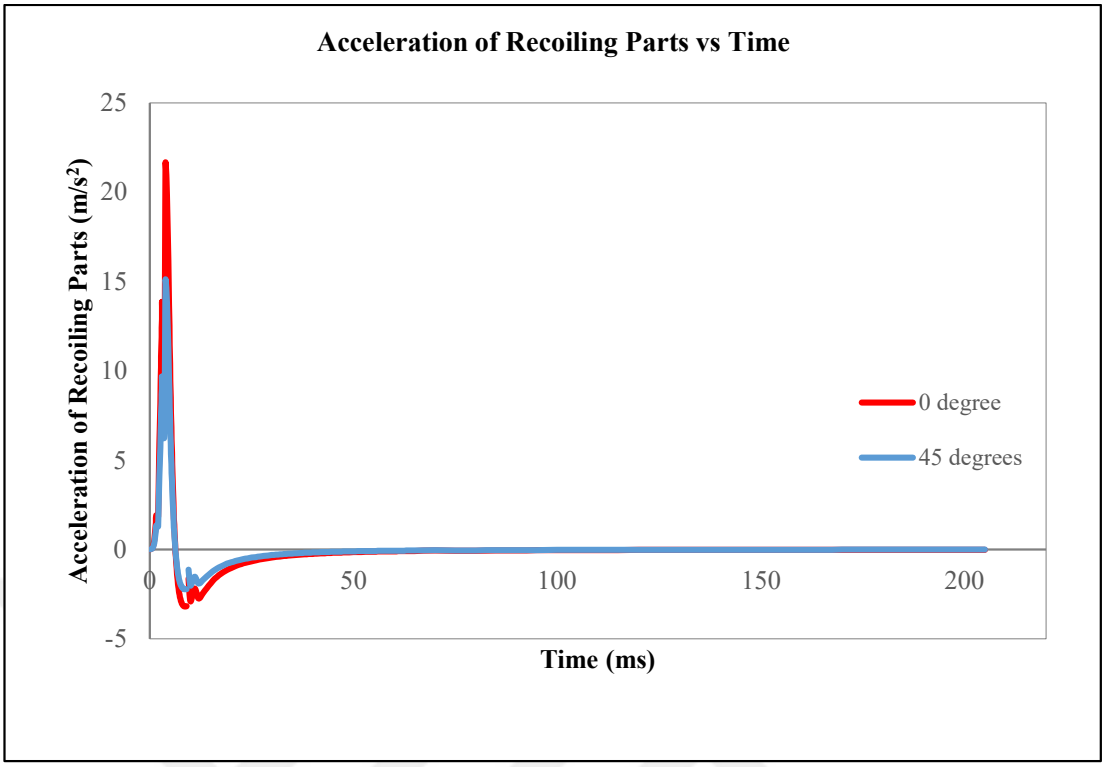

Figure 3.14 Effect of firing angle on acceleration of recoiling parts

3.10 Effect of Recoiling Weight on Recoil Displacement

Effect of recoiling weight on recoil displacement is studied by using the validated model. The model is solved for original weight, 20 % lighter, 10 % lighter, 20 % heavier and 10 % heavier weights at 0° and results are given in Figure 3.15.

The maximum recoil displacement values for 20 % lighter, 10 % lighter, original, 10 % heavier and 20 % heavier weights are 1297 mm, 1187 mm, 1109 mm, 1031 mm and 921 mm respectively and these results are given in Table 3.2.

Table 3.2 Effect of recoiling weight on recoil displacement

Weight	Maximum recoil displacement (mm)
20 % lighter	1297
10 % lighter	1187
original	1109
10 % heavier	1031
20 % heavier	921

It is seen from figure and table that maximum recoil displacement decreases with increasing weight. This result is compatible with equation of motion for recoiling parts (Eq. 2.86).

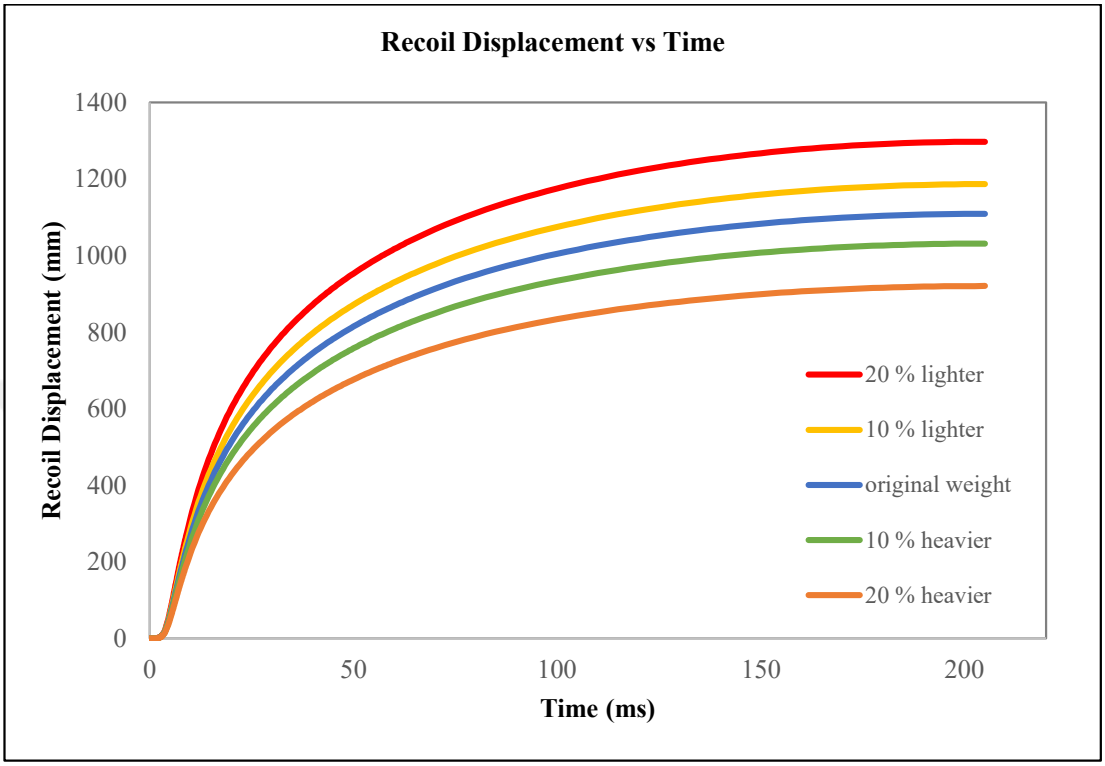

Figure 3.15 Effect of recoiling weight on recoil displacement

3.11 Effect of Recoiling Weight on Velocity of Recoiling Parts

Effect of recoiling weight on velocity of recoiling parts is investigated by using the validated model. The model is solved for original weight, 20 % lighter, 10 % lighter, 20 % heavier and 10 % heavier weights at 0° and results are given in Figure 3.16 and 3.17.

The maximum velocity values of recoiling parts for 20 % lighter, 10 % lighter, original, 10 % heavier and 20 % heavier weights are 52.87 m/s, 48.35 m/s, 45.19 m/s, 42.02 m/s and 37.51 m/s respectively and these results are given in Table 3.3.

Table 3.3 Effect of recoiling weight on velocity of recoiling parts

Weight	Maximum recoil velocity (m/s)
20 % lighter	52.87
10 % lighter	48.35
original	45.19
10 % heavier	42.02
20 % heavier	37.51

It is seen from figures and table that increasing the weight of recoiling parts results in decrease in velocity of recoiling parts which is in accordance with the equation of motion.

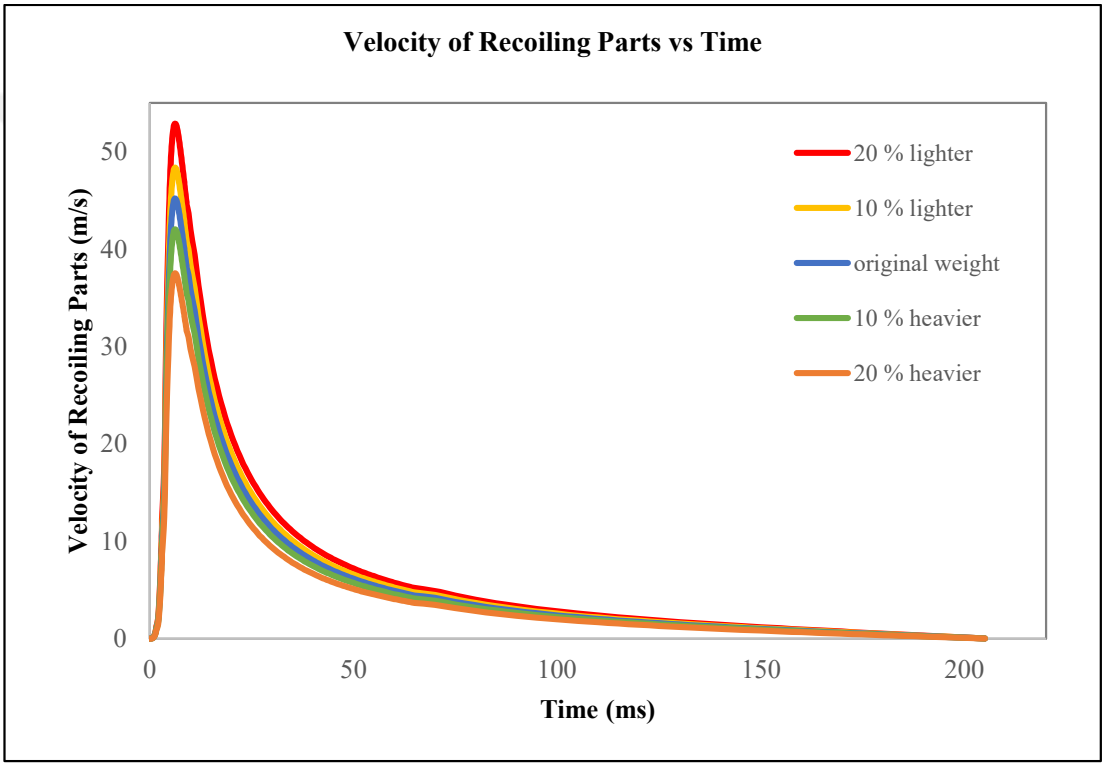

Figure 3.16 Effect of recoiling weight on velocity of recoiling parts

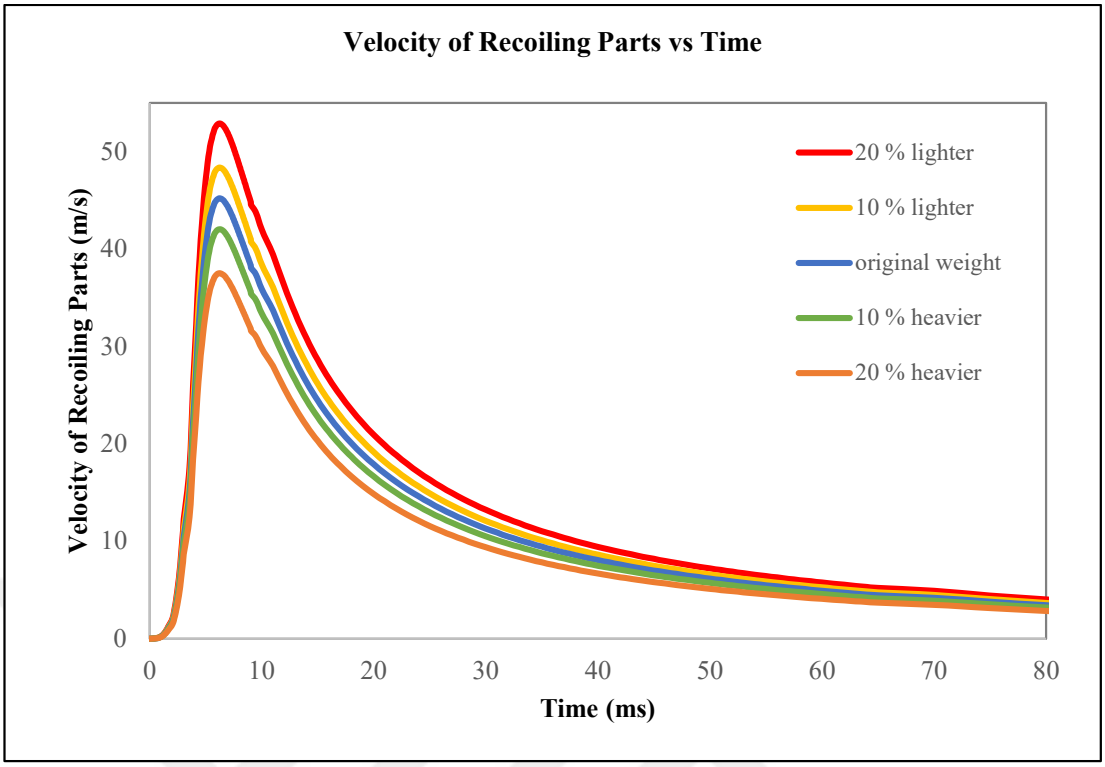

Figure 3.17 Effect of recoiling weight on velocity of recoiling parts (0-80 ms)

3.12 Effect of Recoiling Weight on Acceleration of Recoiling Parts

Effect of recoiling weight on acceleration of recoiling parts is analyzed by using the validated model. The model is solved for original weight, 20 % lighter, 10 % lighter, 20 % heavier and 10 % heavier weights at 0° and results are given in Figure 3.18 and 3.19.

The maximum acceleration values of recoiling parts for 20 % lighter, 10 % lighter, original, 10 % heavier and 20 % heavier weights are 25.23 m/s^2, 23.08 m/s^2, 21.57 m/s^2, 20.06 m/s^2, 17.90 m/s^2 and minimum acceleration values are -3.74 m/s^2, -3.42 m/s^2, -3.20 m/s^2, -2.97 m/s^2, -2.65 m/s^2 respectively and these results are given in Table 3.4.

Table 3.4 Effect of recoiling weight on acceleration of recoiling parts

Weight	Maximum recoil acceleration (m/s^2)	Minimum recoil acceleration (m/s^2)
20 % lighter	25.23	-3.74
10 % lighter	23.08	-3.42
original	21.57	-3.20
10 % heavier	20.06	-2.97
20 % heavier	17.90	-2.65

It is seen from figures and table that increasing the weight of recoiling parts decreases maximum acceleration and increases minimum acceleration values. These results obey the Newton's law of motion.

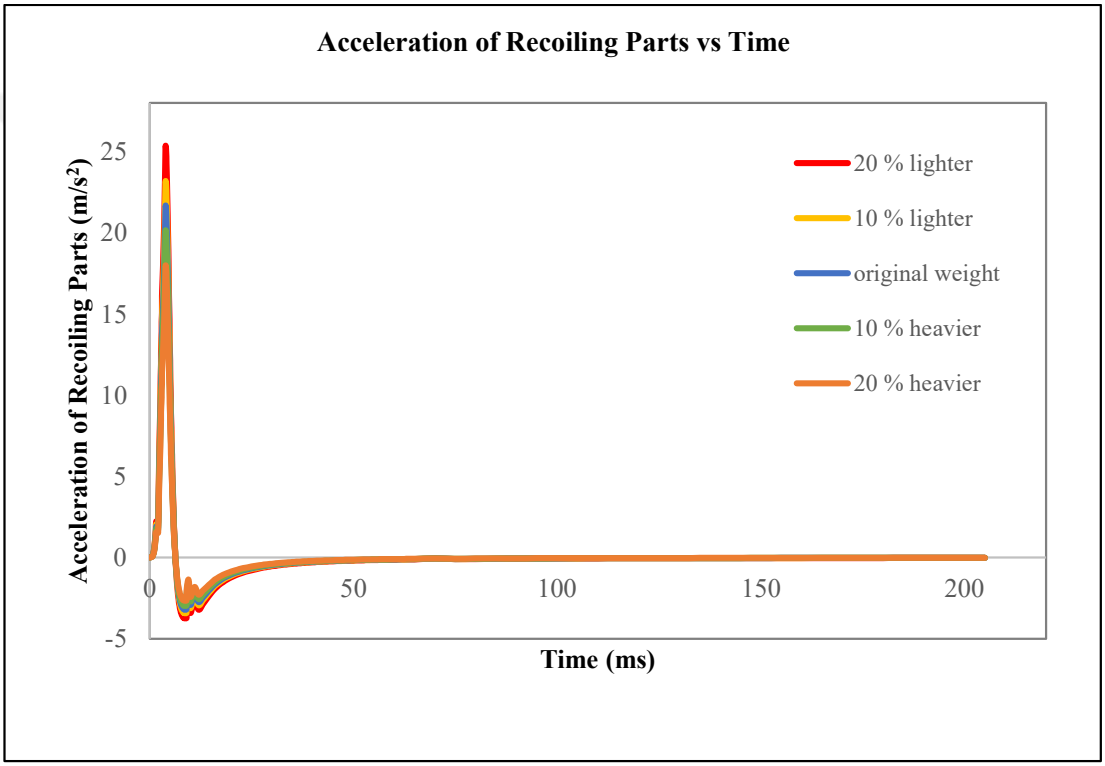

Figure 3.18 Effect of recoiling weight on acceleration of recoiling parts

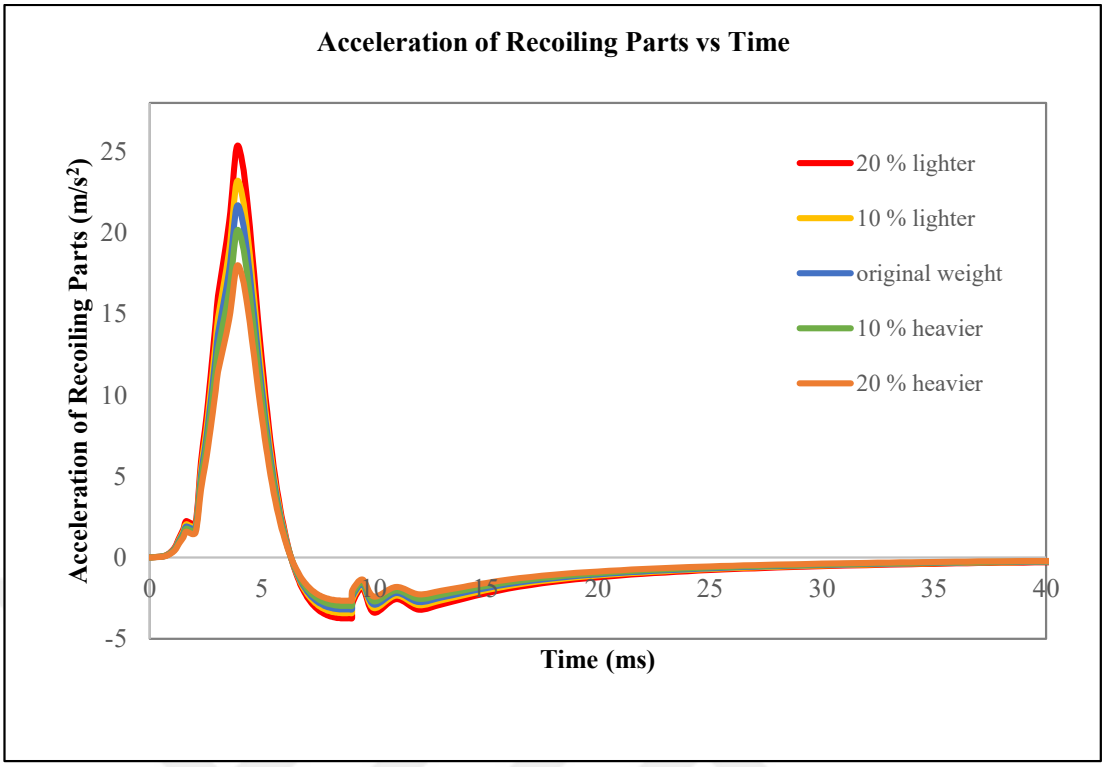

Figure 3.19 Effect of recoiling weight on acceleration of recoiling parts (0-40 ms)

3.13 Effect of Orifice Discharge Coefficient on Recoil Displacement

Effect of orifice discharge coefficient on recoil displacement is studied by using the validated model. The model is solved for original orifice discharge coefficient, 20 % lower, 10 % lower, 20 % higher and 10 % higher orifice discharge coefficients at 0° and results are given in Figure 3.20.

The maximum recoil displacement values for 20 % lower, 10 % lower, original, 10 % higher and 20 % higher orifice discharge coefficients are 998 mm, 1065 mm, 1109 mm, 1153 mm and 1220 mm respectively and these results are given in Table 3.5.

Table 3.5 Effect of orifice discharge coefficient on recoil displacement

Orifice discharge coefficient	Maximum recoil displacement (mm)
20 % lower	998
10 % lower	1065
original	1109
10 % higher	1153
20 % higher	1220

It is seen from figure and table that maximum recoil displacement increases with increasing orifice discharge coefficient.

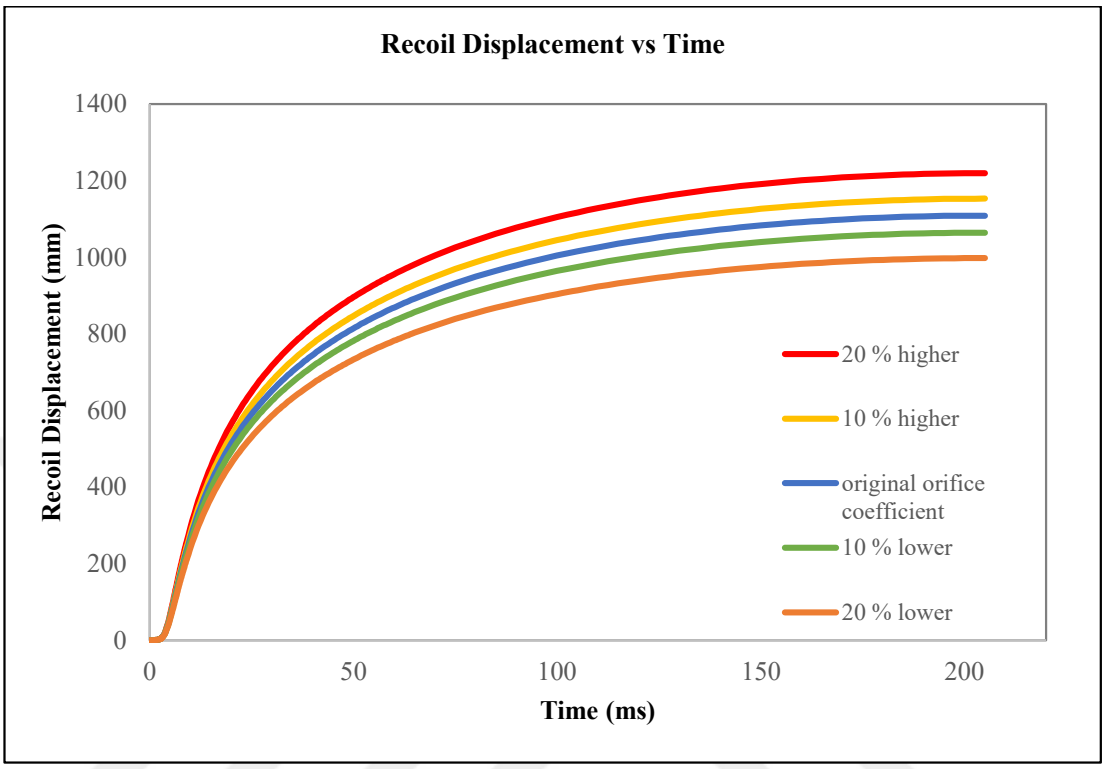

Figure 3.20 Effect of orifice discharge coefficient on recoil displacement

3.14 Effect of Orifice Discharge Coefficient on Recoil Velocity

Effect of orifice discharge coefficient on velocity of recoiling parts is investigated by using the validated model. The model is solved for original orifice discharge coefficient, 20 % lower, 10 % lower, 20 % higher and 10 % higher orifice discharge coefficients at 0° and results are given in Figure 3.21 and 3.22.

The maximum velocity values of recoiling parts for 20 % lower, 10 % lower, original, 10 % higher and 20 % higher orifice discharge coefficients are 40.67 m/s, 43.38 m/s, 45.19 m/s, 46.99 m/s and 49.71 m/s respectively and these results are given in Table 3.6.

Table 3.6 Effect of orifice discharge coefficient on velocity of recoiling parts

Orifice discharge coefficient	Maximum recoil velocity (m/s)
20 % lower	40.67
10 % lower	43.38
original	45.19
10 % higher	46.99
20 % higher	49.71

It is seen from figures and table that increasing the orifice discharge coefficient results in increase in velocity of recoiling parts.

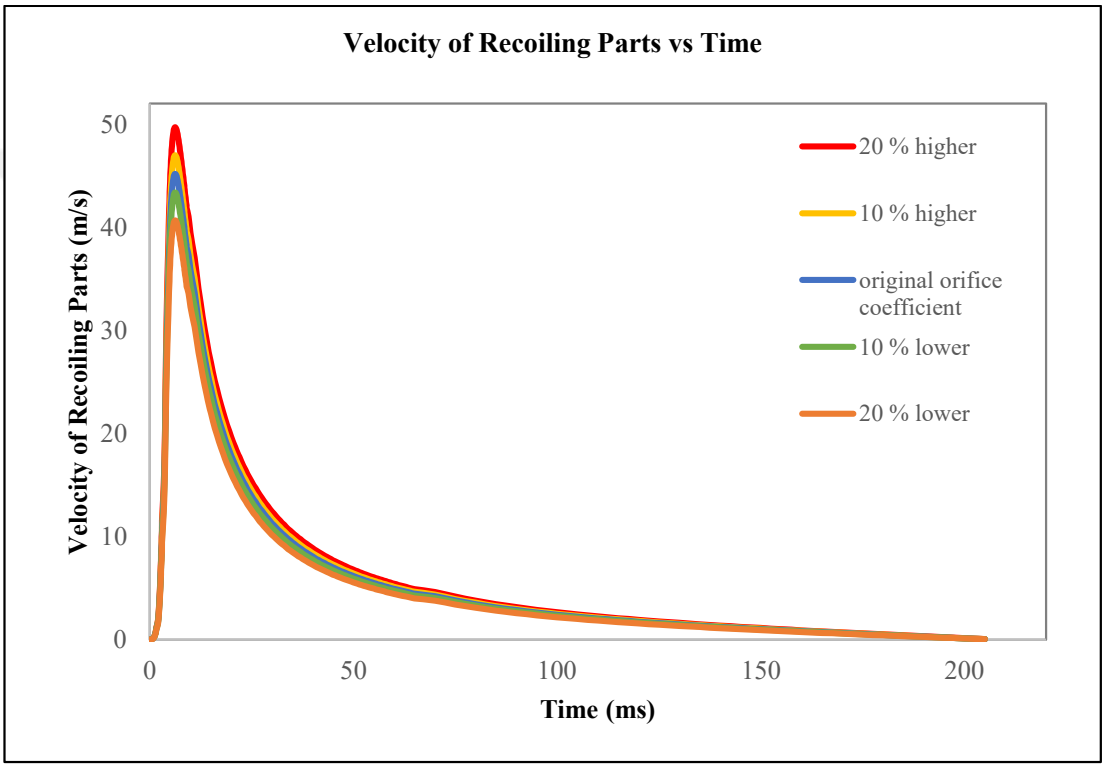

Figure 3.21 Effect of orifice discharge coefficient on velocity of recoiling parts

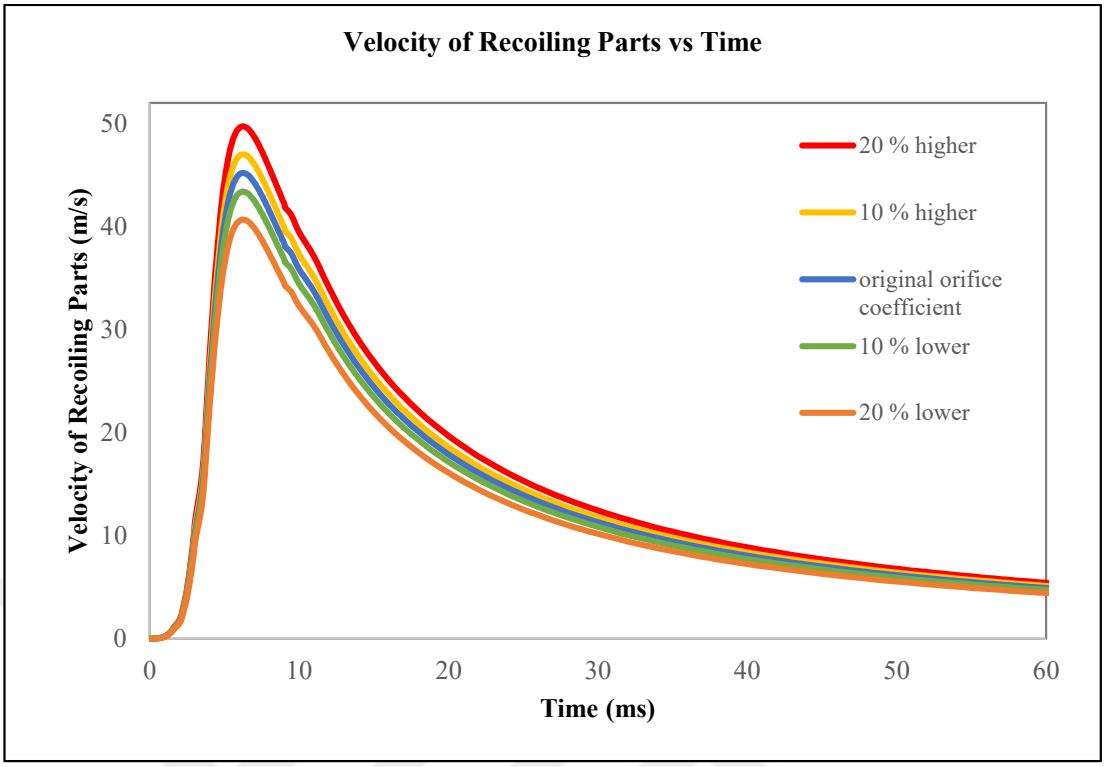

Figure 3.22 Effect of orifice discharge coefficient on velocity of recoiling parts (0-60 ms)

3.15 Effect of Orifice Discharge Coefficient on Recoil Acceleration

Effect of orifice discharge coefficient on acceleration of recoiling parts is analyzed by using the validated model. The model is solved for original orifice discharge coefficient, 20 % lower, 10 % lower, 20 % higher and 10 % higher orifice discharge coefficients at 0° and results are given in Figure 3.23 and 3.24.

The maximum acceleration values of recoiling parts for 20 % lower, 10 % lower, original, 10 % higher and 20 % higher orifice discharge coefficients are 19.41 m/s^2, 20.71 m/s^2, 21.57 m/s^2, 22.43 m/s^2 and 23.72 m/s^2 and minimum acceleration values are -2.88 m/s^2, -3.07 m/s^2, -3.20 m/s^2, -3.33 m/s^2 and -3.52 m/s^2 respectively and these results are given in Table 3.7.

Table 3.7 Effect of orifice discharge coefficient on acceleration of recoiling parts

Orifice discharge coefficient	Maximum recoil acceleration (m/s^2)	Minimum recoil acceleration (m/s^2)
20 % lower	19.41	-2.88
10 % lower	20.71	-3.07
original	21.57	-3.20
10 % higher	22.43	-3.33
20 % higher	23.72	-3.52

It is seen from figures and table that increasing the orifice discharge coefficient increases maximum acceleration and decreases minimum acceleration values.

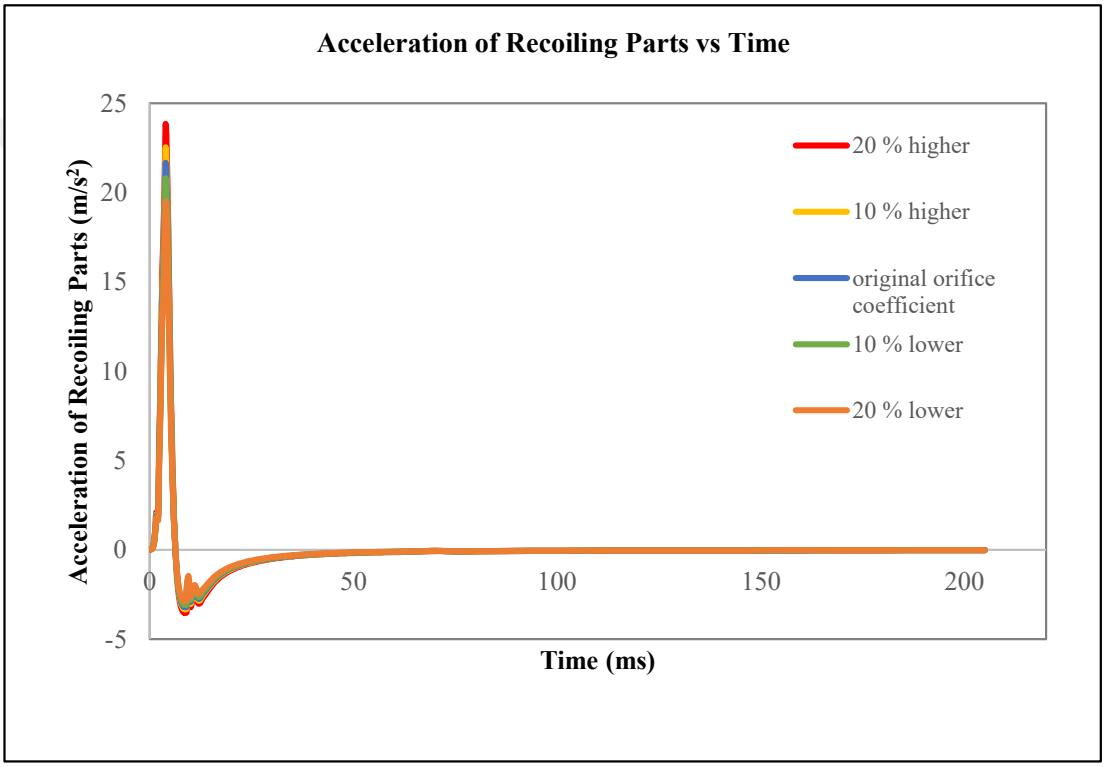

Figure 3.23 Effect of orifice discharge coefficient on acceleration of recoiling parts

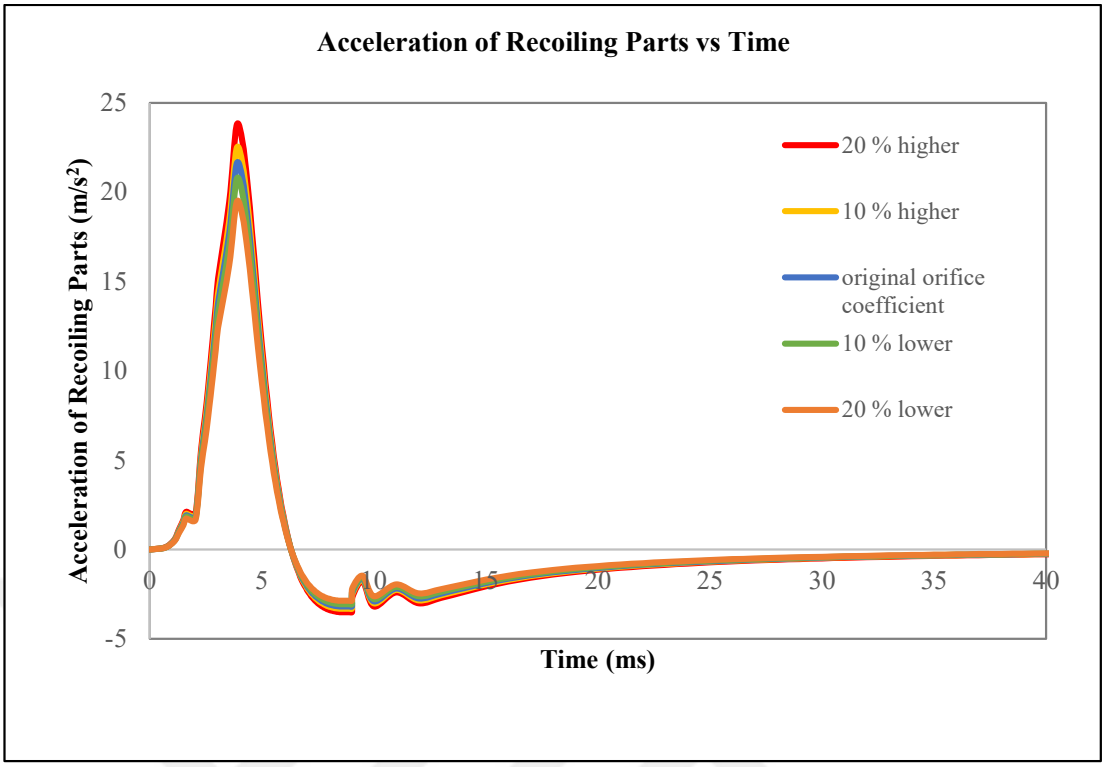

Figure 3.24 Effect of orifice discharge coefficient on acceleration of recoiling parts (0-40 ms)

3.16 Effect of Muzzle Brake Efficiency on Breech Force

Muzzle brake efficiency is a parameter that affects breech force especially for gas ejection period. Effect of this parameter on breech force is investigated via validated model. The model is solved for 0.5, 1 and 1.5 muzzle brake efficiency at 0° firing angle and results are given in Figure 3.25.

It is seen from figure that during gas ejection period 0.5 muzzle brake efficiency has the highest breech force while 1.5 efficiency has the lowest breech force. It can be said that designing a muzzle brake with higher efficiency contribute recoil mechanism by decreasing breech force during gas ejection period.

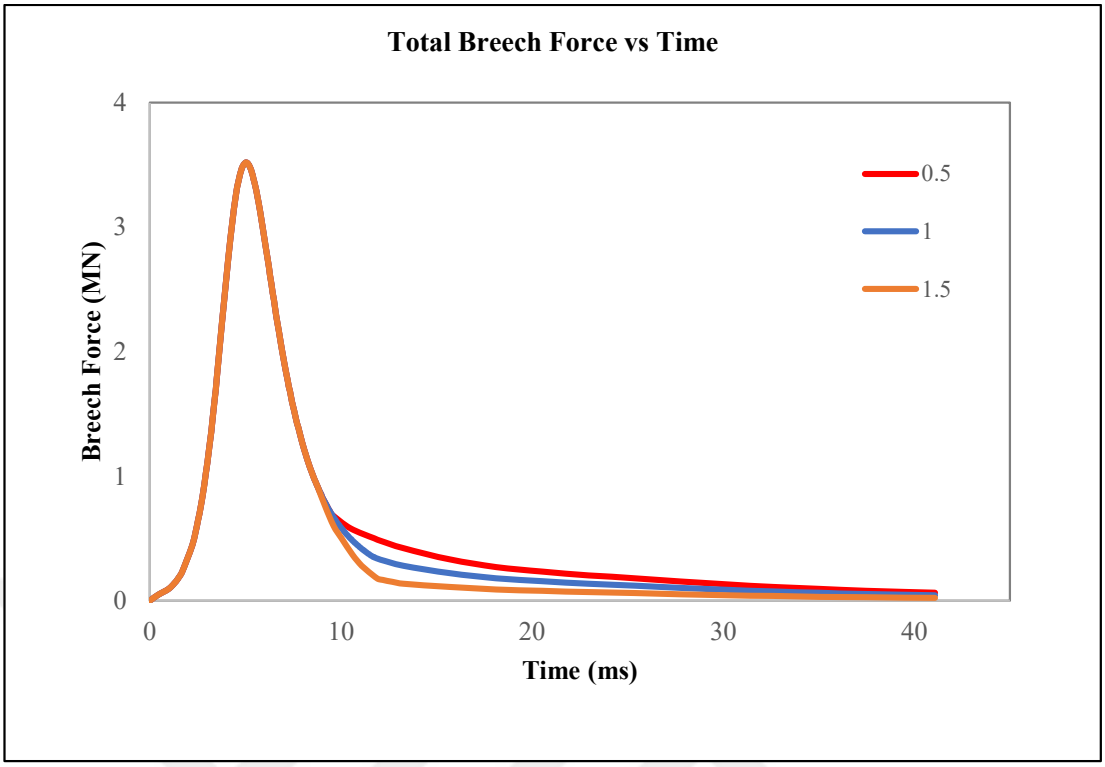

Figure 3.25 Effect of muzzle brake efficiency on breech force

3.17 Effect of Muzzle Brake Efficiency on Recoil Displacement

Effect of muzzle brake efficiency on recoil displacement is studied by using the validated model. The model is solved for 0.5, 0.75, 1, 1.25 and 1.5 muzzle brake efficiency values at 0° and results are given in Figure 3.26 and 3.27.

The maximum recoil displacement values for 0.5, 0.75, 1, 1.25, 1.5 muzzle brake efficiencies are 1142 mm, 1122 mm, 1109 mm, 1096 mm and 1075 mm respectively and these results are given in Table 3.8.

Table 3.8 Effect of muzzle brake efficiency on recoil displacement

Muzzle brake efficiency	Maximum recoil displacement (mm)
0.5	1142
0.75	1122
1	1109
1.25	1096
1.5	1075

It is seen from figures and table that maximum recoil displacement decreases with increasing muzzle brake efficiency. Because breech force during gas ejection period is decreased.

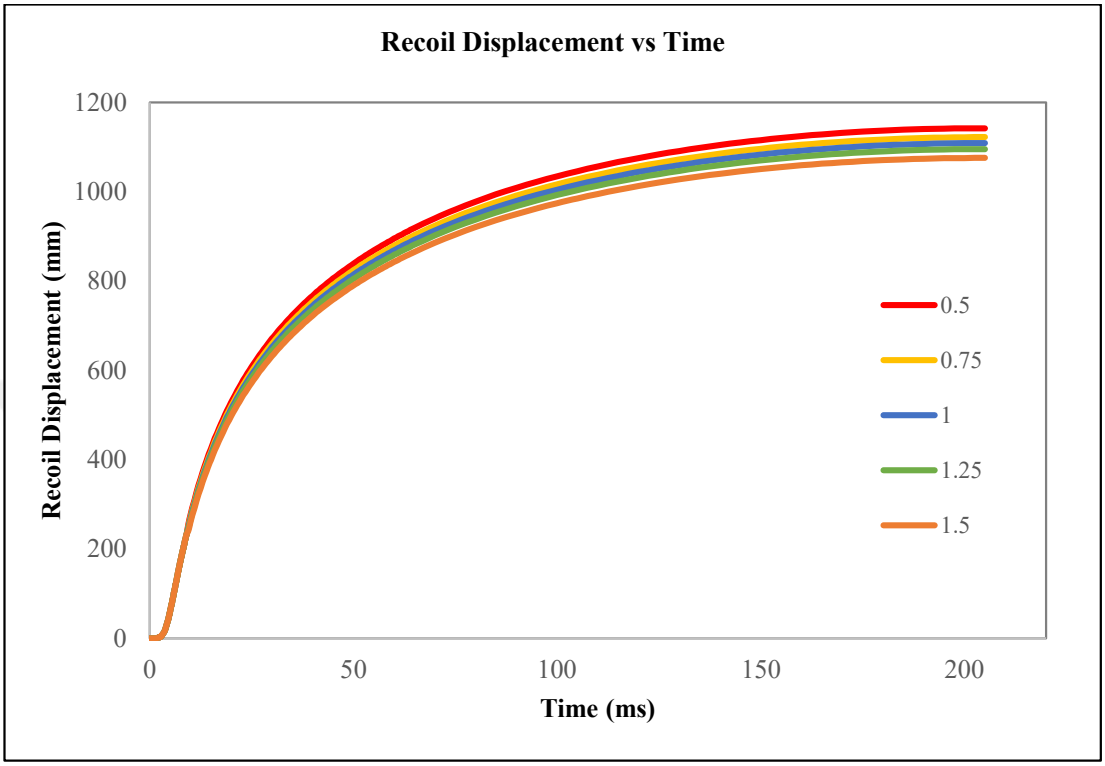

Figure 3.26 Effect of muzzle brake efficiency on recoil displacement

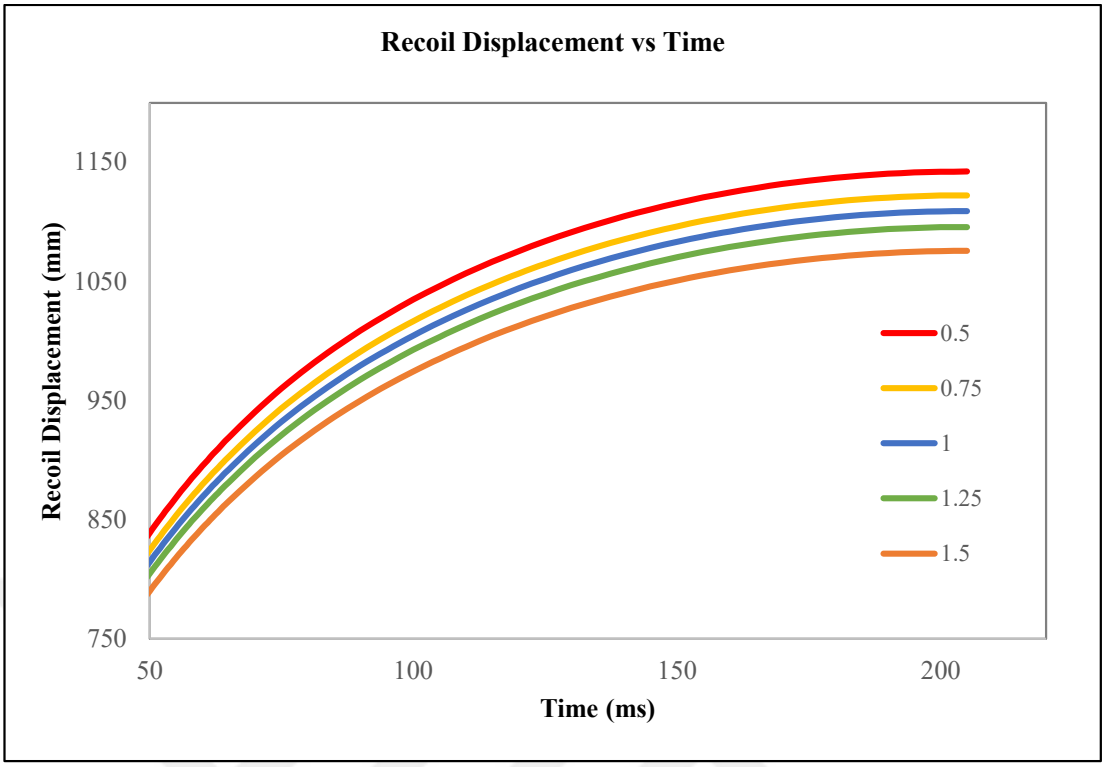

Figure 3.27 Effect of muzzle brake efficiency on recoil displacement (50-205 ms)

3.18 Effect of Muzzle Brake Efficiency on Recoil Velocity

Effect of muzzle brake efficiency on velocity of recoiling parts is investigated by using the validated model. The model is solved for 0.5, 0.75, 1, 1.25 and 1.5 muzzle brake efficiency values at 0° and results are given in Figure 3.28 and 3.29.

The maximum velocity values of recoiling parts for 0.5, 0.75, 1, 1.25 and 1.5 muzzle brake efficiencies are 46.54 m/s, 45.73 m/s, 45.19 m/s, 44.64 m/s and 43.83 m/s respectively and these results are given in Table 3.9.

Table 3.9 Effect of muzzle brake efficiency on velocity of recoiling parts

Muzzle brake efficiency	Maximum recoil velocity (m/s)
0.5	46.54
0.75	45.73
1	45.19
1.25	44.64
1.5	43.83

It is seen from figures and table that increasing the muzzle brake efficiency results in decrease in velocity of recoiling parts as expected. Because increasing muzzle brake efficiency causes decrease in breech force during gas ejection period.

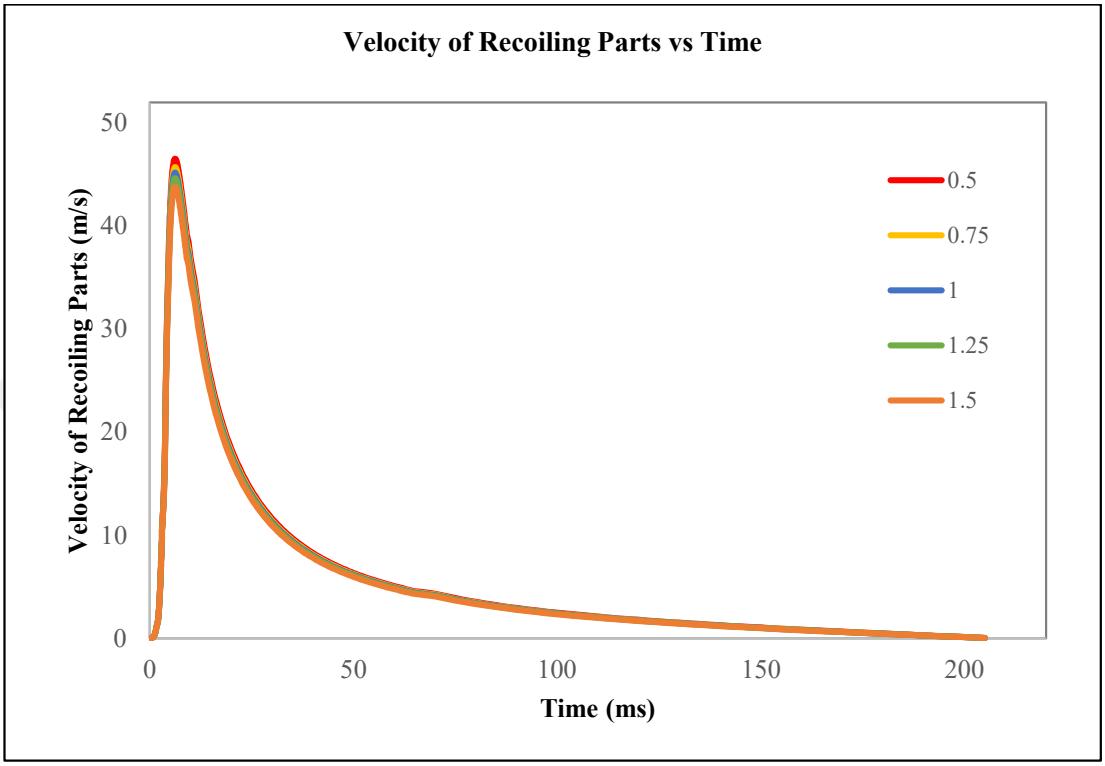

Figure 3.28 Effect of muzzle brake efficiency on velocity of recoiling parts

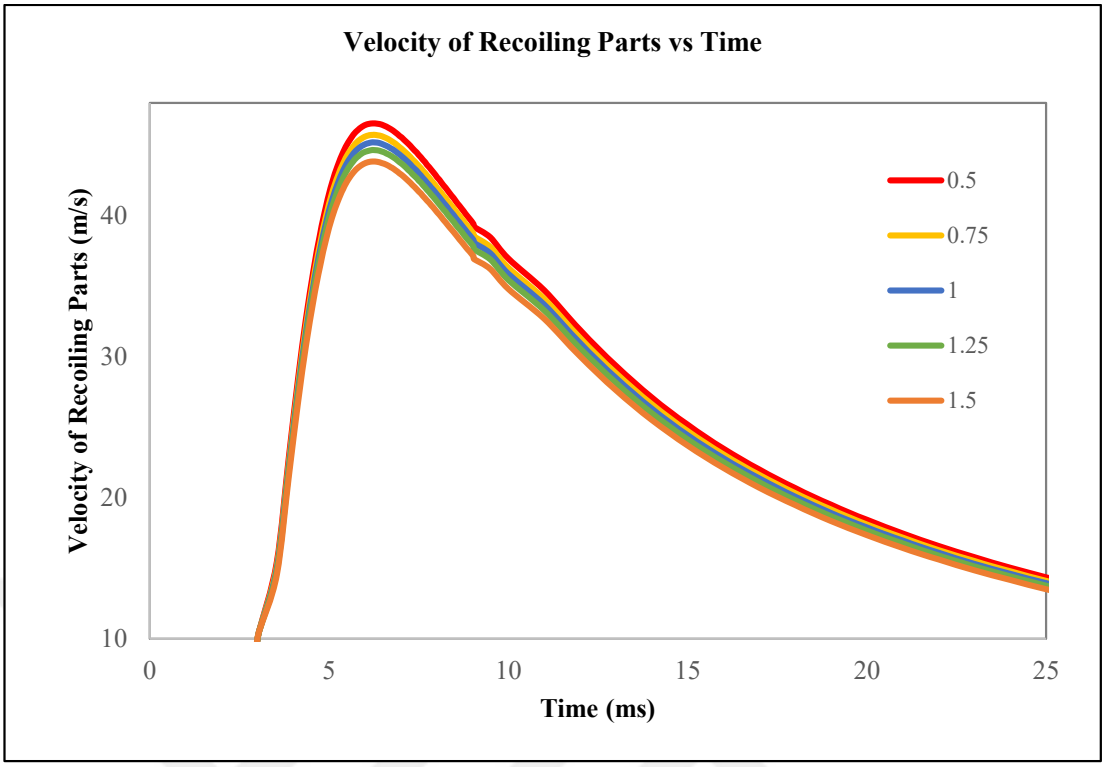

Figure 3.29 Effect of muzzle brake efficiency on velocity of recoiling parts (0-25 ms)

3.19 Effect of Muzzle Brake Efficiency on Recoil Acceleration

Effect of muzzle brake efficiency on acceleration of recoiling parts is analyzed by using the validated model. The model is solved for 0.5, 0.75, 1, 1.25 and 1.5 muzzle brake efficiency values at 0° and results are given in Figure 3.30 and 3.31.

The maximum acceleration value of recoiling parts is equal for 0.5, 0.75, 1, 1.25 and 1.5 muzzle brake efficiencies that is 21.57 m/s^2 and minimum acceleration values are -3.29 m/s^2, -3.24 m/s^2, -3.20 m/s^2, -3.16 m/s^2, -3.10 m/s^2 respectively and these results are given in Table 3.10.

Table 3.10 Effect of orifice discharge coefficient on acceleration of recoiling parts

Orifice discharge coefficient	Maximum recoil acceleration (m/s^2)	Minimum recoil acceleration (m/s^2)
20 % lower	21.57	-3.29
10 % lower	21.57	-3.24
original	21.57	-3.20
20 % higher	21.57	-3.16
20 % higher	21.57	-3.10

It is seen from figure and table that changing muzzle brake efficiency does not affect maximum acceleration of recoiling parts due to that recoiling parts reach the maximum acceleration before the projectile leaves the muzzle. However, increasing muzzle brake efficiency increasing the minimum acceleration of recoiling parts.

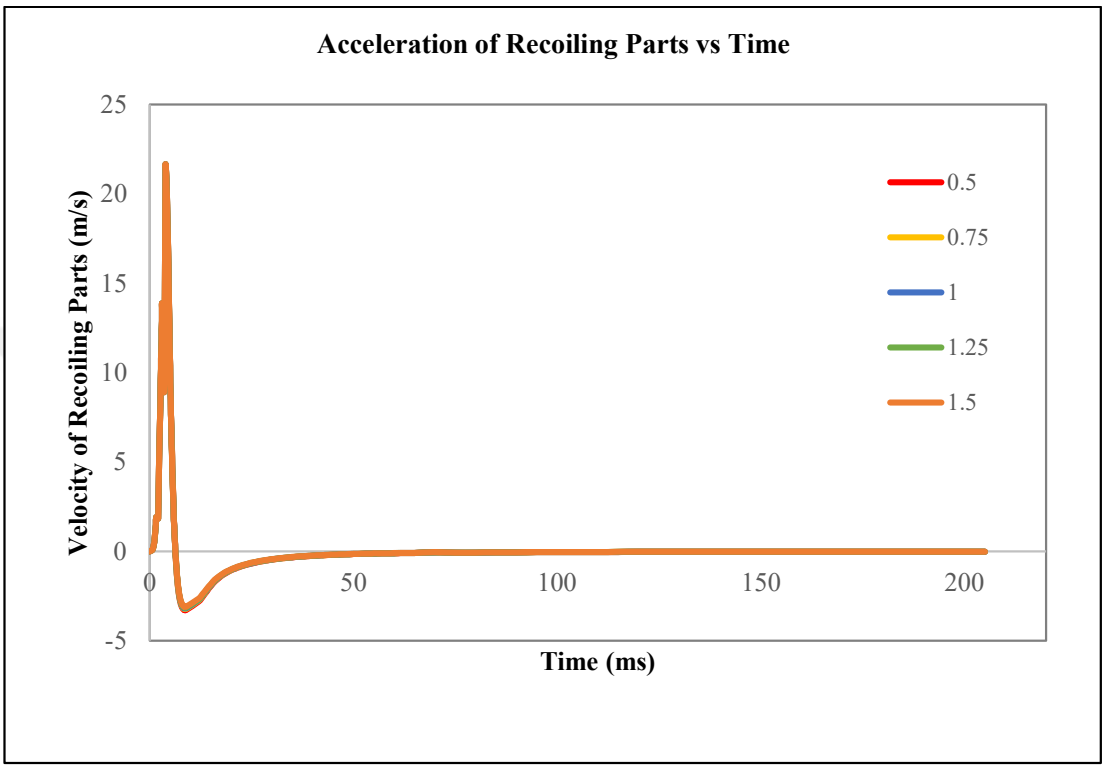

Figure 3.30 Effect of muzzle brake efficiency on acceleration of recoiling parts

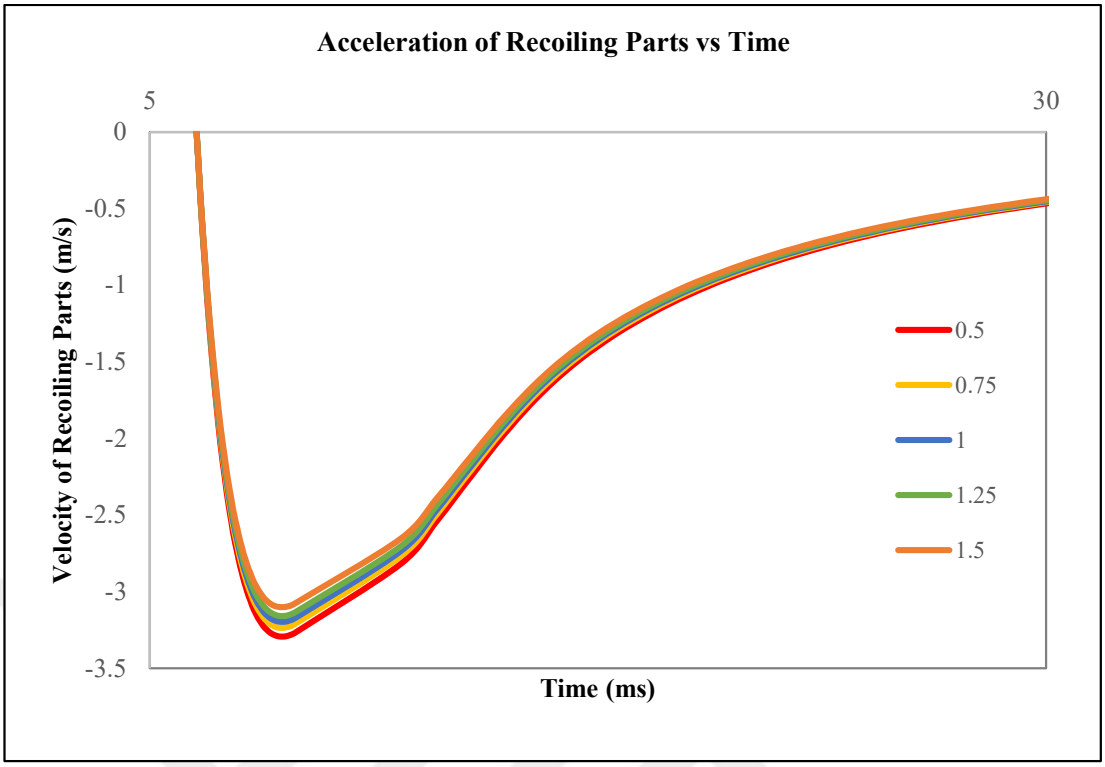

Figure 3.31 Effect of muzzle brake efficiency on acceleration of recoiling parts (5-30 ms)

CHAPTER 4

CONCLUSION AND FUTURE WORKS

4.1 Conclusion

In this study, the recoil movement of heavy weapons with hydropneumatic recoil mechanism is modeled. The primary purpose of the study is to obtain the equation of motion of the recoiling parts in the weapon systems. For this purpose, the forces acting on the recoiling parts were determined, and the effects of each force were examined.

Firstly, breech force is calculated via LeDuc equations for in bore period and verified by comparing with experimental studies. These experimental data are taken from literature for a typical 105 mm howitzer and from MKEK for a new generation lighter 105 mm weapon system. Secondly, the breech force which is generated during the discharge of the remaining gases after the projectile leaves the barrel is also calculated and the total breech force is obtained. Additionally, velocity of projectile in barrel is calculated from the model and compared with the result from literature and MKEK.

Recoil motion caused by breech force is retarded by hydraulic brake and recuperator force in the recoil mechanism and friction. After determining breech and net retarding forces, the equation of motion is obtained, and solved via MATLAB and recoil distance is calculated. Calculated recoil distance is compared with test data.

Comparison of model with test data from two different weapon systems for breech force shows that model results are compatible with real data and the average difference between them is less than three percent.

Model results for velocity of projectile is similar with firing test data from both literature and MKEK. Difference between muzzle velocity values are only about two percent. Muzzle velocity is measured from firing test as 695 m/s and calculated from the model as 680 m/s for the new generation lighter 105 mm weapon system. Firing test and model data for the typical 105 mm weapon system are 455.4 m/s and 455.2 m/s respectively.

Experimental data for recoil displacement is only valid from MKEK and these data are compared with model results. Deviation from test data in model results is in acceptable range which is about two percent. Maximum recoil distance is calculated from model as 1109 mm and measured from firing tests as 1135 mm.

After the validation of model by comparing results from literature and MKEK for breech force, velocity of projectile and recoil displacement, velocity and acceleration of recoiling parts are calculated from the model. In addition, effect of some parameters such as, firing angle, weight of recoiling parts, orifice discharge coefficient and muzzle brake efficiency is investigated.

Velocity and acceleration of the recoiling parts vs time graphics are obtained from the validated model. Results show that recoil mechanism does its duty successfully which is dissipating recoil energy that is formed in very short duration by extremely high internal ballistic forces.

Effect of firing angle on recoil displacement, velocity of recoiling parts and acceleration of recoiling parts is investigated by solving model for 0° and 45°. Results show that the maximum recoil displacement, maximum velocity and maximum acceleration of recoiling parts values are increasing, and minimum acceleration value is decreasing when the firing angle is increased.

Effect of the weight of recoiling parts on recoil displacement, velocity of recoiling parts and acceleration of recoiling parts is also analyzed by solving model for original weight, 20 % lighter weight, 10 % lighter weight, 20 % heavier weight and 10 % heavier weight. Increasing the recoiling weight give opposite results with increasing firing angle. According to the model results, peak values of recoil displacement, velocity and acceleration of the recoiling parts decreasing when the recoiling weight is increased. Those values are decreased from 1109 mm to 921 mm, from 45.2 m/s to 37.5 m/s and from 21.6 m/s^2 to 17.9 m/s^2, respectively as weight of recoiling parts is increased by 20 percent.

Other parameter that is studied is orifice discharge coefficient which is very important for hydraulic cylinder design and hydraulic brake force as well. Effect of this

parameter is studied via validated model by solving it for original, 20 % lower, 10 % lower, 20 % higher and 10 % higher orifice discharge coefficients. Increasing orifice discharge coefficient decrease the hydraulic brake force. Therefore, if orifice discharge is increased, peak values of recoil displacement, velocity and acceleration of the recoiling parts also increase. Those values are increased from 1109 mm to 1220 mm, from 45.2 m/s to 49.7 m/s and from 21.6 m/s^2 to 23.7 m/s^2, respectively when orifice discharge coefficient is increased by 20 percent.

Last parameter whose effects on recoil displacement, velocity of recoiling parts and acceleration of recoiling parts are investigated is muzzle brake efficiency. Muzzle brake efficiency affects breech force especially for gas ejection period. Effect of this parameter is investigated by solving model for 0.5, 0.75, 1, 1.25 and 1.5 muzzle brake efficiency values. Higher muzzle brake efficiency means lower breech force in gas ejection period and lower peak values for recoil displacement, velocity and acceleration of recoiling parts. Results are compatible with expectations and increasing muzzle brake efficiency, decreases maximum recoil displacement and peak velocity values for recoiling parts. When muzzle brake efficiency is increased from 0.5 to 1.5, those values are decreased from 1142 mm to 1075 mm, 46.5 m/s to 43.8 m/s, respectively.

This study shows that a validated model for recoil mechanism can help designers to predict maximum recoil distance or determine some critical parameters such as orifice discharge coefficient, initial gas pressure etc. to stop recoiling parts in a specified recoil distance.

4.2 Future Works

Some further studies about improving and applying the model can be focused on and these are listed below.

- There are two types of frictional forces that contribute net retarding force. One included in this model is the friction between sliding surfaces. Other one is frictional resistance of packing and seals and model can be improved via including this frictional force.

- This study is focused on hydropneumatic recoil mechanisms in 105 mm howitzers. The model can also be applied on other weapon systems that have hydropneumatic recoil systems.
- Some of the parameters whose effects are investigated in this thesis are not studied experimentally. The effect of recoiling weight, orifice discharge coefficient and muzzle brake efficiency values can be studied experimentally.
- Hydraulic brake force is calculated via numerical modelling in this study. Additionally, fluid behavior inside the hydraulic cylinder can be analyzed by using computational fluid dynamics.

REFERENCES

[1] Headquarters Department of the Army, “Technical Manual, Principles of Artillery Weapons” TM 9-3305, Washington DC, 1981.

[2] William, T. Z., “The Designer’s Dilemma - Recoil: What to do with it?” NATO Functional and Mechanical Integration of Weapons with Land and Air Vehicles Symposium, RTO-MP-AVT-108, 7-9 June 2004, Williamsburg, VA, USA.

[3] Department of Defense, “Military Handbook, Recoil Systems, Metric” DOD-HDBK- 778, Washington DC, 1988.

[4] Arora, J. S., and Haug, J. S., “A Guide to Design of Artillery Recoil Mechanisms” Technical Report, US Army Armament Research and Development Command, Dover, NJ, 1977.

[5] Yang, Z. Dynamic Simulation Analysis and Optimization of Recoil Mechanism. Master’s thesis. National Chiao Tung University Institute of Mechanical Engineering. 2005.

[6] Tuncer, D. G. and Alli, H., “Ağır Silahların Geri Tepme Mekanizmaları Tasarımında İç Balistik Modelin Oluşturulması ve Kama Kuvvetinin Hesaplanması” 2. Ulusal Tasarım İmalat ve Analiz Kongresi, 11-12 November 2010, Balıkesir, Turkey.

[7] Tuncer, D. G. Ağır Silahlardaki Geri Tepme Mekanizmalarının Dinamik Modellenmesi ve Sayısal Benzetimi. Master’s thesis. Fırat University Institute of Natural Sciences. 2010.

[8] Taşkıran, E. Ağır Silahlardaki Geri Tepme Mekanizmalarının Dinamiği Üzerine. Master’s thesis. Gazi University Institute of Natural Sciences. 2010.

[9] Elaldı, F. and Akçay, M., “Design and Testing of a Recoil Mechanism Used For Self Propelled Howitzers” Bulletin of the Technical University of Istanbul, 49 (3-4), 301-316, 1996.

[10] Zaloğlu, H. Finite Element Modelling and Analysis of Recoil Springs in Automatic Weapons. Master's thesis. Middle East Technical University The Graduate School of Natural and Applied Sciences. 2013.

[11] Lin, T. Y., Ping, H. C., Yang, T. Y., Chan, C. T. and Yang, C. C., "Dynamic Simulation of the Recoil Mechanism on Artillery Weapons" The International Conference on Computational & Experimental Engineering and Sciences, 9-13 Nisan 2009, 11(4), 115-121.

[12] Hassaan, G.A., "Dynamics of a Cannon Barrel - Recoil Mechanism with Nonlinear Air-Springs" Int J. Innovation and Applied Sciences, 8(4), 1669-1680, 2014.

[13] Hassaan, G.A., "Dynamics of a Cannon Barrel - Recoil Mechanism with a Nonlinear Hydraulic Damper" Int J. Modern Sciences and Engineering Technology, 1(5), 82-91, 2014.

[14] Hassaan G.A., "On Dynamics of a Cannon Barrel - Recoil Mechanism with Nonlinear Hydraulic Damper and Air-Springs, Int J. Research in Information Technology, 2(9), 704-714, 2014.

[15] Hajihosseinloo, M. A., Hooke, C. J. and Walton, D., "Gun Recoil System Performance Measurement and Prediction" Proceedings of the Institution of Mechanical Engineers, Part C: Mechanical Engineering Science, 203(2), 85-92, 1989.

[16] Tiwari, N., Patil, M., Shankar, R., Saraswat, A. and Dwivedi, R., "Rigid body dynamics modeling, experimental characterization, and performance analysis of a howitzer" Defence Technology, 12, 480-489, 2016.

[17] Ahmadian, M. and Poynor, J. C., "An Evaluation of Magneto Rheological Dampers for Controlling Gun Recoil Dynamics", Shock and Vibration, 8, 147-155, 2001.

[18] Ahmadian, M., Appleton, R. and Norris, J. A., “An analytical study of fire out of battery using magneto rheological dampers” Shock and Vibration, 9, 129-142, 2002.

[19] Ahmadian, M., Appleton, R. J., Norris J.A., “Designing Magneto-Rheological Dampers in a Fire Out-of-Battery Recoil System” IEEE Transactions on Magnetics, 39(1), 480-485, 2003.

[20] Headquarters US Army Material Command, “Engineering Design Handbook, Ballistics Series, Interior Ballistics of Guns” AMCP 706-150, Washington DC, 1965.

[21] Corner, J., “Theory of the Interior Ballistics of Guns” John Wiley & Sons Inc., New York, 1950.

[22] Coberly, R., “Interior Ballistics” Technical Note 3-54, Rock Island, Arsenal, 1954.

[23] Headquarters US Army Material Command, “Engineering Design Handbook, Guns Series, Muzzle Devices”, AMCP 706-251, Washington DC, 1968.

[24] Backstein, G., Bettermann, P., Bisping, B., Böder, D., Boutteville, S. V., Dechow, H. and others, “Handbook on Weaponry”, Rheinmetall GmbH, Düsseldorf, 1982.

[25] Baer, P. G. and Frankle, J. M., “The Simulation of Interior Ballistic Performance of Guns by Digital Computer Program”, Ballistic Research Laboratories, Maryland, 1962.